Phase-Noise-Canceling and Multichannel Coherent Optical Fiber Communications

（位相雑音相殺型および多チャネルコヒーレント光ファイバ通信に関する研究）

Thesis by

Yi-Hao Cheng
（程　　頤浩）

in Partial Fulfillment of the Requirements for
the degree of Doctor of Philosophy in
Electronic Engineering in the Graduate School of
the University of Tokyo

December 22, 1989

Dissertation Supervisor

Professor **Takanori Okoshi**

ACKNOWLEDGMENTS

It is a pleasure to express the utmost gratitude to my dissertation supervisor, Professor Takanori Okoshi, for his continuous guidance, encouragement, and help throughout the course of this work. His professional and private supports made this thesis possible.

I am indeed grateful to Dr. K.Kikuchi for his continuous encouragement and inspiring discussion. His advisable comments and suggestions have helped me complete this work.

I would like to thank Mr. A.Hirose and Ms. S.Kitazawa for their technical assistance in construction and supply of the experimental apparatures. Their continuous encouragement and assistance are indispensable for the completion of this thesis. Acknowledgements are also due to the members of Okoshi & Kikuchi's Lab. and Okoshi & Hotate's Lab.. The collaboration with them was pleasant and fruitful.

I greatly appreciated valuable comments from Prof. E.A.J. Marcatili, Prof. T.Kamiya, Prof. Y.Fujii, Prof. H.Sakaki, Prof. Y.Arakawa, and Prof. K.Hotate.

Encouragement and help from Ms. K.Miyakawa are greatly apprecited and her support is most unforgettable.

Scholarship supports from the Chinese government and Foundation for C&C Promotion are gratefully acknowledged.

Finally, with all my heart I wish to thank my dear wife Hai-Mong. Her love, understanding, support and encouragement have always been a source of inspiration and hope.

Table of Contents

CHAPTER 1

General Introduction

1.1 Background

Optical communication has a long history, which had been an only communication medium until the appearance of electric communication in the nineteenth century. After nearly one century, optical communication was brought back to revival, when optical *fiber* communication was born in 1970, with the advent of practical low loss (about 20dB/km) fibers[1] and semiconductor lasers[2]. Since then lot of efforts have been made to reduce further the fiber loss and to improve the performances of transmitter (laser) and receiver. As results, optical fiber communication systems are now utilized in practical communication networks.

The modulation/demodulation scheme used in present optical fiber communication systems is so called intensity-modulation/direct-detection (IM/DD) scheme, in which the intensity of light is modulated linearly with respect to the input electrical signal, and detected directly by a photodetector. Such system has advantages in system simplicity and low cost. In the wavelength region around 0.85μm, receiver sensitivity near to shot-noise-limit can be obtained because Si-APDs used as photodetectors have excellent noise performance in this region. However, the present optical fiber communication systems are preferably used in the wavelength regions around 1.3μm and

around 1.55μm, because in the former wavelength region the dispersion of fibers is zero, and in the latter the loss of fibers is minimal. At such longer wavelengths, Ge or III-V compound APDs are used as photodetectors, and the receiver sensitivity will be deteriorated due to the poor noise performance of this kind of photodetector[3]. In order to achieve a near shot-noise-limit detection at 1.3 or 1.55μm, coherent (heterodyne/homodyne) optical fiber communications are presently considered to be an only practical method.

1.2 Brief description of coherent optical fiber communications

Heterodyne-type coherent optical communication was proposed in the late 1960's[4]. However, in that system, lens type waveguides and gas lasers were considered to be used, which seems impractical. A new type of coherent optical *fiber* communication system based on the use of optical fiber and semiconductor lasers was developed for the first time in 1979[5],[6], and investigated theoretically and experimentally since that[7]-[9].

Basic constructions of coherent (heterodyne/homodyne) receivers are shown in Fig.1.1. In a heterodyne receiver (Fig.1.1(a)), the transmitted signal light is mixed with local oscillator (LO) light, and detected by a photodetector. The obtained intermediate frequency (IF; the frequency difference between signal carrier frequency and LO frequency) signal is then amplified and demodulated. In a homodyne receiver (Fig.1.1(b)), the LO frequency and phase are controlled to be the same as that of the received signal carrier, so that baseband signals can be obtained directly. In a coherent optical receiver, light power of the LO is so large that the shot noise due to the LO light becomes a predominant source of receiver noise, thereby the remaining noises of the receiver can be neglected, resulting in an achievement of the shot-noise-limited detection.

1.3 Features of and problems with coherent optical fiber communication systems

Compared with IM/DD optical fiber communication systems, coherent optical fiber systems have mainly two features; one is the possibility of receiver sensitivity improvement of about 10~25dB at wavelength of 1.3 or 1.55μm, which leads to the elongation of repeater separation, and the other is the possibility of frequency-division multiplexing (FDM) with very densely spaced channels, which offers an access to vast transmission capacity of single-mode fiber by transmitting many channels into one fiber.

However, before coherent optical fiber communication systems are utilized in practical networks, following technical problems have to be overcome:

[1] *Frequency stability of semiconductor lasers.* Since the typical IF in coherent systems is about 10^{-6}~10^{-5} times the carrier frequency of semiconductor lasers, the requirement for frequency stability of lasers is very serious. Particularly in multichannel coherent systems, frequency stabilization methods have to be developed to set and maintain a desired channel spacing.

[2] *Reduction of laser phase noise (spectral linewidth).* It is understood that when the carrier of transmitter or LO has frequency or/and phase fluctuations, bit-error rate (BER) of coherent systems will be deteriorated, causing an increase of required signal level. On the other hand, semiconductor lasers have relatively large phase noise (wide linewidth) due to spontaneous emission events, carrier fluctuation effect, and 1/f noise. Therefore, new types of detection scheme with large tolerance for laser phase noise are necessary to be developed.

[3] *Random fluctuations of state of polarization (SOP) of signal lights.* Three methods (using polarization maintaining fiber, polarization controlling devices, and polarization diversity scheme, respectively) have been proposed and demonstrated[10]-[12].

So far, researches and developments have been performed on the improvement of receiver sensitivity of single-channel coherent systems in many laboratories, aiming to achievements of shot-noise-limited detection and very long distance transmission[13]-[18]. Successful transmissions have been achieved in laboratories over distance of 300km[19], and under bit-rate as high as 5Gbit/s[20]. A first field transmission with coherent optical fiber system was also reported[21]. Recently, attention is being attracted in multichannel coherent systems.

Unlike that of single-channel coherent systems, the performance of multichannel coherent systems will be deteriorated due to several physical phenomena which are crosstalks caused by excess shot noise, intermodulation interference and nonlinear effects in the single-mode fiber[22]-[25], which do not exist in single-channel systems. It has been found that crosstalk can also be induced by optical amplifier (if used)[26]-[29].

First theoretical investigation on the multichannel coherent system was performed in Ref.[30] with respect to intermodulation interference. The results show that homodyne detection with single-detector receiver should be avoided to use, because it gives poor intermodulation performance, independent of channel spacing (i.e., frequency difference between the channels). Then a kind of balanced receiver was investigated for multichannel coherent system[31]. The results show that a balanced receiver can eliminate direct-detection- and signal-cross-signal interferences. However, detailed theoretical investigation on the crosstalk of multichannel coherent system has not been

reported, in spite of its importance.

On the contrary, experimental studies on multichannel coherent system have become active. Many experimental results have been published with respect to the crosstalks due to the intermodulation interference[32]-[35], and the nonlinear effects in the single-mode fiber[36]-[38] and in the optical amplifier[39]-[41].

1.4 Purpose and construction of the thesis

The purpose of this work is twofold; one is to develop and demonstrate novel transmission schemes suitable for low bit-rate coherent optical fiber communications, in which conventional semiconductor lasers can be used as both transmitter and LO even at low bit-rate (<500Mbit/s). In the research, phase-noise-canceling heterodyne schemes (PNCHSs) are proposed, and investigated theoretically and experimentally. The experimental results show the successful cancellation of laser phase noise, suggesting the feasibility of PNCHSs.

The other purpose is to analyze the crosstalk performance of multichannel coherent optical communication systems. In the analysis, crosstalks caused by excess shot noise and image-band interference are calculated, and influences of laser linewidth, types of IF filter, and pulse shape are discussed. The construction of this thesis is as follows:

In Chapter 2, the performance of a dual-polarization PNCHS (DP-PNCHS) is investigated theoretically. General BER formula and the influence of loss in orthogonality of polarization are clarified, and the orthogonality of polarization in a single-mode optical fiber and in a fiber coupler is also discussed.

Chapter 3 describes the performance of a dual-frequency PNCHS (DF-PNCHS), in which sensitivity of the scheme is analyzed, and a BER measurement experiment is performed to confirm the principle of the scheme. A polarization diversity DF-PNCHS is also proposed and discussed.

In Chapter 4, a new type of PNCHS called dual-waveguide PNCHS (DW-PNCHS) is proposed and analyzed theoretically. Effect of propagating characteristics of fibers is examined.

Another new type of PNCHS called time-division PNCHS (TD-PNCHS) is proposed and investigated in Chapter 5, in which the performance of the scheme is analyzed considering the influence of optical path difference, and a simulated experiment is performed to confirm the principle of the scheme. A polarization diversity TD-PNCHS is also proposed and discussed.

In Chapter 6, detailed theoretical investigations on crosstalk performance of multichannel coherent optical fiber communication systems are described, in which sensitivity penalties caused by crosstalks due to excess shot noise and image-band interference are analyzed, and the influences of various parameters determining the crosstalk are discussed.

Results obtained in this work are summarized in Chapter 7.

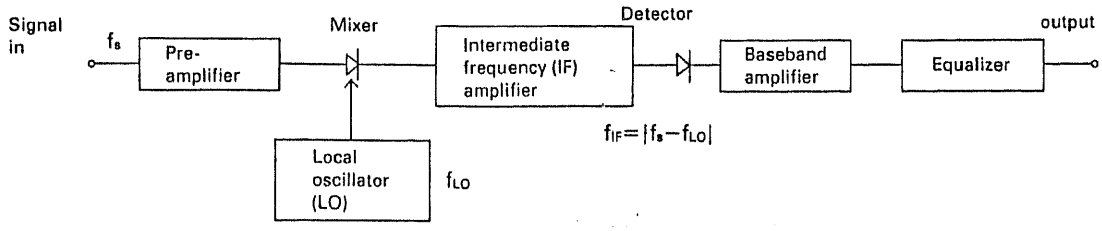

(a)

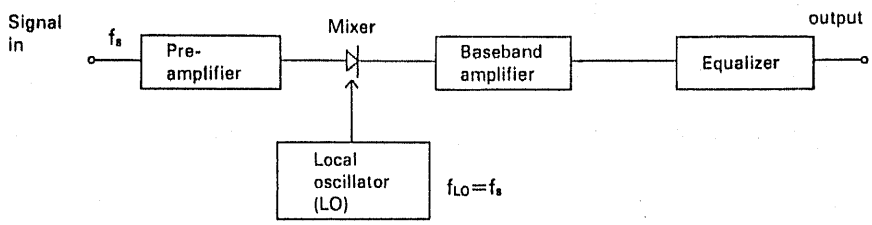

(b)

Fig. 1.1 Basic constructions of coherent receivers, (a) heterodyne receiver, and (b) homodyne receiver.

CHAPTER 2

Dual-Polarization Phase-Noise-Canceling Heterodyne Scheme

Abstract

Dual-polarization phase-noise-canceling heterodyne scheme (DP-PNCHS) is investigated theoretically, and BER performance of the scheme is analyzed taking into account the influence of loss in orthogonality of polarization. Calculated results show that receiver sensitivity of the scheme is better than that of the conventional DPSK heterodyne scheme when laser linewidth is larger than 0.007 times bit-rate. The orthogonalities of polarization in a single-mode optical fiber and in a fiber coupler are also discussed. It is found that the orthogonality of polarization will be maintained in a fiber if it has the same attenuation coefficient for both polarization components, and that in a fiber coupler the polarization dependence of power splitting ratio will cause loss in orthogonality of polarization. Experimental results show that the loss in orthogonality of polarization is small in a typical fiber coupler, suggesting the feasibility of the scheme.

2.1 Introduction

Since the concept of coherent optical fiber communications using semiconductor lasers as transmitter and/or LO was proposed in 1979, researches have been actively performed on improvement of frequency stability and spectral purity (reduction of linewidth) of the semiconductor laser, because the broad laser linewidth due to phase noise often causes degradation of receiver sensitivity. Previous works show that the maximal permissible ratio of laser linewidth to bit-rate ($\Delta\nu/R_b$) is generally 9% for ASK system, several percent for FSK system (depending on frequency deviation and detection scheme), and below 0.5% for PSK (or DPSK) system to confine the sensitivity degradation within 1dB at BER=10^{-9} [42]-[44].

Among many coherent optical fiber communication systems, it is predicted that medial or low bit-rate (below several hundred Mbit/s) PSK systems will be commonly utilized in optical local area networks (LANs) or in optical broadband subscriber systems in the future. However, according to theoretical and experimental estimations, such systems require lasers having linewidth less than about 1MHz. But this is difficult to realize as far as solitary distributed feedback (DFB) lasers are used, although some improvements are achieved by using recently developed MQW DFB lasers having relative narrow linewidth[45].

One countermeasure against the problem of laser phase noise is to use semiconductor lasers with external cavity as transmitter and/or LO. In fact, some experiments concerned have been reported at low bit-rates[46],[47]. However, those systems are considered to be not useful for practical communication networks, because of problems of stability, mode-hopping and lifetime.

Another countermeasure is to use phase-noise-canceling heterodyne schemes (PNCHSs). One of them (called dual-polarization phase-noise-canceling heterodyne scheme: hereafter DP-PNCHS) was proposed by K.Tamura et al. in 1988[48], in which two orthogonally polarized lights are used to cancel laser phase noise. Preliminary experiment showed that the scheme is useful in low bit-rate system. However, detailed performance of the scheme and the requirement for orthogonality of polarization have not been analyzed.

In this Chapter, performance of the DP-PNCHS is investigated theoretically taking into account the influence of loss in orthogonality of polarization, and the losses in orthogonality of polarization in a single-mode fiber and in a fiber coupler are studied theoretically and experimentally.

In Section 2.2, a general BER formula of the scheme is derived, and the influence of loss in orthogonality of polarization is discussed. Section 2.3 describes theoretically and experimentally the losses in orthogonality of polarization in a single-mode fiber and in a fiber coupler. Results of this Chapter are summarized in Section 2.4.

2.2 Theoretical analysis of DP-PNCHS

In optical communication systems, one of the important factors is receiver sensitivity (BER characteristic), here the sensitivity of the DP-PNCHS is calculated. The shot-noise-limited state is assumed in the analysis for simplicity.

2.2.1 Calculation of BER

In the DP-PNCHS shown in Fig.2.1, two orthogonally polarized light

beams having the same intensity are transmitted. One beam (e.g., x-polarized one) is used as signal channel and contains the information to be transmitted and phase noise of transmitting laser, whereas the second beam (e.g., y-polarized one) is used as reference channel and includes the laser phase noise only. At the receiving end, with a proper polarization control the received signal and the LO lights are split into vertically and horizontally polarized components by a polarizing beam splitter. The signals of two channels can be separated completely, provided that the orthogonality of polarization is maintained in transmitting path (e.g., single-mode optical fibers) between the transmitter and receiver. However, as will be described in Section 2.3, when two optical waves with orthogonal polarizations are launched into a single-mode fiber, in general, they will not remain orthogonal, and a sensitivity degradation is thereby caused.

Considering here the case that the orthogonality of polarization can not be maintained, i.e., at receiving end the difference of inclination angles of state of polarization (SOP) of the two light beams is no longer 90 but $90+\rho$ degrees, and a phase difference ψ may be also produced between them (see Fig. 2.2). The complex electric field amplitudes of the signals and LO lights at the detectors, E_{sx}, E_{sy}, E_{Lx} and E_{Ly} (s: signal, L: LO, x: horizontal, y: vertical) can be expressed as

$$E_{sx} = \sqrt{\frac{P_s}{2}} \exp[j(\omega_s t + \theta(t) + \phi_s)] + \sqrt{\frac{P_s}{2}} \sin\rho \exp[j(\omega_s t + \phi_s + \psi)] \quad (2.2.1)$$

$$E_{sy} = \sqrt{\frac{P_s}{2}} \cos\rho \exp[j(\omega_s t + \phi_s + \psi)] \quad (2.2.2)$$

$$E_{Lx} = \sqrt{\frac{P_L}{2}} \exp[j(\omega_L t + \phi_L)] \quad (2.2.3)$$

$$E_{Ly} = \sqrt{\frac{P_L}{2}} \exp[j(\omega_L t + \phi_L)] \quad (2.2.4)$$

where P_s denotes the received signal power, ϕ_s the signal phase noise including laser phase noise, P_L the LO power, ϕ_L the LO phase noise, ω_s and ω_L the angular frequencies of the signal and LO light, respectively, and $\theta(t)$ denotes the phase modulation by signals to be transmitted. Assuming that $P_L >> P_s$, by ignoring the DC terms and considering a mark signal($\theta(t) = 0$), the obtained photocurrents in a narrow band approach [49] can be expressed as

$$I_x = [R\sqrt{P_sP_L} + R\sqrt{P_sP_L}\sin\rho\cos\psi + n_1]\cos(\Delta\omega t + \Delta\phi) - [R\sqrt{P_sP_L}\sin\rho\sin\psi + n_2]\sin(\Delta\omega t + \Delta\phi) \quad (2.2.5)$$

$$I_y = [R\sqrt{P_sP_L}\cos\rho\cos\psi + n_3]\cos(\Delta\omega t + \Delta\phi) - [R\sqrt{P_sP_L}\cos\rho\sin\psi + n_4]\sin(\Delta\omega t + \Delta\phi) \quad (2.2.6)$$

where $\Delta\omega = \omega_s - \omega_{LO}$, $\Delta\phi = \phi_s - \phi_{LO}$, and R denotes the detector responsivity, n_i (i=1,2,3,4) the shot-noise currents having zero-mean Gaussian distributions whose root-mean-square (rms) values are given as:

$$\overline{n_1^2} = \overline{n_2^2} = eR(R_b + K\Delta\nu)P_L = \sigma_{p1}^2 \quad (2.2.7)$$

$$\overline{n_3^2} = \overline{n_4^2} = eRK\Delta\nu P_L = \sigma_{p2}^2 \quad (2.2.8)$$

$$<n_i> = 0 \qquad \text{for} \quad i=1,2,3,4 \quad (2.2.9)$$

where e is the electron charge, $\Delta\nu$ the IF linewidth, and K is a constant depending on the filter bandwidth. Here the use of two bandpass filters having bandwidths of $R_b+K\Delta\nu$ for the signal channel and $K\Delta\nu$ for the reference channel is assumed.

The two IF signals, I_x and I_y, are amplified, and multiplied by each other. Here ten stochastic variables are defined for further computations:

$$X_1 = R\sqrt{P_sP_L} + R\sqrt{P_sP_L}\sin\rho\cos\psi + n_1$$

$$X_2 = R\sqrt{P_sP_L}\cos\rho\cos\psi + n_3$$

$$Y_1 = R\sqrt{P_sP_L}\sin\rho\sin\psi + n_2$$

$$Y_2 = R\sqrt{P_sP_L}\cos\rho\sin\psi + n_4$$

$$x_1 = X_1 + X_2 \qquad x_2 = X_1 - X_2$$

$$x_3 = Y_1 + Y_2 \qquad x_4 = Y_1 - Y_2$$

$$r_m^2 = x_1^2 + x_3^2 \qquad r_n^2 = x_2^2 + x_4^2 \tag{2.2.10}$$

The product thus obtained can be expressed as

$$\begin{aligned} V &= \frac{1}{2}(X_1X_2 + Y_1Y_2) \\ &= \frac{1}{8}(r_m^2 - r_n^2) \end{aligned} \tag{2.2.11}$$

where r_m and r_n are norms of corresponding 2-dimensional vectors.

In PSK scheme, BER for mark signals is given as probability for generating a negative output; i.e., for $r_m < r_n$

$$\begin{aligned} P_e &= prob.(r_m < r_n) \\ &= \int_0^\infty q_m(r_m) \int_{r_m}^\infty q_n(r_n)\, dr_m\, dr_n \end{aligned} \tag{2.2.12}$$

where $q_m(r_m)$ and $q_n(r_n)$ are the probability density function of r_m and r_n, respectively, which have the forms[50]

$$q_m(r_m) = \frac{r_m}{\sigma^2} I_0\left[\frac{A_m r_m}{\sigma^2}\right] \exp\left[-\frac{r_m^2 + A_m^2}{2\sigma^2}\right] \tag{2.2.13}$$

$$q_n(r_n) = \frac{r_n}{\sigma^2} I_0\left[\frac{A_n r_n}{\sigma^2}\right] \exp\left[-\frac{r_n^2 + A_n^2}{2\sigma^2}\right] \tag{2.2.14}$$

where

$$\sigma^2 = \sigma_{p1}^2 + \sigma_{p2}^2 \tag{2.2.15}$$

$$A_m^2 = \overline{x_1}^2 + \overline{x_3}^2 \tag{2.2.16}$$

$$A_n^2 = \overline{x_2}^2 + \overline{x_4}^2 \tag{2.2.17}$$

Considering first an ideal case of the orthogonality of polarization is maintained (i.e., $\rho = 0, \psi = 0$). Thus

$$A_m^2 = 2R^2 P_s P_L, \qquad A_n^2 = 0 \tag{2.2.18}$$

and

$$q_n(r_n) = \frac{r_n}{\sigma^2} \exp\left(-\frac{r_n^2}{2\sigma^2}\right) \tag{2.2.19}$$

The BER can then be calculated analytically by substituting Eqs.(2.2.13)-

(2.2.19) into Eq.(2.2.12) to give

$$P_e = \frac{1}{2}\exp\left(-\frac{1}{1+K\cdot\Delta\nu/R_b}\frac{N}{2}\right) \tag{2.2.20}$$

where N is the number of signal photons in one bit period. It is understood that BER of the conventional phase-noise free DPSK heterodyne scheme is given as[51]

$$P_e = \frac{1}{2}\exp(-N) \tag{2.2.21}$$

Thus power penalty of the DP-PNCHS can be obtained by comparing Eqs.(2.2.21) and (2.2.21), and given as

$$P_{enalty} = 10\log_{10}[2(1+K\Delta\nu/R_b)]\ (dB) \tag{2.2.22}$$

Figure 2.3 shows the calculated power penalty at BER=10^{-9} as a function of the ratio of IF linewidth to bit-rate ($\Delta\nu/R_b$). The result for the conventional DPSK heterodyne receiver is also shown for comparison in dotted curve. It is found that the performance of the DP-PNCHS is better than that of the conventional DPSK heterodyne receiver when $\Delta\nu/R_b$>0.007. It should be noted that because σ_{p1}^2 and σ_{p2}^2 are determined by the bandwidth of IF BPFs, the receiver sensitivity of individual system may be different from the present calculated results if different filter bandwidth is chosen, but the conclusion will be not changed remarkably. In addition, there may be an optimum choice for BPF bandwidth because larger bandwidth will cause larger sensitivity degradation, whereas the phase noise cancellation will become incomplete if the bandwidth is too narrow.

2.2.2 Influence of loss in orthogonality of polarization

In the case of $\rho \neq 0$ and $\psi \neq 0$, BER of the DP-PNCHS can be calcu-

lated numerically by Eq.(2.2.12) to give

$$P_e = 4e^{-\alpha-\beta}\int_0^\infty \epsilon I_0[2\sqrt{\alpha}\epsilon]e^{-\epsilon^2}\int_\epsilon^\infty \xi I_0[2\sqrt{\beta}\xi]e^{-\xi^2}d\xi\, d\epsilon \qquad (2.2.23)$$

where

$$\alpha = \frac{A_m^2}{2\sigma^2} \qquad \beta = \frac{A_n^2}{2\sigma^2}$$

Equation (2.2.23) can be rewritten with a series as

$$P_e = e^{-\alpha-\beta}\sum_{n=0}^{\infty} a_n \qquad (2.2.24)$$

where

$$a_0 = \frac{1}{2}e^{\frac{\alpha}{2}} \qquad (2.2.25)$$

$$a_n = \frac{\beta}{n}a_{n-1} + \frac{1}{2}\frac{\left(\frac{\beta}{2}\right)^n}{n!}e^{\frac{\alpha}{2}}\sum_{l=0}^{n}\frac{n!}{(n-l)!(l!)^2}\left(\frac{\alpha}{2}\right)^l \qquad (2.2.26)$$

Figure 2.4 shows the calculated power penalties under various phase differences, as functions of the deviation in inclination angle at BER=10^{-9}. It is found that the existence of phase difference ψ will cause increase of power penalty due to inclination angle difference ρ. Figure 2.5 shows the maximal permissible phase difference to achieve a power penalty less than desired level at BER=10^{-9}, as a function of the deviation in inclination angle. It is found that the power penalty is strongly dependent on ρ rather than on ψ, and that the deviation in inclination angle should be less than about 9 degrees to confine the power penalty within 1dB when $\psi = 0$.

2.3 Orthogonality of polarization in a single-mode fiber and a fiber coupler

The theoretical results calculated above show that the loss in orthogonality of polarization will be detrimental to the performance of the DP-PNCHS. Therefore, it is important to understand the relationship between the

SOPs of two signal lights at the output end of a fiber, when the two signal lights are orthogonal at the input end of the fiber. This section describes the loss in orthogonality of polarization in a single-mode optical fiber, and in a fiber directional coupler which is commonly used in coherent optical fiber communication systems.

2.3.1 Theory

A linear optical system (e.g., a single-mode fiber) can be represented by a 2×2 complex-amplitude Jones transmission matrix T. Assuming that E_{1i} and E_{2i} are complex unit vectors (normalized Jones vectors) describing the SOPs of input lights, and E_{1o} and E_{2o} are the corresponding complex vectors describing the SOPs of output lights, then the scalar product of E_{1o} and E_{2o} can be expressed as

$$E_{2o}^{*} \cdot E_{1o} = E_{2i}^{*} T^{*} T E_{1i} \tag{2.3.1}$$

where * indicates the transpose complex conjugate. It can be found from Eq.(2.3.1) that if the input lights are orthogonally polarized, that is,

$$E_{2i}^{*} \cdot E_{1i} = 0 \tag{2.3.2}$$

and the Jones matrix T is a unitary matrix, i.e., $T^{*}T = I$, where I is a unit matrix, then the orthogonality of polarization will be maintained in the system, that is, the SOPs of the output lights will be also orthogonally polarized. In other words, a linear optical system having the unitary transmission matrix will maintain the orthogonality of polarization.

When polarization fluctuations due to changes of external environment (such as temperature, mechanical conditions, and so on) are ignored in a single-mode optical fiber, the transmission matrix of the fiber, T_f, can be expressed as

$$T_f = \begin{pmatrix} e^{-j(\beta+\Delta\beta)-\alpha_x} & 0 \\ 0 & e^{-j(\beta-\Delta\beta)-\alpha_y} \end{pmatrix} \tag{2.3.3}$$

where $\beta+\Delta\beta$ and $\beta-\Delta\beta$ are the propagation constants for x- and y-polarized lights, and α_x and α_y are the attenuation coefficients for x- and y-polarized lights, respectively. It is found that T will become a unitary matrix, when $\alpha_x = \alpha_y$. That is, the orthogonality of polarization can be maintained in a fiber if it has the same attenuation coefficient for both polarization components.

The polarization fluctuations due to the changes of external environment in the fiber can be considered equivalently as a result of effects of optical phase shifters and rotators. The transmission matrix of a phase shifter, T_p, can be expressed as

$$T_p = \begin{pmatrix} e^{j\frac{\delta}{2}} & 0 \\ 0 & e^{-j\frac{\delta}{2}} \end{pmatrix} \tag{2.3.4}$$

and the transmission matrix of a rotator, T_r, is given as

$$T_r = \begin{pmatrix} \cos\theta & \sin\theta \\ -\sin\theta & \cos\theta \end{pmatrix} \tag{2.3.5}$$

It is found that although the changes of external environment will cause the fluctuation of SOP of lights, they do not give any influence on the orthogonality of polarization in the fiber, because both T_p and T_r are unitary matrices.

On the other hand, fiber coupler is often used to mix the signal and LO lights in coherent systems. Assuming that the power splitting ratio of the fiber coupler for x- and y-polarized components are p_x and p_y respectively, the transmission matrix of the fiber coupler from one port of inputs to one port of outputs, T_c, can be expressed as

$$T_c = \begin{pmatrix} \sqrt{p_x}\, e^{j\delta} & 0 \\ 0 & \sqrt{p_y}\, e^{j\delta} \end{pmatrix} \tag{2.3.6}$$

It is found that T_c will become to be a unitary matrix when $p_x = p_y$. However, since the power splitting ratio of a fiber coupler has generally a polarization dependence, it is difficult to realize $p_x = p_y$, so that the orthogonality of polarization can not be maintained in practical fiber couplers.

2.3.2 Measurement of loss in orthogonality of polarization in a fiber coupler

Experiment by R.E.Wagner et al.[52] showed that the loss in orthogonality of polarization in a 150km single-mode optical fiber was about 6 degrees. It is found from Fig.2.3 that the corresponding power penalty is 0.5dB in the DP-PNCHS. However, loss in orthogonality of polarization in a fiber coupler has never been reported. Experimental results of the measurement of loss in orthogonality of polarization in a fiber coupler are investigated here.

The experimental set-up is shown in Fig.2.6, in which SOP of the laser light is changed by a Babinet-Soleil compensator and a polarizer, and SOP of output light from the coupler is measured using another polarizer (analyzer) and a power meter.

In the measurement, the Babinet-Soleil compensator is adjusted to give a circularly polarized light, and the polarizer (PL.1) is fixed to give a linearly polarized light. The inclination angle of the obtained linearly polarized light can be changed by rotating PL.1. The maximal and minimal output powers, P_{max1} and P_{min1}, of the output light and corresponding inclination angles, θ_{max1} and θ_{min1} are at first measured by rotating the analyzer. The inclination angle of PL.1 is then rotated by 90 degrees, and the maximal and minimal output powers, P_{max2} and P_{min2}, and the corresponding inclination angles θ_{max2} and θ_{min2} are measured again. This procedure is repeated for the inclination angle of PL.1 from 0 to 90 degrees. The fiber coupler under test is a commercially

available 1.3μm 50/50 single-mode fiber coupler.

Figure 2.7 shows measured ellipticity defined as P_{min1}/P_{max1} of SOP of the output light as a function of the inclination angle of PL.1, where $P_{min1}/P_{max1} = 0$ corresponds to a linearly polarized light, and $P_{min1}/P_{max1} = 1$ corresponds to a circularly polarized light. It is found that the SOP of the output light varies with the inclination angle of PL.1. The loss in orthogonality of polarization can be calculated as $\theta_{max1} - \theta_{max2} - 90$ or $\theta_{min1} - \theta_{min2} - 90$. The measured results are shown in Fig.2.8 as a function of the inclination angle of PL.1. It is found that the loss in orthogonality of polarization in the coupler is varied with the inclination angle of PL.1, and has a maximal value of 6 degrees, causing a power penalty of about 0.5dB in the DP-PNCHS.

Figure 2.9 shows measured fluctuation of power splitting ratio of the coupler as a function of the inclination angle of PL.1. It is found that the maximal loss in orthogonality of polarization and the maximal deviation of power splitting ratio are appeared at the same inclination angle, suggesting the validity of the theory.

2.4 Conclusions

In this Chapter, the performance of the DP-PNCHS is analyzed taking into account the influence of orthogonality of polarization, and losses in orthogonality of polarization in a single-mode fiber and in a directional fiber coupler are investigated theoretically and experimentally. It is found from the results obtained in this Chapter that

(1) DP-PNCHS has better receiver sensitivity than the conventional DPSK heterodyne scheme when IF linewidth to bit-rate is larger than 0.007, and can be used even in a system having IF linewidth larger than bit-rate.

(2) The loss in orthogonality of polarization in transmitting path between the transmitter and receiver will cause degradation of the performance of the DP-PNCHS, and it should be smaller than 9 degrees to keep the power penalty below 1dB at BER=10^{-9}.

(3) Although the SOP of lights will be fluctuated in a non-polarization maintaining fiber due to changes of external environment, the orthogonality of polarization will be still maintained in the fiber, provided that attenuation coefficients of the fiber are independent of the SOP of signal lights.

(4) The orthogonality of polarization can not be generally maintained in a fiber coupler because of the polarization dependence of its power splitting ratio. However, experimental results show that the loss in orthogonality of polarization in a fiber coupler is as low as about 6 degrees, resulting in very small power penalty in the DP-PNCHS.

These results suggest that the DP-PNCHS is quite feasible for low bit-rate coherent optical system because in which conventional solitary DFB lasers can be used as both transmitter and LO.

The only disadvantage of the DP-PNCHS is the requirement for polarization control to obtain two linearly orthogonally polarized lights at the receiving end. In conventional coherent systems employment of polarization diversity receiver is found to be a useful solution to the polarization problem. However, in the DP-PNCHS the polarization diversity receiver is difficult to be used because the polarization informations of light are used to perform the cancellation of laser phase noise. Therefore, some polarization control schemes have to be used.

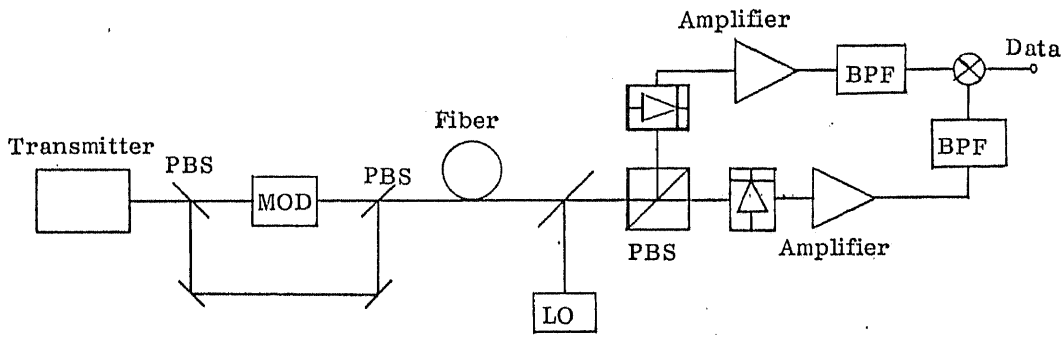

Fig. 2.1 Basic construction of the DP-PNCHS.

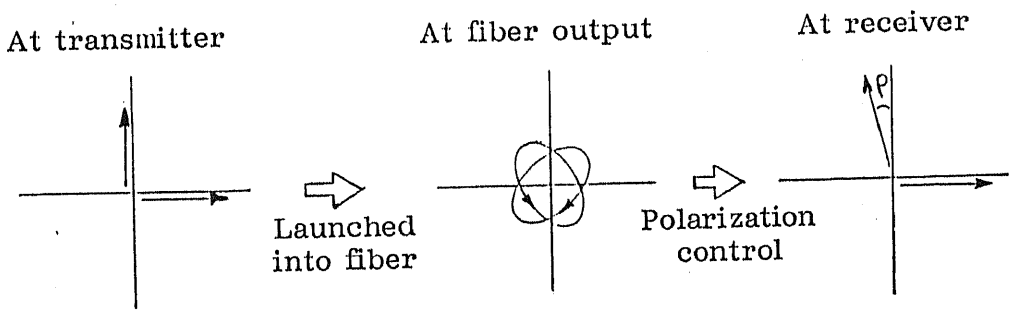

Fig. 2.2 SOP of signal lights at the transmitter and receiver of the DP-PNCHS.

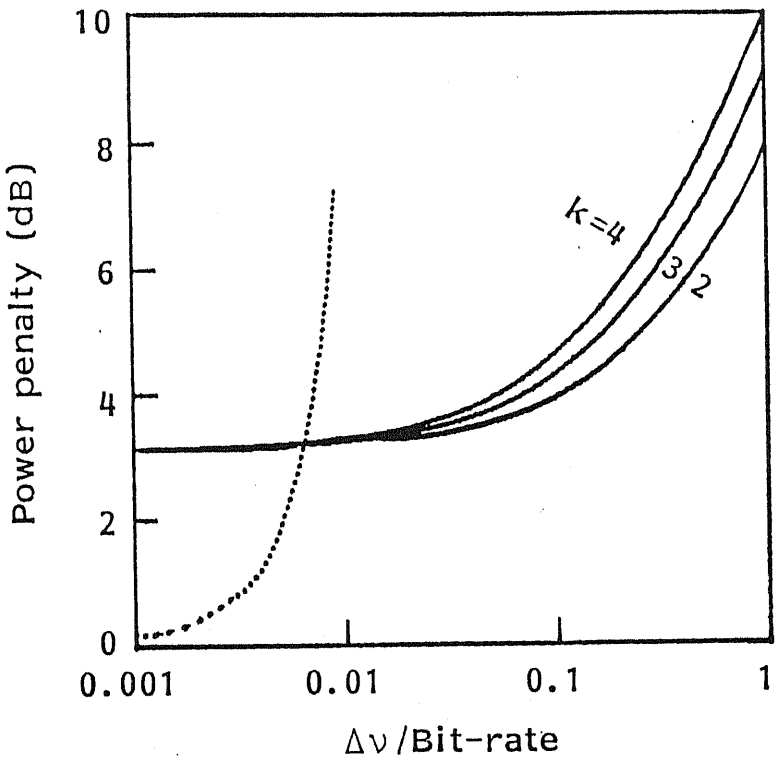

Fig. 2.3 Power-penalty comparison of the DP-PNCHS and the conventional DPSK heterodyne scheme at BER=10^{-9}.

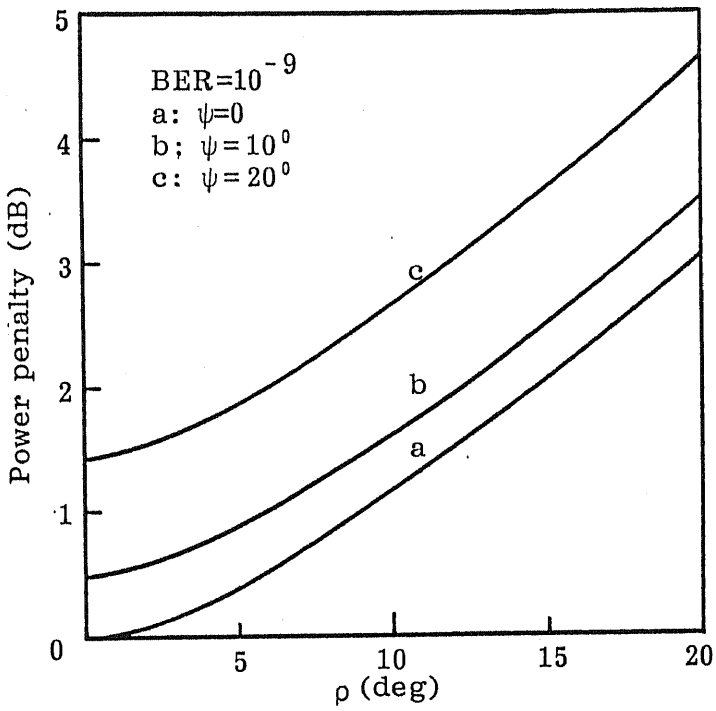

Fig. 2.4 Calculated power penalty due to the loss in orthogonality of polarization under various phase differences.

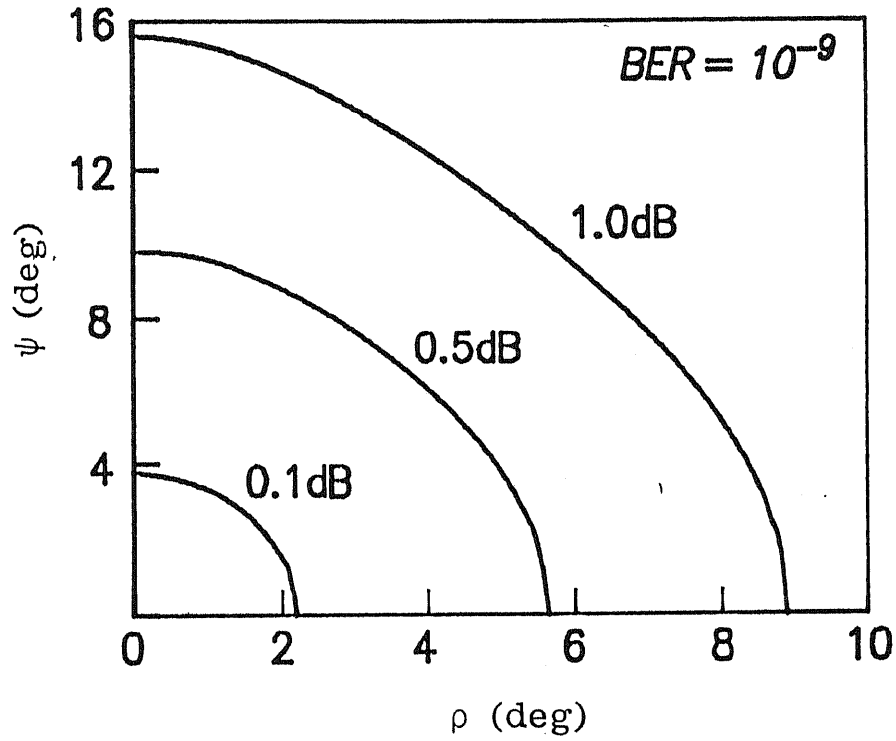

Fig. 2.5 The maximal permissible phase difference and inclination angle to achieve a power penalty below desired levels at BER=10^{-9}.

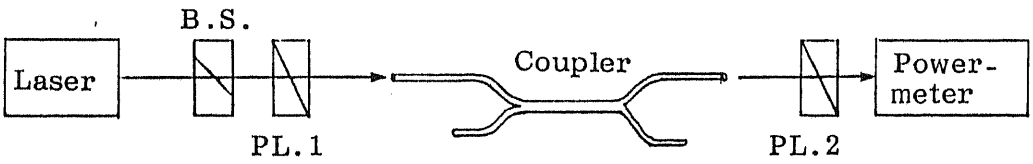

B.S.:Babinet-Soleil Compensator
PL. :Polarizer

Fig. 2.6 Experimental set-up of the measurement of orthogonality of polarization in a directional fiber coupler.

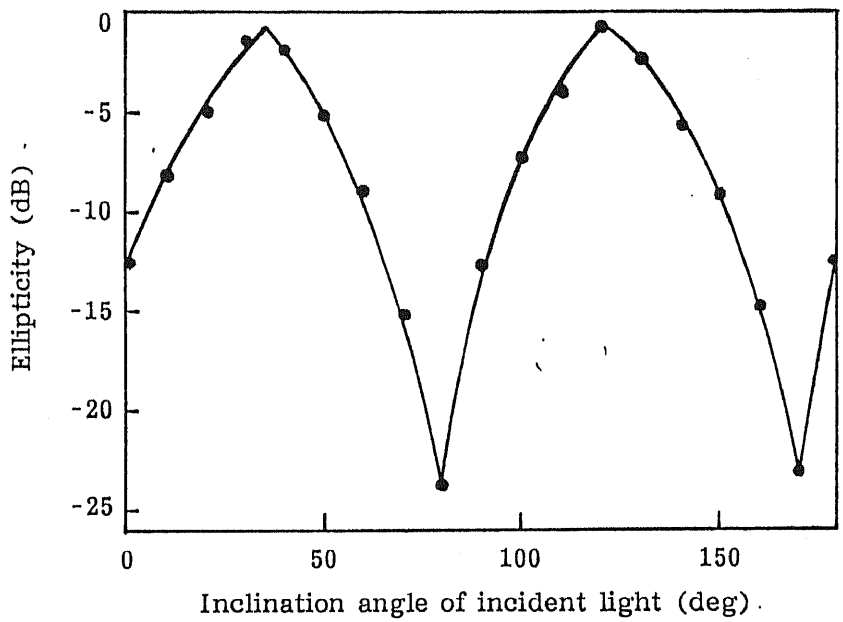

Fig. 2.7 Measured ellipticity of SOP of the output light as a function of inclination angle of the input light.

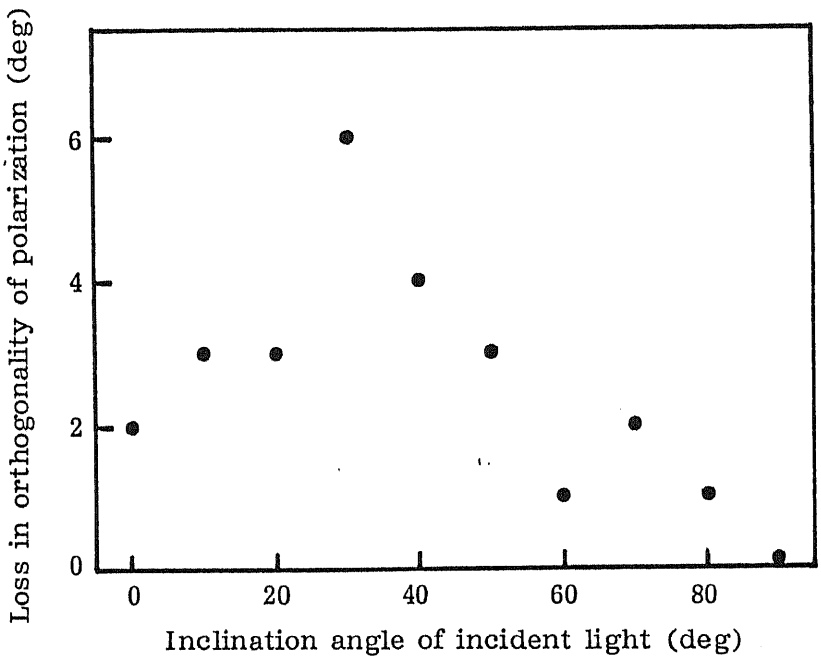

Fig. 2.8 Measured loss in orthogonality of polarization in the coupler as a function of inclination angle of the input light.

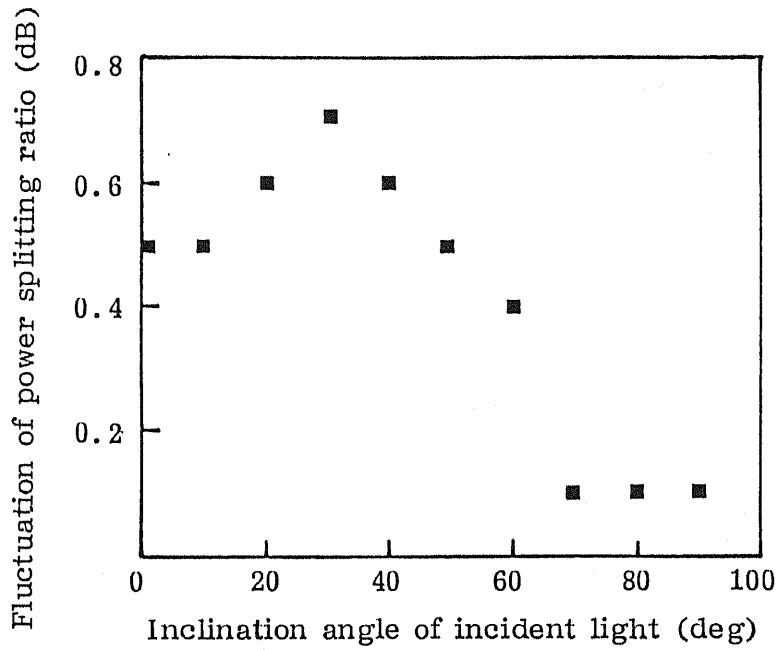

Fig. 2.9 Measured fluctuation of power splitting ratio of the coupler as a function of inclination angle of the input light.

CHAPTER 3

Dual-Frequency Phase-Noise-Canceling Heterodyne Scheme: Theoretical and Experimental Studies

Abstract

The performance of dual-frequency PNCHS (DF-PNCHS) is analyzed theoretically, and a phase noise cancellation is succeeded for the first time in experiment of BER measurement with a 20Mbit/s PSK DF-PNCHS. The theoretical results show that receiver sensitivity of the scheme is the same as that of the DP-PNCHS described in the preceding chapter. The experimental result shows that there is no appearance of so called BER floor even when the ratio of IF linewidth to bit-rate is about 1, suggesting the success of cancellation of laser phase noise. A polarization independent DF-PNCHS is also proposed and discussed. It is found that the proposed polarization diversity DF-PNCHS can be used in a low bit-rate system having small frequency separation and using a fiber with little difference in propagation delay times for two principal states.

3.1 Introduction

The DP-PNCHS described in Chapter 2 is advantageous for simple system construction, however, because the polarization-domain in which is used to achieve phase noise cancellation (that is, two separate signals are carried onto two orthogonally polarized components of light), a polarization controller is needed to compensate polarization fluctuations of signal lights, and it is difficult to use a polarization diversity receiver. On the contrary, frequency-domain PNCHS (called dual-frequency PNCHS) seems to be possible to use polarization diversity receiver. The principle of the DF-PNCHS shown in Fig.3.1 has been proposed by J.P.Dakin et al.[53], in which two carrier lights having different frequencies were used. At the receiving end the two carrier lights were mixed with LO, and detected by a photodetector. Obtained IF current was demodulated by a square-law detector after passed through a bandpass filter (BPF), generating a phase noise free second IF. However, the detailed system structure and performance of the scheme have never been investigated.

In this chapter, the performance of a PSK DF-PNCHS is investigated theoretically and experimentally. A theoretical BER formula of the scheme is given in Section 3.2. Section 3.3 describes the experimental results of BER measurement of a 20Mbit/s PSK DF-PNCHS. A polarization diversity version of the DF-PNCHS is proposed and discussed in Section 3.4, and results of this chapter are summarized in Section 3.5.

3.2 BER analysis of the DF-PNCHS

Figure 3.2 shows the detailed construction of a PSK DF-PNCHS under investigation, in which light from the transmitter laser is divided into two beams having the same intensity. One beam is frequency shifted by a

frequency shifter to $\omega_s + 2\pi\Delta f$, whereas the other is phase modulated by signal $\theta(t)$ to be transmitted. Therefore, the complex electric field amplitudes of the two beams can be expressed as

$$E_1 = \sqrt{\frac{P_s}{2}} \exp[j(\omega_s t + \theta(t) + \phi_s)] \tag{3.2.1}$$

$$E_2 = \sqrt{\frac{P_s}{2}} \exp[j(\omega_s + 2\pi\Delta f)t + j\phi_s] \tag{3.2.2}$$

where ϕ_s is phase noise of the signal laser, which is time dependent. These two beams are combined again, and launched into a fiber.

At the receiving end, after mixed with LO, two IF signals having frequencies of $\Delta\omega$ and $\Delta\omega + 2\pi\Delta f$ are obtained, and then separated by two bandpass filters (BPFs) having the bandwidths of $R_b + K\Delta\nu$ and $K\Delta\nu$ respectively, where $\Delta\omega = \omega_s - \omega_L$, ω_L is the frequency of LO, and R_b the bit-rate. The two separated IF signals are

$$I_1 = [R\sqrt{2P_sP_L} + n_1]\cos(\Delta\omega t + \Delta\phi) + n_2\sin(\Delta\omega t + \Delta\phi) \tag{3.2.3}$$

$$I_2 = [R\sqrt{2P_sP_L} + n_3]\cos[(\Delta\omega + 2\pi\Delta f)t + \Delta\phi] + n_4\sin[(\Delta\omega + 2\pi\Delta f)t + \Delta\phi] \tag{3.2.4}$$

Here $\Delta\phi = \phi_s - \phi_L$, and n_i (i=1,2,3,4) denote the shot-noise currents having zero-mean Gaussian distributions whose root-mean-square (rms) values are given as

$$\overline{n_1^2} = \overline{n_2^2} = 2eR(R_b + K\Delta\nu)P_L = \sigma_{f1}^2 \tag{3.2.5}$$

$$\overline{n_3^2} = \overline{n_4^2} = 2eRK\Delta\nu P_L = \sigma_{f2}^2 \tag{3.2.6}$$

Note that $\sigma_{f1}^2 = 2\sigma_{p1}^2$ and $\sigma_{f2}^2 = 2\sigma_{p2}^2$

The two IF signals, I_1 and I_2, are amplified and multiplied by each other to generate a second IF. The output of the multiplier is expressed as

$$I_{IF} = \frac{1}{2}[(X_1X_2 + Y_1Y_2)\cos(2\pi\Delta ft) + (Y_1X_2 - X_1Y_2)\sin(2\pi\Delta ft)] \tag{3.2.7}$$

where X_i and Y_i are defined as

$$X_1 = R\sqrt{2P_sP_L} + n_1$$
$$X_2 = R\sqrt{2P_sP_L} + n_3$$
$$Y_1 = n_2, \qquad Y_2 = n_4$$

It can be seen that the phase noise $\Delta\phi$ is canceled in Eq.(3.2.7).

In this receiver a second detector is necessary, because the output of the multiplier is not a baseband signal but an IF signal. In this case a coherent detection (or the differential detection) is advantageous and convenient, because the second IF, Δf, is equal to the frequency shifted in the transmitter and hence can be very stable. If a coherent detector is used as the second detector, the output is expressed as

$$\begin{aligned} V &= \frac{1}{4}(X_1X_2 + Y_1Y_2) \\ &= \frac{1}{16}(r_m^2 - r_n^2) \end{aligned} \tag{3.2.8}$$

where r_m and r_n are norms of corresponding 2-dimensional vectors, whose probability density function are the same as what have been described in Chapter 2. Thus BER of the scheme can be calculated in a similar way as in Chapter 2. Note that in this case $A_m^2 = 4R^2P_sP_L$, and $A_n^2 = 0$, then the BER can be given as

$$\begin{aligned} P_e &= prob.(r_m < r_n) \\ &= \int_0^\infty q_m(r_m)\int_{r_m}^\infty q_n(r_n)dr_m\,dr_n \\ &= \frac{1}{2}\exp\left(-\frac{1}{1+K\cdot\Delta\nu/R_b}\frac{N}{2}\right) \end{aligned} \tag{3.2.9}$$

which is the same as that of the DP-PNCHS. That is, the DF-PNCHS has a better sensitivity than the conventional DPSK heterodyne scheme when $\Delta\nu/R_b > 0.007$.

3.3 BER measurement of the DF-PNCHS

Since laser phase noise will cause so called "floor" (saturation of BER) to appear in BER curve, one can measure the BER curve of a system to evaluate the influence of laser phase noise. To confirm the principle of the DF-PNCHS, BER measurement is performed for a 20Mbit/s PSK DF-PNCHS for the first time.

The experimental set-up is shown in Fig.3.3. Both transmitter and LO used in the experiment are temperature controlled 1.3μm DFB lasers having linewidths of about 10MHz, so that the IF linewidth is about 20MHz. Light of the transmitting laser is split into two beams by a half-mirror. Two acousto-optic modulators (AOMs) are used in cascade to give frequency separation, Δf, of 200MHz to one beam. A $LiTaO_3$ phase modulator is used to modulate the phase of the other beam with 20Mbit/s non-return-to-zero (NRZ) format pseudorandom bit sequence (2^{15}-1), giving $\Delta\nu/R_b = 1$. Two intermediate frequencies are arranged at 500MHz and 700MHz and separated by two BPFs centered at 500MHz and 700MHz respectively. The bandwidths of both filters are 80MHz, giving K=4. The two separated IFs are amplified and multiplied by each other, generating a second IF of 200MHz, which is free from the laser phase noise.

The eye pattern obtained after demodulation and the measured BER curve (circles) are shown in Figs.3.4(a) and (b), respectively. A receiver sensitivity of -48.9dBm at BER=10^{-9} is obtained. The power penalty is about 10dB more than the estimated result (solid curve) by the theory considering the phase noise effect. However, no floor is found in the BER curve, suggesting that the laser phase noise is canceled. The appearance of power penalty of 10dB is believed to be due to imperfect phase modulation, deviation from ideal operation of the multiplier (double balanced mixer) and other electronic

circuit noise.

3.4 Polarization diversity DF-PNCHS

It is understood that in coherent optical fiber communications the fluctuation of SOP of signal lights during transmission in a fiber will cause the degradation of receiver sensitivity. So far a few polarization control schemes and polarization diversity receivers have been proposed to solve the polarization problem. Experiment results showed that the polarization diversity schemes can be used in any conventional coherent systems and are relatively practical schemes[54]-[57]. Here the possible combination of DF-PNCHS with polarization diversity receiver is discussed.

One of the possible constructions of polarization diversity DF-PNCHS proposed here is shown in Fig.3.5, in which transmitter is the same one as shown in Fig.3.2, but at receiving end the signal light transmitted by a fiber and the LO are divided into two orthogonally polarized components by a polarizing beam splitter, and then detected separately by two photodetectors. The obtained two IF signals can be expressed as

$$\begin{aligned} I_H &= R\sqrt{2P_sP_L\alpha}\cos(\Delta\omega t + \theta(t) + \Delta\phi) \\ &\quad + R\sqrt{2P_sP_L\beta}\cos(\Delta\omega t + 2\pi\Delta f t + \Delta\phi) \qquad (3.4.1) \\ I_V &= R\sqrt{2P_sP_L(1-\alpha)}\cos(\Delta\omega t + \theta(t) + \Delta\phi + \delta) \\ &\quad + R\sqrt{2P_sP_L(1-\beta)}\cos(\Delta\omega t + 2\pi\Delta f t + \Delta\phi + \eta) \qquad (3.4.2) \end{aligned}$$

where α and β are the power splitting ratios for two signal lights having different frequencies, and δ and η the corresponding phase differences between the two orthogonal polarization components. In general α, β, η and δ will change with the SOP of signal lights.

The two IFs, I_H and I_V, are then separated by two BPFs respectively, and multiplied by each other, giving

$$I_1 = R^2 2P_s P_L \sqrt{\alpha\beta}\cos(\theta(t) - 2\pi\Delta ft) \tag{3.4.3}$$

and

$$I_2 = R^2 2P_s P_L \sqrt{(1-\alpha)(1-\beta)}\cos(\theta(t) - 2\pi\Delta ft + \eta - \delta) \tag{3.4.4}$$

Note that the phase noise is canceled in Eqs.(3.4.3) and (3.4.4).

When the two signal lights experience the same polarization fluctuation in a fiber, the SOPs of the signals will become the same with each other at the fiber output, resulting in $\alpha = \beta$ and $\eta = \delta$. In this case a second IF is obtained by summing I_1 and I_2, so that

$$I = R^2 2P_s P_L \cos(\theta(t) - 2\pi\Delta ft) \tag{3.4.5}$$

which is independent of the SOPs of the two signals. This IF can be demodulated by coherent detection or differential detection to recover the data.

In general, SOPs of two signals with different frequencies are slightly different at fiber output end, because of the polarization dispersion in fiber and frequency difference between two signal lights, giving $\alpha \neq \beta$ and $\eta \neq \delta$. In this case, observing the relative positions of the SOPs of such two signals on a Poincare sphere, the SOP of one signal changes its position on the Poincare sphere within a circular area centered around the SOP of another signal. Figure 3.6 shows the possible positions of SOPs of the two signals on the Poincare sphere. The maximal angle, γ, corresponding to the maximal radius of the circular area, is expressed as

$$\gamma = 2\pi\Delta\tau\cdot\Delta f \tag{3.4.6}$$

where $\Delta\tau$ is the difference in propagation delay times for two principal states[58].

Because the fluctuation of the SOP of light is relatively slow in a fiber, η and δ can be considered to be constants in a bit period. Therefore, I_1 and I_2 can first be demodulated by differential detection, generating two baseband

signals which are free from the phase differences η and δ, and the receiver output can then be obtained by summing the two baseband signals. In this case the maximal sensitivity penalty can be calculated as

$$\begin{aligned} Penalty &= 10\cdot\log_{10}(\cos^2\gamma) \\ &= 20\cdot\log_{10}[\cos(2\pi\Delta\tau\cdot\Delta f)] \end{aligned} \tag{3.4.7}$$

It is found that the penalty due to the SOP difference between the two signals depends on the product of the difference in propagation delay times $\Delta\tau$ and frequency shift Δf. Calculated power penalty at BER=10^{-9} is shown in Fig.3.7 as a function of $(\Delta\tau\cdot\Delta f)$. It is found that $(\Delta\tau\cdot\Delta f)$ should be less than 53.5ps·GHz to achieve a power penalty below 0.5dB, and that the polarization diversity DF-PNCHS can be used in a system with a fiber having a difference in propagation delay times below 10ps and having a frequency separation of several GHz.

3.5 Conclusions

In this chapter, the performance of DF-PNCHS is investigated theoretically and experimentally, and a polarization diversity DF-PNCHS is developed and discussed. The results of BER analysis and experimental demonstration show that

(1) Receiver sensitivity of the DF-PNCHS is the same as that of the DP-PNCHS, and is better than that of the conventional DPSK heterodyne scheme when $\Delta\nu/R_b > 0.007$.

(2) Experiment result of BER measurement of a 20Mbit/s PSK DF-PNCHS shows a successful cancellation of phase noise, suggesting the feasibility of the scheme even for $\Delta\nu/R_b = 1$.

(3) The DF-PNCHS can be combined with polarization diversity receiver without causing any power penalty when two carrier lights having different frequencies experience the same polarization fluctuation in a fiber.

(4) When two carrier lights having different frequencies experience different polarization fluctuation in a fiber, the power penalty of polarization diversity DF-PNCHS will depend on the product, $\Delta\tau \cdot \Delta f$, of the difference in propagation delay times and the frequency separation between two carrier lights, and will be below 0.5dB for $\Delta\tau \cdot \Delta f < 53.5$ps·GHz.

There are several advantages for the DF-PNCHS, demand for only one photodetector, freedom from the fluctuation of laser frequency and possibility of using polarization diversity receiver. On the other hand, there are also a few drawbacks for the scheme such as requirement of a wide-band frequency shifter and an additional detection, and limited bit-rate owing to the bandwidth of frequency shifter.

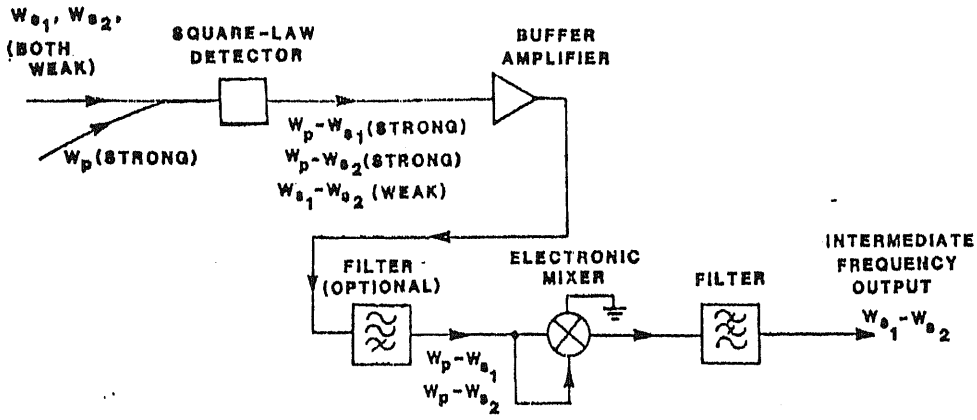

Fig. 3.1 Basic principle of the DF-PNCHS proposed by J.P.Dakin et al..

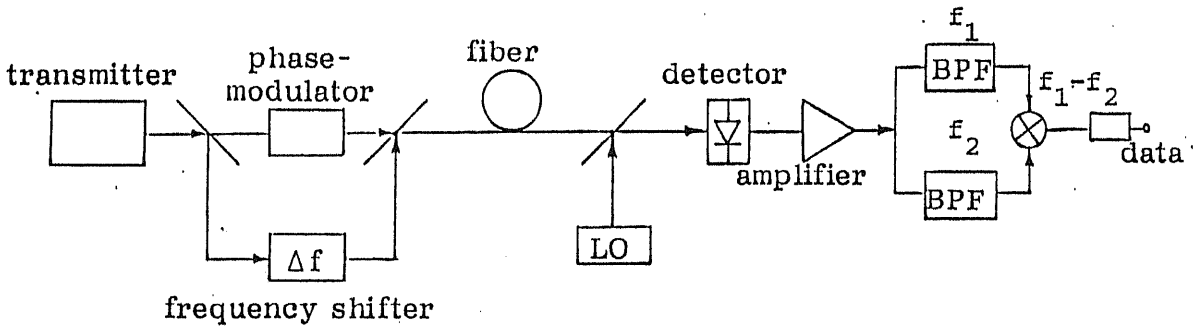

Fig. 3.2 Construction of the PSK DF-PNCHS under investigation.

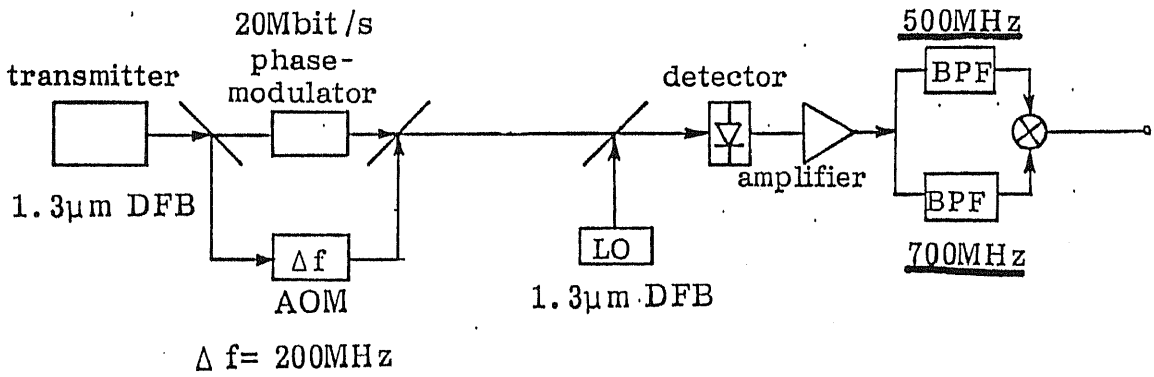

Fig. 3.3 Experimental set-up for BER measurement of a 20Mbit/s PSK DF-PNCHS.

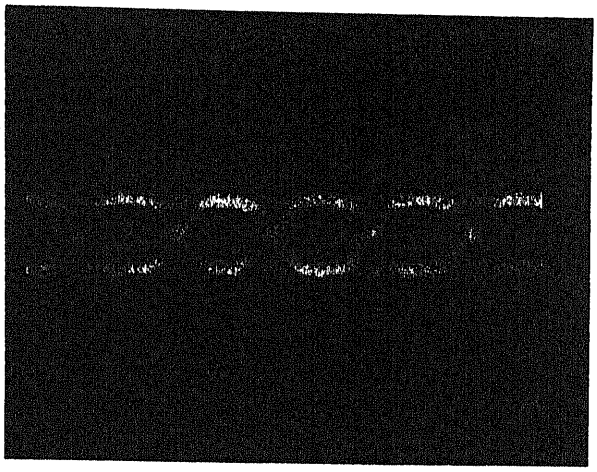

(a)

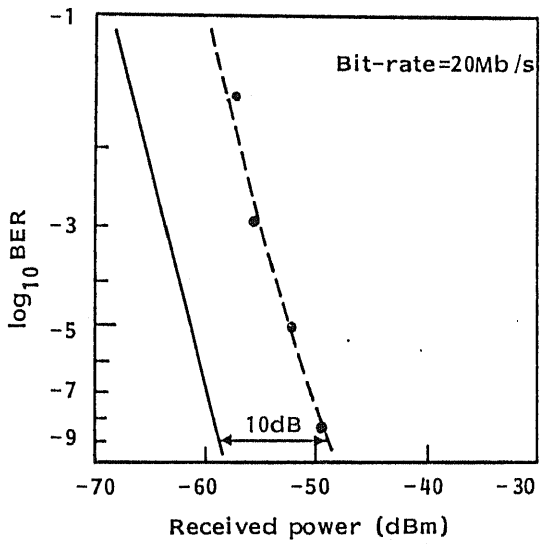

(b)

Fig. 3.4 Experimental results (a) Eye pattern of demodulated signals, (b) Measured BER curve. The solid curve shows the theoretical result for $\Delta\nu/R_b = 1$.

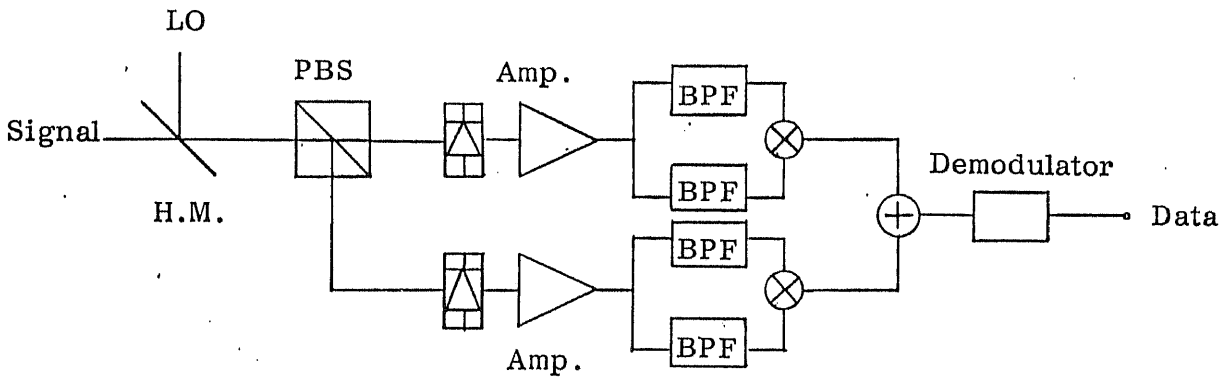

Fig. 3.5 One of the constructions of the proposed polarization diversity DF-PNCHS.

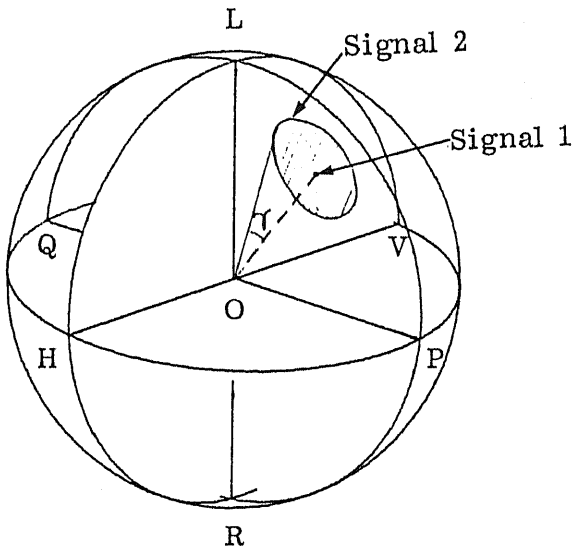

Fig. 3.6 Possible positions of SOPs of two signals having different frequencies on a Poincare sphere.

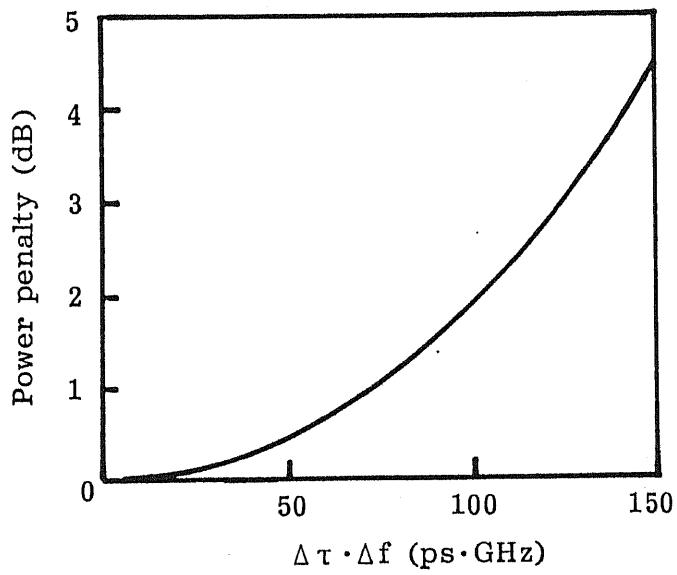

Fig. 3.7 Calculated maximal power penalty versus product ($\Delta\tau \cdot \Delta f$) at BER=$10^{-9}$.

CHAPTER 4

Dual-Waveguide Phase-Noise-Canceling Heterodyne Scheme: Proposal and Analysis

Abstract

A dual-waveguide PNCHS (DW-PNCHS) is proposed and its performance is investigated theoretically. The results of BER analysis show that the receiver sensitivity of the scheme is the same as that of the DP-PNCHS and is dependent on the propagating characteristics of waveguides. Improvements of the DW-PNCHS are also discussed to remove the influences of characteristic difference of waveguides, and of polarization fluctuations.

4.1 Introduction

Based on the principles of the DP- and the DF-PNCHSs described in Chapters 2 and 3, the common principles of PNCHSs can be summarized as follows:

(1) Two lightwave signals are transmitted separately at the transmitting end, one includes laser phase noise and information to be transmitted, while the other includes the laser phase noise only.

(2) At the receiving end, the two signals are received separately (or separated at IF stage), and are multiplied by themselves after frequency conversion. Thus obtained baseband signal will be free from the laser phase noise, because the two IF signals include the same laser phase noise which are canceled at the output of multiplier.

Following to the principle, two new types of PNCHS can be developed. One is called dual-waveguide PNCHS (DW-PNCHS) described in this chapter, and the other is call time-division PNCHS (TD-PNCHS) which will be described in next chapter.

In this chapter, the DW-PNCHS is proposed and analyzed theoretically. In Section 4.2 the performance of the scheme is analyzed, and the influence of difference of waveguide characteristics is discussed. Section 4.3 describes some improvements on the DW-PNCHS, and the results of this chapter is summarized in Section 4.4.

4.2 Analysis of the DW-PNCHS

4.2.1 Principle of the proposed DW-PNCHS

Figure 4.1 shows a basic construction of the proposed DW-PNCHS, in which a space-domain (i.e., two separate fibers) is used to achieve the phase

noise cancellation. The basic principle of the scheme is as following:

Light of the transmitter laser is split into two beams having the same intensity, one beam is phase modulated by signal $\theta(t)$ before launched into a fiber, and the other beam is directly launched into another fiber. At the receiving end, two signal lights transmitted by the two fibers are mixed with the LO lights respectively, and detected separately by two detectors. The obtained two IF signals are passed through two BPFs respectively, and multiplied by each other. If the two fibers have the same propagating characteristics, then the obtained baseband signal will become to be free from phase noise, because the two IF signals contain the same laser phase noise which can be canceled by the multiplying process.

4.2.2 BER analysis of the DW-PNCHS

Referring to Fig.4.1, the two signal lights passed through the two fibers can be expressed as

$$E_1 = \sqrt{\frac{P_s}{2}} \exp[j(\omega_s t + \theta(t) + \phi_s + \beta_1)] \tag{4.2.1}$$

$$E_2 = \sqrt{\frac{P_s}{2}} \exp[j(\omega_s t + \phi_s + \beta_2)] \tag{4.2.2}$$

where β_1 and β_2 denote the phase depending on propagating characteristics of the fibers including propagation constant, fiber length, dispersion, and so on.

As the two signal lights are mixed with the LO lights, and detected by two photodetectors, the received two IF signals passed through two BPFs can be expressed as follows, considering mark signals ($\theta(t) = 0$),

$$I_1 = (R\sqrt{P_t P_L} + n_1)\cos(\Delta\omega t + \Delta\phi + \beta_1) + n_2\sin(\Delta\omega t + \Delta\phi + \beta_1) \tag{4.2.3}$$

$$I_2 = (R\sqrt{P_t P_L}\cos\Delta\beta + n_3)\cos(\Delta\omega t + \Delta\phi + \beta_1) + (R\sqrt{P_t P_L}\sin\Delta\beta + n_4)\sin(\Delta\omega t + \Delta\phi + \beta_1) \tag{4.2.4}$$

where $\Delta\beta = \beta_1 - \beta_2$, and n_i (i=1,2,3,4) denote the shot-noise currents having

zero-mean Gaussian distributions whose root-mean-square (rms) values are given as

$$\overline{n_1^2} = \overline{n_2^2} = eR(R_b + K\Delta\nu)P_L = \sigma_{w1}^2 \tag{4.2.5}$$

$$\overline{n_3^2} = \overline{n_4^2} = eRK\Delta\nu P_L = \sigma_{w2}^2 \tag{4.2.6}$$

Note that $\sigma_{w1}^2 = \sigma_{p1}^2$ and $\sigma_{w2}^2 = \sigma_{p2}^2$.

Considering first an ideal case that the two fibers used in the system have the same propagating characteristics, then we have $\Delta\beta = 0$. Then BER can be calculated similarly as in Chapter 2 using $A_m^2 = 2R^2P_sP_L$ and $A_n^2 = 0$, and is consequently given as

$$P_e = \frac{1}{2}\exp\left(-\frac{1}{1+K\cdot\Delta\nu/R_b}\frac{N}{2}\right) \tag{4.2.7}$$

It is found that Eq.(4.2.7) is equal to Eq.(2.2.19) of Chapter 2, indicating that the DW-PNCHS has the same sensitivity as that of the DP-PNCHS.

4.2.3 Influence of phase difference $\Delta\beta$

In general, propagation constant and dispersion are different for different fibers, i.e., $\Delta\beta \neq 0$, thereby the degradation of receiver sensitivity will be caused. In this case, BER can be calculated with Eq.(2.2.12) of Chapter 2 using

$$A_m^2 = 2R^2P_sP_L\cos^2\frac{\Delta\beta}{2} \tag{4.2.8}$$

$$A_n^2 = 2R^2P_sP_L\sin^2\frac{\Delta\beta}{2} \tag{4.2.9}$$

Figure 4.2 shows the calculated power penalty due to phase difference $\Delta\beta$ at BER=10^{-9}. It is found that $\Delta\beta$ should be less than about 0.08π to confine power penalty within 1dB.

4.3 Discussion

4.3.1 Improvement of the DW-PNCHS

The theoretical results show that in the DW-PNCHS shown in Fig.4.1, the difference in propagating characteristics between two fibers used as transmission lines will cause a sensitivity penalty. Figure 4.3 shows an improved DW-PNCHS with IF shift technique[20] to remove the influence of propagating characteristics of fibers. The basic construction of the developed scheme is similar to that in Fig.4.1, but at the receiving end, one of the obtained two IFs is frequency shifted by ω_c using an electric oscillator, and an additional differential detection is used to recover the data.

Referring to Eqs.(4.2.3) and (4.2.4), by ignoring the noise terms, the received two IF signals, I_1 and I_2, are given as

$$I_1 = R\sqrt{P_s P_L}\cos(\Delta\omega t + \Delta\phi + \beta_1) \tag{4.3.1}$$

$$I_2 = R\sqrt{P_s P_L}\cos(\Delta\omega t + \theta(t) + \Delta\phi + \beta_2) \tag{4.3.2}$$

which vary with β_1 and β_2.

In the scheme proposed here, the frequency $\Delta\omega$ of I_1 is shifted to $\Delta\omega + \omega_c$ using an electric local oscillator and a double balanced mixer. Thus a second IF signal I_{IF} can be obtained, after multiplying I_1 with I_2, as

$$I_{IF} = R^2 P_s P_L \cos(\omega_c t + \theta(t) + \Delta\beta). \tag{4.3.3}$$

This second IF signal is then demodulated by a differential detection to recover the data. Since the fluctuations of β_1 and β_2 are negligibly small in bit interval, the obtained baseband signal of the receiver becomes independent of $\Delta\beta$.

4.3.2 Polarization diversity DW-PNCHS

As described in Chapter 3, It is desired to combine PNCHS with polarization diversity receiver to remove the effect of fluctuations of SOP of signal lights. Possibility for realizing of polarization diversity DW-PNCHS is discussed here.

A possible structure of the polarization diversity DW-PNCHS is shown in Fig.4.4, in which two signal lights transmitted from two fibers are separated into a horizontally and a vertically polarized component by two polarizing beam splitters respectively. Obtained four beams are mixed with LO lights and detected separately by four photodetectors. Assuming that the two fibers have identical propagating characteristics, and ignoring the noise terms, obtained four IF currents can be expressed as

$$I_{1H} = R\sqrt{P_s P_L\ \alpha}\cos(\Delta\omega t + \theta(t) + \Delta\phi) \tag{4.3.4}$$

$$I_{1V} = R\sqrt{P_s P_L\ (1-\alpha)}\cos(\Delta\omega t + \theta(t) + \Delta\phi + \delta) \tag{4.3.5}$$

$$I_{2H} = R\sqrt{P_s P_L\ \beta}\cos(\Delta\omega t + \Delta\phi) \tag{4.3.6}$$

$$I_{2V} = R\sqrt{P_s P_L\ (1-\beta)}\cos(\Delta\omega t + \Delta\phi + \eta) \tag{4.3.7}$$

where α and β are power splitting ratios of polarizing beam splitters for two signals transmitted from different fibers, and δ and η are the corresponding phase differences.

Considering an ideal case that the two signal lights experience the same fluctuations of SOP, then the SOP of the two signal lights become to be identical at the fiber output, bringing on $\alpha = \beta$ and $\delta = \eta$. In this case, the four IF currents can be processed as $(I_{1H}\ I_{2H} + I_{1V}\ I_{2V})$ leading to a baseband signal

$$I = R^2 P_s P_L\ \cos\theta(t) \tag{4.3.8}$$

which is independent of both laser phase noise and fluctuation of SOP of signal lights.

However, it is predicted that the SOPs of lights launched into different fibers will be different at the fiber output end, because of the difference in polarization dispersion and birefringence of fibers, resulting in that $\alpha \neq \beta$ and $\delta \neq \eta$. In this case, some extent of degradation of receiver sensitivity will be caused as described in Chapter 3. Therefore, the polarization diversity DW-PNCHS can only be used in a special case that two signal lights transmitted from two fibers are identical in SOP.

4.4 Conclusions

In this chapter, a DW-PNCHS is proposed and analyzed theoretically, and a polarization diversity DW-PNCHS is also discussed. Theoretical results show that receiver sensitivity of the scheme is equal to that of the DP-PNCHS, and is dependent on the propagating characteristics of fibers used as transmission lines. The difference in propagating characteristics of fibers will cause degradation of receiver sensitivity, and should be less than 0.08π to confine penalty within 1dB. This problem can be solved by using an IF shift technique. And an improved DW-PNCHS to remove the influence of non-identification of waveguides is also proposed and discussed.

The DW-PNCHS can be combined with polarization diversity receiver, provided that SOPs of two lightwaves experience the same fluctuations during the propagation in two different fibers. However, in general it is predicted that SOP of lightwaves is separately fluctuated in different fibers when the fibers have different birefringences and polarization dispersions, so that the polarization diversity DW-PNCHS will be confined to special use.

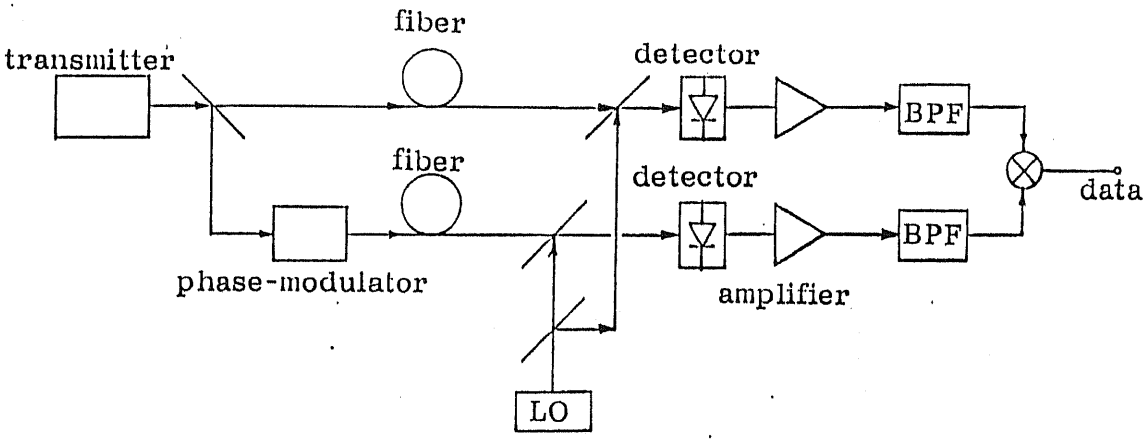

Fig. 4.1 Basic construction of the proposed DW-PNCHS.

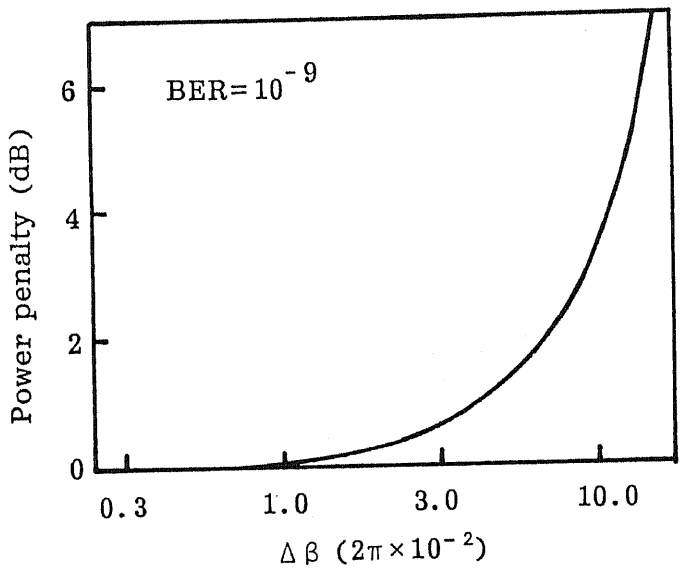

Fig. 4.2 Calculated power penalty due to phase difference $\Delta\beta$ at BER=10^{-9}.

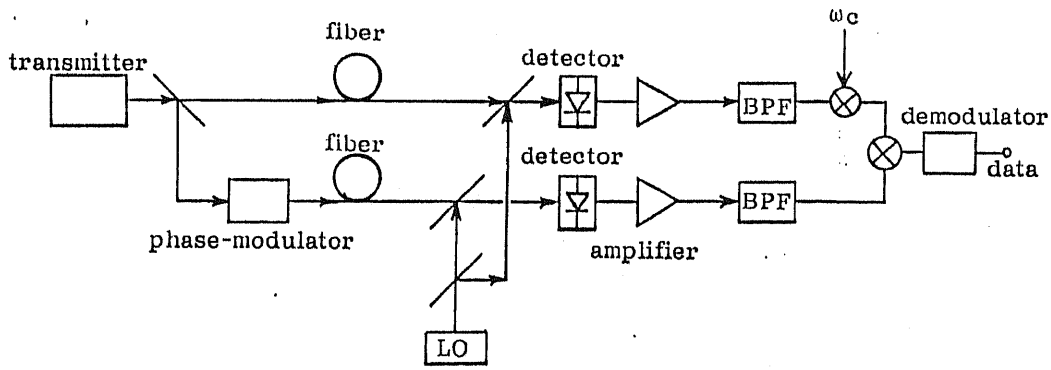

Fig. 4.3 Basic construction of the proposed improved DW-PNCHS to remove the influence of phase noise $\Delta\beta$ due to non-identification of fibers.

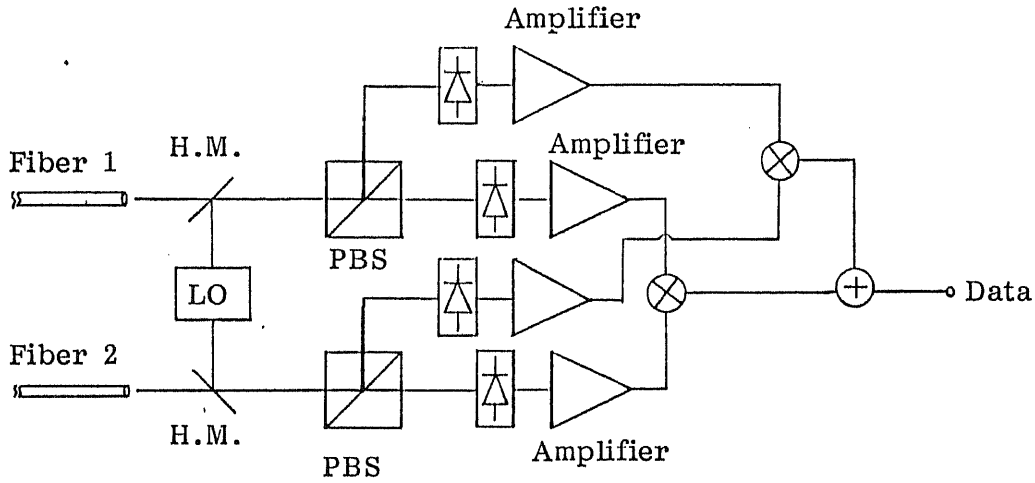

H.M. : Half mirror

PBS : Polarizing beam splitter

Fig. 4.4 Basic construction of a polarization diversity DW-PNCHS.

CHAPTER 5

Time-Division Phase-Noise-Canceling Heterodyne Scheme: Theory and Experiment

Abstract

A time-division PNCHS (TD-PNCHS) is proposed and investigated theoretically and experimentally. The theoretical results show that the scheme has better sensitivity than the conventional DPSK heterodyne scheme when IF linewidth is larger than 0.009 times bit-rate, and that the difference in optical path lengths (delay times) will cause degradation of receiver sensitivity. A polarization diversity TD-PNCHS is also proposed and discussed. It is found that the TD-PNCHS can be combined with polarization diversity receiver without causing extra any power penalty. The results of experiment by an electronic simulation model show a successful cancellation of laser phase noise, suggesting the feasibility of the scheme.

5.1 Introduction

In the preceding three chapters, three types of PNCHS are investigated. It is found that although the DP-PNCHS is advantageous for its simple system construction, there is difficulty for introduction of polarization diversity receiver into it, and that the DF-PNCHS can be conditionally combined with polarization diversity receiver, but it needs wider bandwidth than conventional heterodyne schemes, which is undesirable in multichannel systems. On the other hand, the DW-PNCHS has an advantage of simple structure, but for which two fibers of the same propagating characteristics are required, and it also has the problem of polarization control. Therefore, a new type of PNCHS needs to be established, which is suitable for using in multichannel coherent systems and is possible to be combined with polarization diversity receiver.

In this chapter, a time-domain PNCHS (called time-division PNCHS: TD-PNCHS) is proposed and investigated theoretically and experimentally. In Section 5.2, the basic principle of the scheme is described, and its performance is analyzed. Section 5.3 develops a polarization diversity TD-PNCHS. The results of experiment by an electronic simulation model of the scheme are discussed in Section 5.4, and a summary of this chapter is given in Section 5.5.

5.2 Analysis of the TD-PNCHS

5.2.1 Principle of the TD-PNCHS

One of the constructions of the proposed TD-PNCHS is shown in Fig.5.1, in which light of the transmitter laser is ON-OFF switched (or intensity modulated) by an optical switch (or an amplitude modulator) with a

switching signal of frequency, f_s, and is then divided into two beams. One beam is phase-modulated by a phase modulator, whereas to the other a delay time of $\frac{1}{2f_s}$ (=T) is applied.

At the receiving end, the signals transmitted by a fiber are divided first into two beams by a switch synchronized with the switch in the transmitter. Then a delay time T is given to one of the beams which was not delayed at the transmitter, so that the obtained two beams contain the same phase noise. These two beams are mixed with LO lights and heterodyne-detected separately. The obtained two IFs are amplified and multiplied by each other. Thus a phase noise free baseband signal can be generated because the two IFs contain the same phase noise. Figure 5.2 shows the schematic diagram of the transmitted and received signals.

5.2.2 BER analysis of the TD-PNCHS

Referring to Figs.5.1 and 5.2, the electric field complex amplitudes of the two beams at the transmitting end are expressed as

$$E_1 = \sqrt{\frac{P_s}{2}} \exp[j(\omega_s t + \theta(t) + \phi_s(t))] \tag{5.2.1}$$

$$E_2 = \sqrt{\frac{P_s}{2}} \exp[j(\omega_s (t + \tau_1) + \phi_s(t + \tau_1))] \tag{5.2.2}$$

where τ_1 is the delay time applied to one of the beam at the transmitting end. In general, $\tau_1 = T$ is chosen to be equal to T, and $T = \frac{1}{R_b}$. The two beams are combined again and transmitted into a fiber.

At the receiving end, the transmitted signal light is divided into two beams by another optical switch synchronized with the switch in the transmitter, and a delay time τ_2 is given to beam E_1 which is not delayed at the transmitting end, thus

$$E_1' = \sqrt{\frac{P_s}{2}} \exp[j(\omega_s(t + \tau_2) + \theta(t) + \phi_s(t + \tau_2))] \tag{5.2.3}$$

Then the two beams, E_1 and E_1', are mixed with LO lights and heterodyne-detected. Considering mark signals ($\theta(t) = 0$), the output photocurrents are expressed as

$$\begin{aligned} I_1 &= (R\sqrt{P_s P_L} + n_1)\cos(\Delta\omega t + \omega_s\tau_2 + \Delta\phi_s) \\ &\quad + n_2 \sin(\Delta\omega t + \omega_s\tau_2 + \Delta\phi_s) \end{aligned} \tag{5.2.4}$$

$$\begin{aligned} I_2 &= [R\sqrt{P_s P_L}\cos(\omega_s\Delta\tau + \Delta\phi) + n_3]\cos(\Delta\omega t + \omega_s\tau_2 + \Delta\phi_s) \\ &\quad + [R\sqrt{P_s P_L}\sin(\omega_s\Delta\tau + \Delta\phi) + n_4]\sin(\Delta\omega t + \omega_s\tau_2 + \Delta\phi_s) \end{aligned} \tag{5.2.5}$$

where $\Delta\tau = \tau_1 - \tau_2$ and $\Delta\phi_s = \phi_s(t+\tau_2) - \phi_s(t+\tau_1)$, and n_i (i=1,2,3,4) denote the shot-noise currents having zero-mean Gaussian distributions whose root-mean-square (rms) values are given as

$$\overline{n_1^2} = \overline{n_2^2} = 2eR(R_b + K\Delta\nu)P_L = \sigma_{t1}^2 = 2\sigma_{p1}^2 \tag{5.2.6}$$

and

$$\overline{n_3^2} = \overline{n_4^2} = 2eRK\Delta\nu P_L = \sigma_{t2}^2 = 2\sigma_{p2}^2 \tag{5.2.7}$$

These two IFs are amplified and multiplied by each other, and the resulted output can be expressed as

$$V = \frac{1}{2}(X_1X_2 + Y_1Y_2) \tag{5.2.8}$$

where X_i and Y_i (i=1,2) are defined as

$$X_1 = R\sqrt{P_s P_L} + n_1 \tag{5.2.9}$$

$$Y_1 = n_2 \tag{5.2.10}$$

$$X_2 = R\sqrt{P_s P_L}\cos(\omega_s\Delta\tau + \Delta\phi) + n_3 \tag{5.2.11}$$

$$Y_2 = R\sqrt{P_s P_L}\sin(\omega_s\Delta\tau + \Delta\phi) + n_4 \tag{5.2.12}$$

It should be noted that when the delay times at the transmitter and the receiver are equal to each other (i.e., $\tau_1 = \tau_2$), then $\Delta\tau = 0$ and $\Delta\phi_s = 0$, giving $A_m^2 = 2R^2P_sP_L$ and $A_n^2 = 0$. In this case laser phase noise will be perfectly

canceled according to Eq.(5.2.8), and BER of the scheme can be calculated similarly as done in Section 2.2.1 of Chapter 2, and consequently

$$P_e = \frac{1}{2}\exp\left(-\frac{1}{1+K\cdot\Delta\nu/R_b}\frac{N}{4}\right) \tag{5.2.13}$$

It is found that receiver sensitivity of the TD-PNCHS exhibits 3dB penalty compared with other three types of PNCHS. This is because that only half the time slot (in other words, half power) can be used to transmit the signals. Figure 5.3 shows calculated power penalty at BER=10^{-9} as a function of the ratio of IF linewidth to bit-rate. The broken curve shows the result for the conventional DPSK heterodyne receiver. It is found that the receiver sensitivity of the TD-PNCHS is better than that of the conventional DPSK receiver when $\Delta\nu/R_b>0.009$.

5.2.3 Influence of delay time difference

In general, it is difficult to adjust the delay times to be exactly equal (i.e., τ_1 is not equal to τ_2), so that the laser phase noise can not be perfectly canceled, then degradation of the receiver sensitivity will be caused. In this case, the BER of the scheme can be calculated similarly as in Section 2.2.2 of Chapter 2 using

$$A_m^2 = 2R^2P_sP_L\cos^2\left(\frac{\omega_s\Delta\tau+\Delta\phi}{2}\right) \tag{5.2.14}$$

and

$$A_n^2 = 2R^2P_sP_L\sin^2\left(\frac{\omega_s\Delta\tau+\Delta\phi}{2}\right) \tag{5.2.15}$$

Figure 5.4 shows calculated power penalty at BER=10^{-9} as a function of $\omega_s\Delta\tau$, where $\Delta\phi$ is assumed to be 0. It is found that $\omega_s\Delta\tau$ for a power penalty of 1dB is about 4%.

Above mentioned theoretical results show that fluctuations of the optical path lengths and the optical delays should be less than 0.006 times one wavelength. But, in a practical system it is difficult to adjust the optical path lengths and optical delay so exactly. This problem can be solved by adopting the IF-shift technique described in the preceding chapter[59].

5.3 Polarization diversity TD-PNCHS

As described in Chapter 3, it is desired to combine PNCHS with polarization diversity receiver to remove sensitivity degradation due to polarization fluctuations. In this section, a polarization diversity TD-PNCHS is proposed, and its performance is discussed.

One of the possible constructions of the polarization diversity TD-PNCHS to be proposed is shown in Fig. 5.5, in which the transmitter is the same one as shown in Fig. 5.1, but at the receiving end the signal light transmitted by a fiber is divided into two orthogonally polarized components by a polarizing beam splitter, and the two beams are then received separately by two receivers similar to those in Fig. 5.1. Assuming that the delay times are equally adjusted, by ignoring the noise terms, the obtained four IF signals can be expressed as

$$I_{H1} = R\sqrt{P_s P_L \alpha}\cos(\Delta\omega t + \theta(t) + \Delta\phi) \tag{5.3.1}$$

$$I_{H2} = R\sqrt{P_s P_L \alpha}\cos(\Delta\omega t + \Delta\phi) \tag{5.3.2}$$

$$I_{V1} = R\sqrt{P_s P_L (1-\alpha)}\cos(\Delta\omega t + \theta(t) + \Delta\phi + \delta) \tag{5.3.3}$$

$$I_{V2} = R\sqrt{P_s P_L (1-\alpha)}\cos(\Delta\omega t + \Delta\phi + \delta) \tag{5.3.4}$$

where α is the power splitting ratio of the polarizing beam splitter, and δ the phase difference between the two polarization components. In general, α and δ will change with the SOP of signal lights.

These four IFs are then amplified and multiplied by each other, giving

$$I_1 = R^2 P_s P_L \alpha \cos(\theta(t)) \tag{5.3.5}$$

and

$$I_2 = R^2 P_s P_L (1-\alpha) \cos(\theta(t)) \tag{5.3.6}$$

Note that laser phase noise is canceled in Eqs.(5.3.5) and (5.3.6).

The data can be recovered by summing I_1 and I_2, giving

$$I = R^2 P_s P_L \cos(\theta(t)) \tag{5.3.7}$$

which is independent of the fluctuation of SOP of the signal light.

5.4 BER measurement of an electronic simulation model of the TD-PNCHS

To confirm the principle of the proposed TD-PNCHS, BER of the scheme is measured with an electronic simulation model of the TD-PNCHS. The experimental set-up is shown in Fig.5.6, in which a noise-contained carrier is generated by adding Gaussian noise from a noise generator to FM input of a wideband voltage controlled oscillator (VCO). Figure 5.7 shows the output spectral of the noise generator used in the experiment. The linewidth of the carrier can be adjusted by changing the input voltage applied on the VCO. In Fig.5.8 photographs of spectrum of carriers with different linewidths are shown. The maximal linewidth of about 1MHz can be obtained.

In the experiment, the carrier is first ON-OFF switched by a sequence of 10001000... with bit-rate of 20Mbit/s, and divided into two parts. One is phase modulated by '101010...' signals of 5Mbit/s, and the other is delayed by 50ns (bit period) using a coaxial cable. The power spectral of the phase modulated carrier is shown in Fig.5.9, it can be seen that it is noisy. Then the

obtained two signals are combined again and detected at the receiving end. Figure 5.10 shows the waveform of the combined signals.

At the receiving end, the transmitted signals are divided into two part, one of which is delayed by 50ns using another coaxial cable. The two signals are then amplified and multiplied by each other, generating a phase noise free baseband signal which is inputted to the BER measurement equipment.

For comparison, BER of a conventional DPSK scheme of 20Mbit/s is first measured using carriers with different linewidths. Figure 5.11 shows measured BER curves as a function of the ratio of signal to noise (S/N), in which solid inverse-triangles show the results for the DPSK system with IF linewidth of about 350kHz, and solid squares show that with IF linewidth of about 250kHz. It is found that floor appeared in the BER curves, because of the large phase noise.

Previous analyses show that in the DPSK heterodyne system, the BER floor can be given as[60],[61]

$$P_{floor} = \frac{1}{2} erfc\left[\frac{1}{4}\sqrt{\frac{\pi}{\Delta\nu T}}\right] \qquad (5.4.1)$$

where T is equal to bit period. Figure 5.12 shows the calculated and measured BER floors as functions of $\Delta\nu T$. It is found that the measured results is agreed well with the theoretical prediction.

The measured BER for the electronic simulation model of TD-PNCHS is shown in Fig.5.11 by solid circles, where the IF linewidth is about 1MHz. It is found that there is no BER floor, suggesting that the phase noise is canceled.

5.5 Conclusions

In this chapter, TD-PNCHS is proposed and investigated theoretically and experimentally, and a polarization diversity TD-PNCHS is also developed. It is found from the results that the receiver sensitivity of the TD-PNCHS is better than that of the conventional DPSK heterodyne receiver when the ratio of IF linewidth to bit-rate is larger than 0.009, and it is 3dB lower than other three types of PNCHS. Delay time difference at the transmitter and receiver should be less than 4% of the frequency of signal light to suppress the power penalty below 1dB, and the influences of fluctuation of optical path lengths and switching instability of optical switch can be removed by using the IF shifting technique. The TD-PNCHS can be combined with polarization diversity receiver without penalty. Simulated experiment of BER measurement of a 20Mbit/s PSK TD-PNCHS proves the successful cancellation of phase noise, suggesting the feasibility of the scheme.

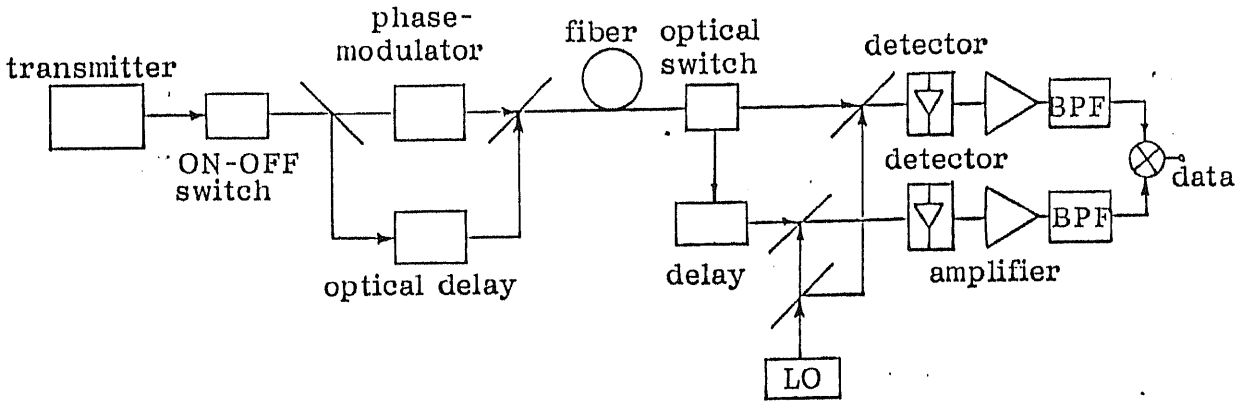

Fig. 5.1 Construction of the proposed TD-PNCHS.

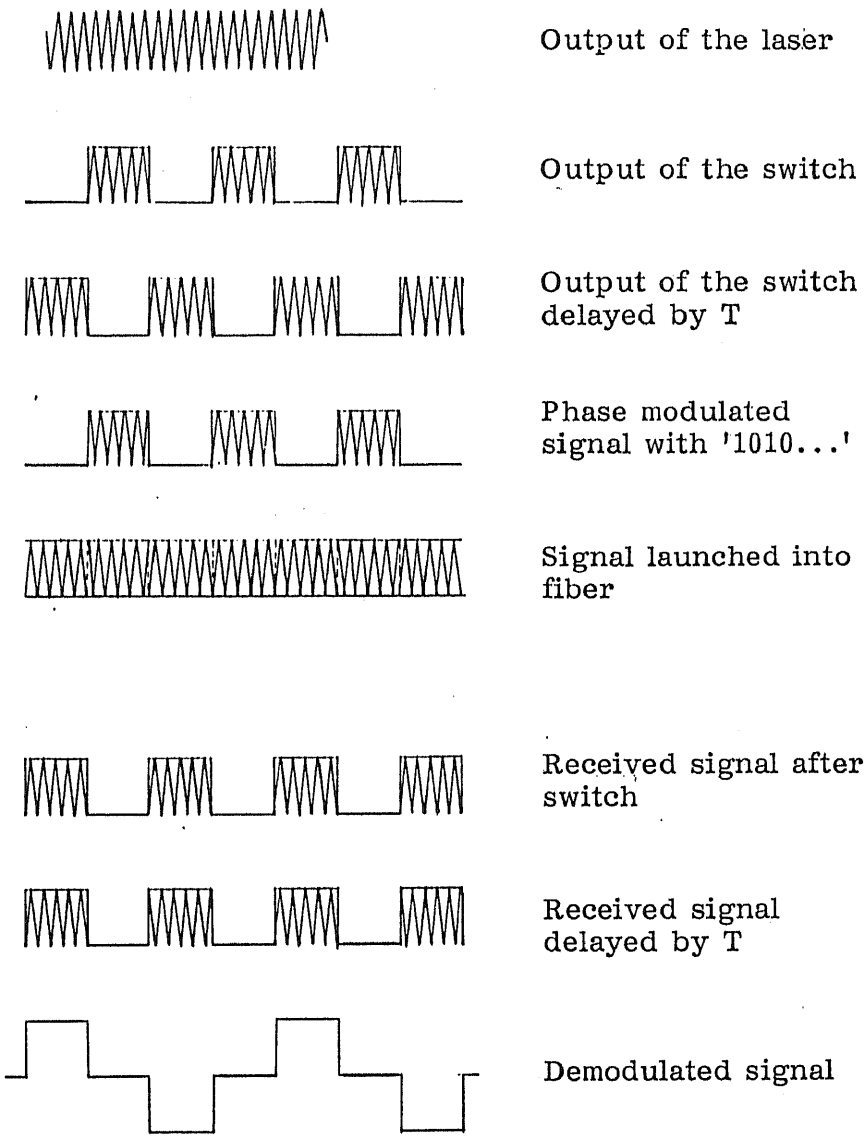

Fig. 5.2 Schematic diagram of the transmitted and received signals.

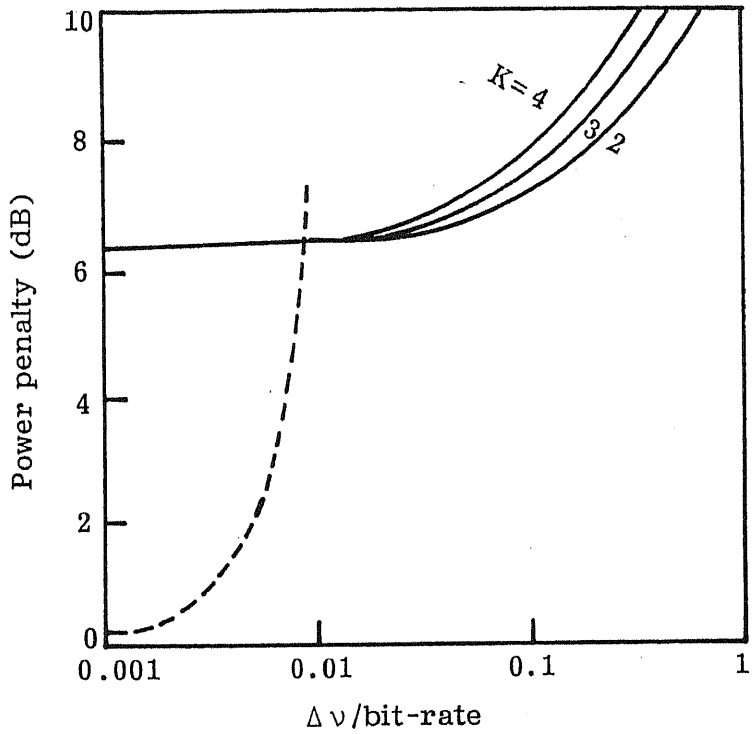

Fig. 5.3 Calculated power penalty at BER=10^{-9} as a function of the ratio of IF linewidth to bit-rate, under various values of K. Similar result for the conventional DPSK heterodyne receiver is shown in the broken curve for comparison.

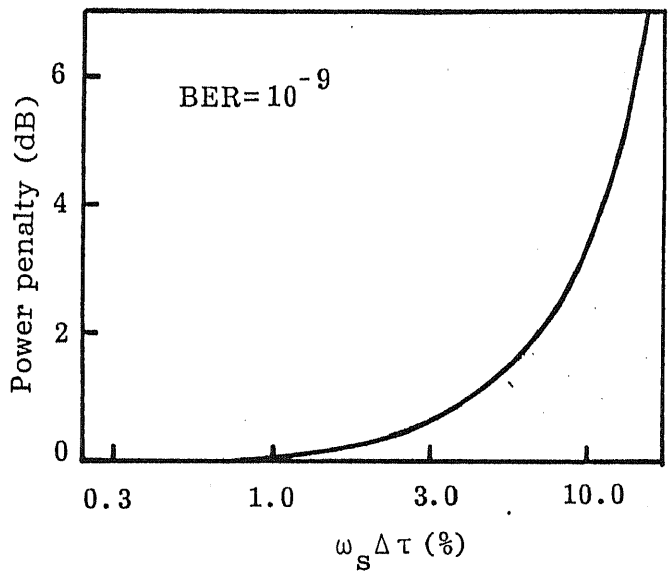

Fig. 5.4 Calculated power penalty as a function of ($\omega_s \Delta\tau$) at BER=10^{-9}.

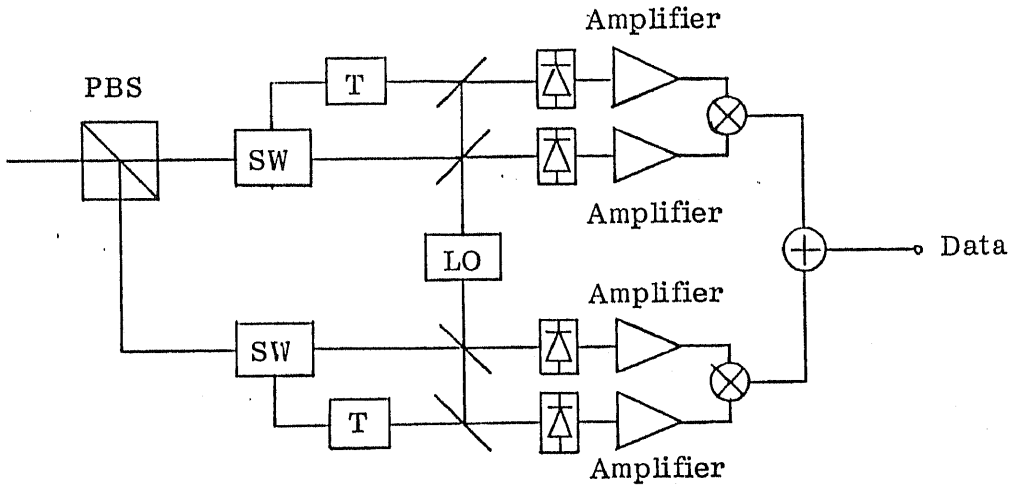

SW : Optical switch

T : Optical delay time

Fig. 5.5 Construction of the proposed polarization diversity TD-PNCHS.

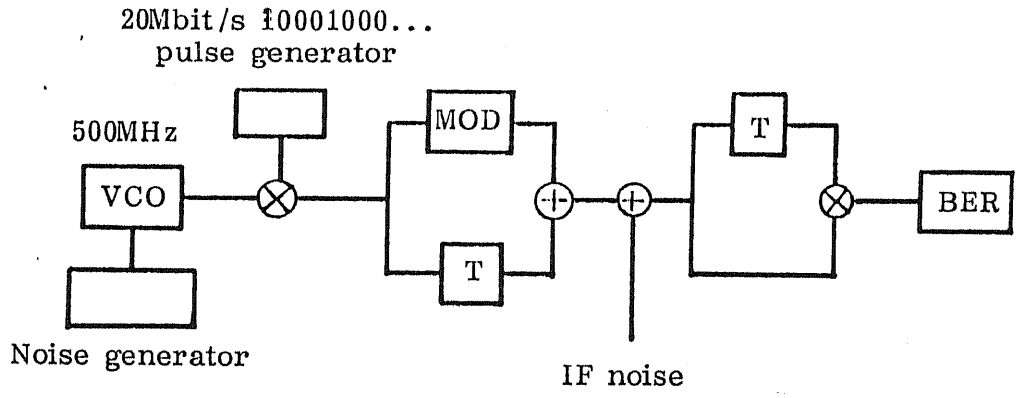

Fig. 5.6 Experiment set-up for BER measurement of the electronic simulation model of the TD-PNCHS.

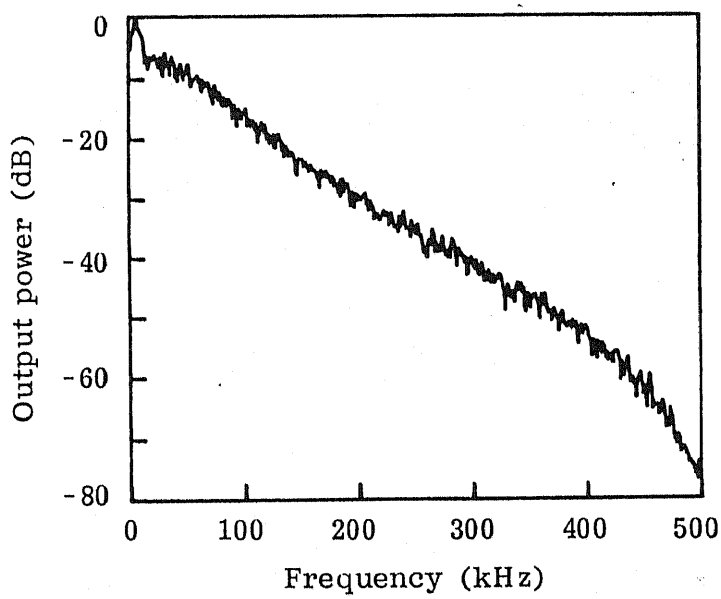

Fig. 5.7 Output spectral of the noise generator used in the experiment.

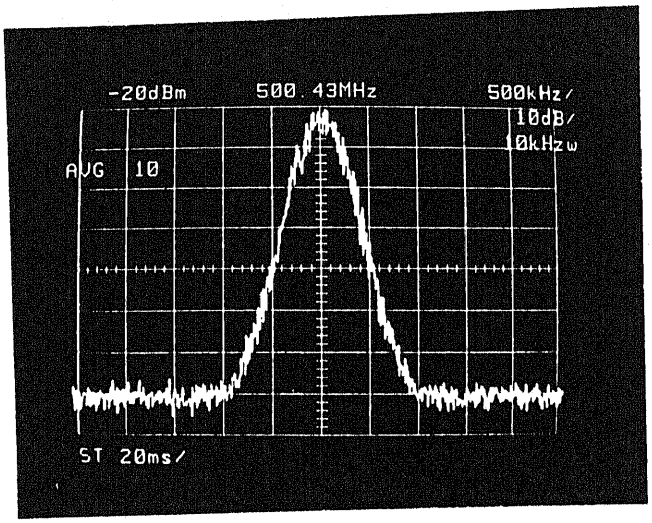

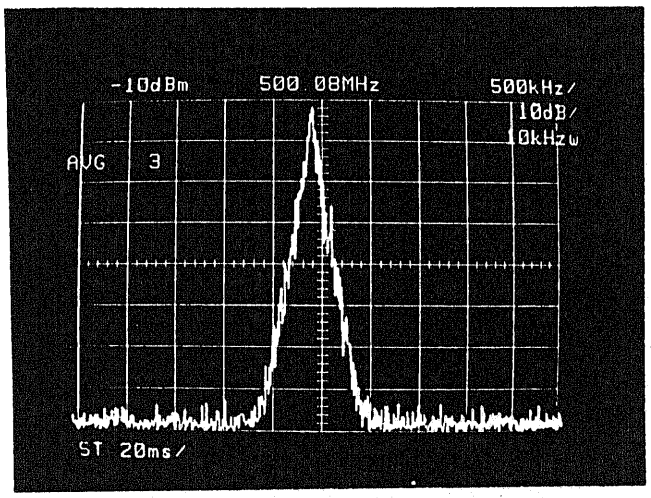

Fig. 5.8 Photographs of spectrum of the carrier with different linewidths.

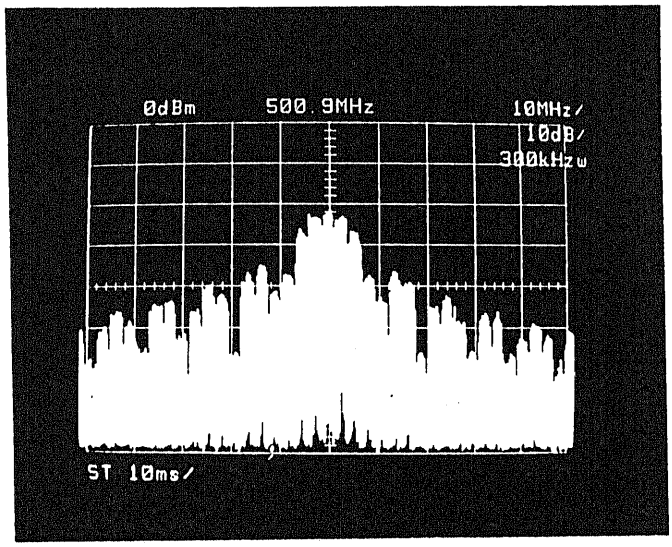

Fig. 5.9 Power spectral of phase modulated carrier with 5Mbit/s '101010...' patterns.

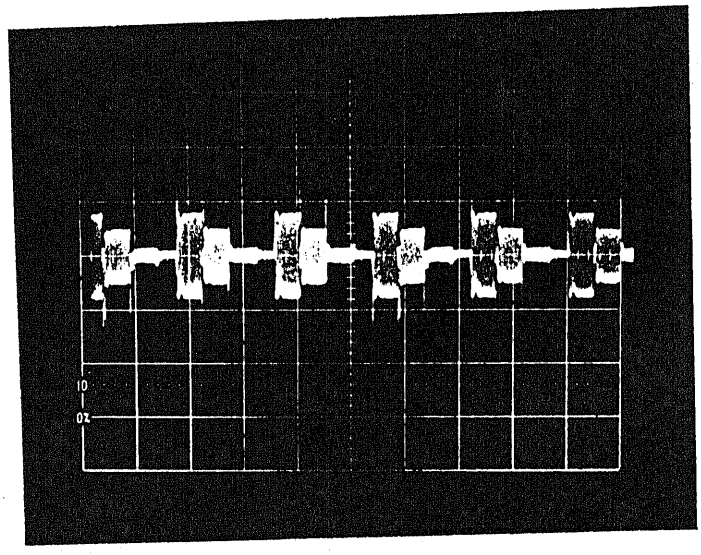

Fig. 5.10 Waveform of combined signals at the transmitting end.

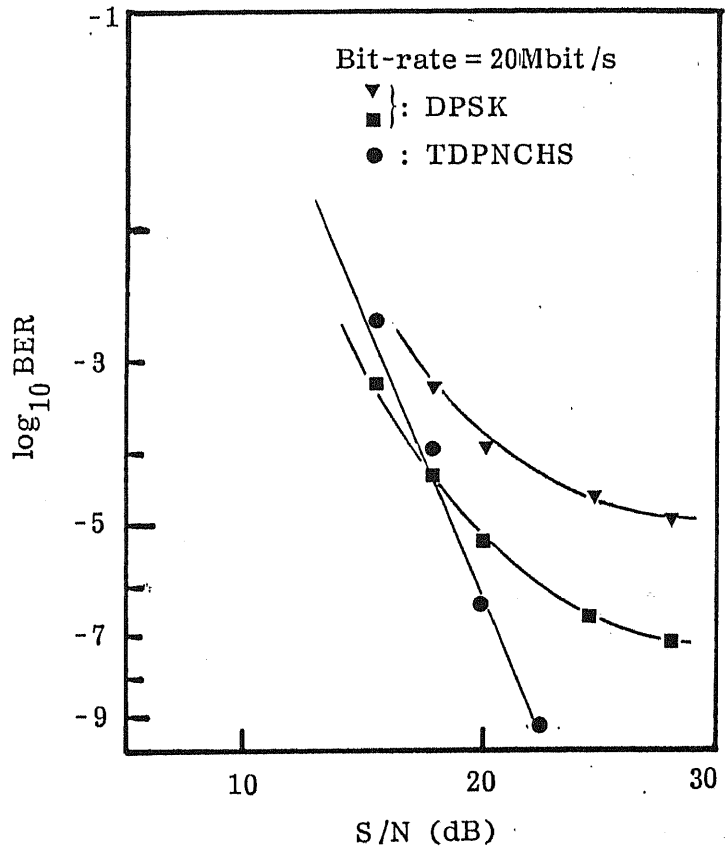

Fig. 5.11 Measured BER curves as functions of the ratio of signal to noise (S/N), among them the solid triangles show the results for DPSK system with IF linewidth of about 350kHz, the solid squares that with IF linewidth of about 250kHz and the solid circles that for the TD-PNCHS with IF linewidth of about 1MHz.

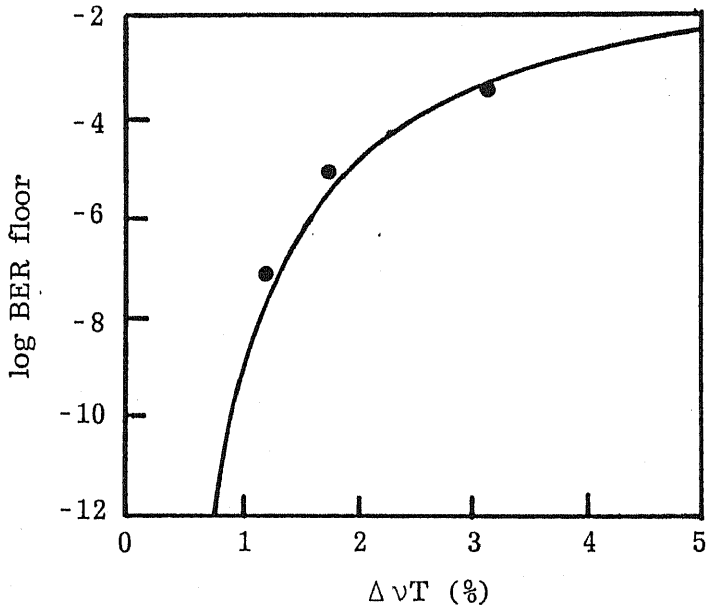

Fig. 5.12 Calculated and measured BER floors as functions of $\Delta\nu T$.

CHAPTER 6

Multichannel Coherent Optical Fiber Communication Systems

Abstract

Crosstalks caused by excess shot noise and by image-band interference in multichannel coherent optical fiber communication systems are investigated theoretically. It is found that the sensitivity penalty caused by excess shot noise is dependent on LO power, and that when a typical LO power of 1mW is used the permissible bit-rate and channel number for a penalty of 0.1dB are 2Gbit/s and 500 respectively. On the other hand, the crosstalk due to image-band interference is dependent on modulation scheme, laser linewidth, type of IF filter, pulse shape and bandwidth of IF filter. In an idealized phase noise free system, ASK and PSK systems require larger channel spacing than FSK systems, and ASK and PSK systems have similar crosstalk induced penalty. In addition, the existence of laser phase noise causes an increase of the crosstalk induced penalty, and FSK system is more sensitive to laser phase noise than ASK and PSK systems. It is also found that the crosstalk induced penalty can be significantly reduced by choosing a proper type of pulse as signal pulse. The calculated results based on the present theory show good agreements with the experimental results reported by others, suggesting the validity of the theory.

6.1 Introduction

The feasibility of single-channel coherent optical communications has been proved by many systematical experiments, and attention is recently being attracted in multichannel systems, because coherent optical fiber communication systems offer a possibility of utilizing large bandwidth of single-mode fibers via frequency division multiplexing (FDM).

In a multichannel coherent system, when more than one channels are transmitted, performance of a coherent receiver will be degraded by several physical phenomena, including excess shot noise generated in the receiver, intermodulation interference due to adjacent channels, and crosstalk caused by nonlinear effects in single-mode optical fiber and in semiconductor laser amplifier (if used). These crosstalk sources determine the design parameters (e.g., channel spacing, channel number, bit-rate, and modulation scheme) of the multichannel system and consequently the receiver sensitivity. Therefore, one of the main subjects of research on multichannel coherent systems is to investigate sensitivity degradation due to above mentioned crosstalk, which has not yet been studied.

In this chapter the sensitivity penalty due to crosstalk in multichannel coherent optical fiber communication systems is theoretically investigated, and optimum parameters of the system are discussed. System description and problem statement are given in Section 6.2. Crosstalk due to excess shot noise is analyzed in Section 6.3. Section 6.4 analyzes the crosstalk due to image-band interference taking into account the effect of laser phase noise. Results obtained are discussed in Section 6.5, and the whole chapter is summarized in Section 6.6.

6.2 System description and problem statement

The block diagram and channel arrangement of the N-channel coherent optical fiber communication system under investigation are shown in Figs.6.1(a) and (b), respectively, where D_{opt} denotes channel spacing between lasers in optical-domain, and D_{ele} that in electrical-domain. In the system, N numbers of transmitting laser are used and modulated by N numbers of information source with ASK, FSK or PSK modulation format. The N numbers of information source are available for each of M numbers of receiver. The frequency of kth laser is

$$f_k = f_1 + (k-1)D_{opt}\ , \qquad \text{for} \quad 1 \le k \le N \tag{6.2.1}$$

Signals of the N numbers of laser are combined with an N×M optical fiber coupler and transmitted to M numbers of receiver. Each receiver is able to tune to any one of the signal channels by adjusting its local oscillator (LO) frequency f_L to such that $f_L = f_k - f_{IF}$, where f_{IF} is the intermediate frequency (IF) of the receiver.

It is understood that in coherent optical fiber communications, it is desired to keep IF to be minimum since the equalized receiver noise spectral density typically increases with the frequency. Thus it is assumed here that the IF is smaller than the optical-domain channel spacing D_{opt}, so that f_L is arranged between the desired channel and the nearest adjacent channel. In this case, two arrangements are possible; one is to locate f_L to be closer to the desired channel than the nearest adjacent channel leading to the smallest IF, and the other is to locate it closer to the nearest adjacent channel than the desired channel leading to the second smallest IF. In the analysis of this chapter, the use of the former arrangement is first considered, and it is assumed that kth channel is a desired channel, so that f_L is located between

*k*th channel and *(k-1)*th channel and is closer to the *k*th channel than the *(k-1)*th channel. With such arrangement, *(k-1)*th channel becomes the nearest adjacent channel and the main source of crosstalk.

Because a balanced receiver can eliminate the direct-detection- and channel-cross-channel interferences in multichannel coherent systems, in the system of Fig.6.1 such kind of receiver is assumed to be used. In this case output photocurrent of each of M numbers of receiver shown in Fig.6.1(a) is given as

$$I(t) = AS(t) + C(t) + n(t) \tag{6.2.2}$$

where

$$A = 2R\sqrt{P_L P_s} \tag{6.2.3}$$

$$S(t) = m_k(t)\cos(2\pi f_{IF} t + \phi_k(t) + \theta_k(t)) \tag{6.2.4}$$

$$C(t) = \sum_{\substack{i=1 \\ i \neq k}}^{N} m_i(t) B_i \cos[2\pi f_{IF} t + 2\pi(i-k)D_{opt} t + \phi_i(t) + \theta_i(t)] \tag{6.2.5}$$

$$B_i = 2R\sqrt{P_L P_{si}} \tag{6.2.6}$$

Here $S(t)$ denotes the desired signal of the desired channel, $C(t)$ the crosstalk terms due to image-band interference of adjacent channels, $n(t)$ the noise term including shot noise and electrical circuit noise, subscript k refers to the desired channel, R is the detector responsivity, P_L the LO power, P_s the signal power of desired channel, P_{si} the signal power of the ith adjacent channel, N the channel number, $m_i(t)$ and $\theta_i(t)$ the amplitude- and phase-modulation signal for the ith channel, and $\phi_i(t)$ the laser phase noise. The single-sided power spectral density of the noise $n(t)$ in the receiver is

$$\eta = 2eRP_T + 2i_n^2 \qquad \text{for} \quad f>0 \tag{6.2.7}$$

where e denotes the electron charge, P_T the detected total power, and i_n is the receiver noise current including the noise of photodetector, load resistor, and preamplifier.

6.3 Analysis of crosstalk due to excess shot noise

In a single-channel coherent system, the detected total power P_T is

$$P_T = P_L + P_s \tag{6.3.1}$$

so that the noise power at the filter output is

$$\sigma_{ns}^2 = 2B[eR(P_L + P_s) + i_n^2] \tag{6.3.2}$$

where B is the bandwidth of the filter. The first and second terms of Eq.(6.3.2) denote shot noise due to LO and signal power, respectively. Because $P_L \gg P_s$, in general the shot noise due to signal power P_s can be ignored compared with that due to LO power P_L, resulting in the achievement of shot-noise-limited detection.

On the contrary, in an N-channel system, the detected total power P_T is

$$P_T = P_L + \sum_{i=1}^{N} P_{si} \tag{6.3.3}$$

thus the noise power at the filter output is

$$\sigma_{nm}^2 = 2B[eR(P_L + \sum_{i=1}^{N} P_{si}) + i_n^2] \tag{6.3.4}$$

In the case that the transmitted optical power for each channel is equal, Eq.(6.3.4) becomes to be

$$\sigma_{nm}^2 = 2B[eR(P_L + NP_s) + i_n^2] \tag{6.3.5}$$

It can be seen from Eq.(6.3.5) that the shot noise in a multichannel system is larger than that in a single-channel system by $2eR(N-1)BP_s$, which is called excess shot noise, and results from undesired channels. Because the LO power is finite, when N is large, the shot-noise-limited detection can not be achieved as in single-channel systems, causing an occurrence of power

penalty. Here sensitivity penalty stemming from the excess shot noise is calculated.

Referring to Eq.(6.3.5), the signal-to-noise ratio (SNR) at the filter output in an N-channel system is expressed as

$$SNR = \frac{RP_s}{eB(1 + \frac{NP_s}{P_L} + \frac{i_n^2}{eRP_L})} \tag{6.3.6}$$

On the other hand, BER of a heterodyne receiver can be approximately given as[3]

$$BER = \frac{1}{2} exp(-\alpha SNR) \tag{6.3.7}$$

where α is a constant depending on modulation formats ($\alpha = \frac{1}{8}$ for ASK scheme and FSK single-filter scheme, $\frac{1}{4}$ for FSK dual-filter scheme, and $\frac{1}{2}$ for PSK scheme). Therefore, the sensitivity penalty caused by the excess shot noise can be calculated using Eqs.(6.3.6) and (6.3.7), and be given as

$$P_{enalty} = \frac{RP_L + Be/\alpha \, log(2BER)}{RP_L + BeN/\alpha \, log(2BER)} \tag{6.3.8}$$

Figure 6.2 shows the calculated maximal permissible bit-rate for ASK scheme under different LO powers to confine power penalty due to the excess shot noise within 0.1dB at BER=10^{-9}, as a function of channel number. It is found that the permissible bit-rate is strongly dependent on LO power. For example, the permissible bit-rate is about 900Mbit/s for an ASK system having a channel number of 500 and an LO power of 0.5mW, however, it becomes to be 1.8Gbit/s when LO power is increased to 1mW. Figure 6.3 shows the calculated maximal permissible bit-rate for ASK scheme to confine power penalty due to the excess shot noise within the desired level at BER=10^{-9}, as a function of channel number, where an LO power of 1mW is

assumed. A comparison of ASK scheme with FSK single-filter scheme, FSK dual-filter scheme and PSK scheme is shown in Fig.6.4, where an LO power of 1mW and a power penalty of 0.1dB are assumed. It is found that the permissible bit-rate of PSK scheme is the largest among these schemes. This is because that PSK scheme has a higher sensitivity than ASK and FSK schemes, so that the needed signal power to achieve BER=10^{-9} is lower than that in ASK and FSK schemes, causing a smaller excess shot noise.

6.4 Analysis of crosstalk due to image-band interference

It is understood from Eq.(6.2.2) that in multichannel coherent systems, signals received by a receiver contain a crosstalk component C(t) due to intermodulation interferences including image-band interference, direct-detection interference, and channel-cross-channel interference. Since the influences of direct-detection interference and channel-cross-channel interference can be removed by using a balanced receiver, image-band interference becomes a main cause for crosstalk. The crosstalk due to image-band interference comes from signal powers of adjacent channels fell within the bandwidth of IF filter for the desired channel. The sensitivity degradation due to image-band interference is calculated here.

6.4.1 General analysis

When channel spacing is large, an approximate frequency domain analysis, in which the noise spectra due to image-band interference are assumed to be Gaussian noise-like spectra (that is, the crosstalk probability density function is approximated to the Gaussian probability density function), leads to simple BER expressions, and gives almost the same results as that of exact time domain analysis[62]. Therefore, a frequency domain

analysis is conducted here. For simplicity, the shot-noise-limited state is assumed, and the excess shot noise is ignored. In this case, noise power, σ^2, of the receiver of desired channel can be expressed such, as the sum of shot noise due to LO power and that due to crosstalk-induced noise, that

$$\sigma^2 = \sigma_n^2 + \sigma_c^2 \tag{6.4.1}$$

where σ_n^2 denotes the shot noise caused by LO power P_L, and σ_c^2 the noise power due to image-band interference, which can be calculated as

$$\sigma_c^2 = \int_{-\infty}^{\infty} G_c(f)\,|H(f)|^2 df \tag{6.4.2}$$

where $G_c(f)$ is the normalized spectral density (NSD) of the crosstalk terms represented by Eq.(6.2.5), and $H(f)$ the transfer function of IF bandpass filter (BPF) used in the receiver for desired channel. Here the use of an ideal BPF having twice Nyquist-limit bandwidth is assumed. That is,

$$|H(f)|^2 = \begin{cases} 1 & \text{for } |f - f_{IF}| \le R_b \\ 0 & \text{for } |f - f_{IF}| > R_b \end{cases} \tag{6.4.3}$$

where R_b is the bit-rate.

Since information signals to be transmitted are independent of laser phase noise, $G_c(f)$ can be expressed as[63]

$$G_c(f) = \sum_{\substack{i=1 \\ i \neq k}}^{N} B_i^2 G_{mi}(f) * G_{bi}(f - f_{IF} + (i-k)D_{opt}) \tag{6.4.4}$$

where * denotes the convolution, $G_{mi}(f)$ the NSD of modulation signals for ith channel, and $G_{bi}(f)$ the NSD of carrier of ith channel. $G_{mi}(f)$ is determined by pulse shape and modulation format. Thus the degradation of sensitivity due to crosstalk can be calculated by Eq.(6.3.7) and Eqs.(6.4.1)-(6.4.4), and gives

$$P_{enalty} = \frac{1}{1 + \dfrac{\sigma_c^2}{A^2\alpha}\log(2BER)} \tag{6.4.5}$$

6.4.2 Crosstalk penalty in an idealized multichannel system

Consider firstly an idealized multichannel coherent system in which the transmitters and the LOs have negligible phase noises, and all the channels have the same bit-rate, the same optical power and the same type of modulation format. In this case, the carrier of each channel can be considered to be a complete sine function, and whose NSD, $G_{bi}(f)$, is given by a Delta function as

$$G_{bi}(f) = \delta(f) \tag{6.4.6}$$

so that the noise power caused by the crosstalk due to image-band interference can be calculated as

$$\sigma_c^2 = A^2 \sum_{\substack{i=1 \\ i \neq k}}^{N} \int_{f_{IF}-R_b}^{f_{IF}+R_b} G_m \left(f - f_{IF} + (i-k)D_{opt} \right) df \tag{6.4.7}$$

A. Crosstalk penalties in multichannel systems with ASK and PSK modulation formats

The single-side NSDs of ASK and PSK signals are[63]

$$G_{mA}(f) = \frac{R_b}{8}|P(f)|^2 + \frac{1}{8}\delta(f) \tag{6.4.8}$$

and

$$G_{mP}(f) = \frac{R_b}{2}|P(f)|^2 \tag{6.4.9}$$

where $|P(f)|$ is the power spectral of signal pulses used as modulation signals. When non-return-to-zero(NRZ) rectangular pulses are used, $|P(f)|^2$ is given as

$$|P(f)|^2 = \frac{1}{R_b^2} sinc^2\left(\frac{f}{R_b}\right)$$

where sinc(·) is a sinc-function defined as

$$sinc(x) = \frac{sin(\pi x)}{\pi x}$$

It is found that the NSDs of ASK and PSK signals are of similar profile, but the NSD of ASK signals contains an additional carrier component $\delta(f)$. By Substituting Eqs.(6.4.8) and (6.4.9) into Eq.(6.4.7), the noise power caused by image-band interference due to adjacent channels can be calculated, and the crosstalk induced penalty can be consequently calculated from Eq.(6.4.5).

Figure 6.5 shows the calculated crosstalk induced penalties at BER=10^{-9} for ASK and PSK schemes under different channel numbers, as a function of optical channel spacing normalized by the bit-rate D_{opt}/R_b. In the analysis an IF of R_b is assumed for simplicity. It is found that the power penalties are decreased with the increase of channel spacing and depend on channel number. However, there are no difference in the calculated results for 10-channel and for 50-channel systems. It is also found that the calculated results for ASK and PSK schemes are equal to each other, in spite of the difference in their NSDs. This is because that in the receiver the Delta-like component of NSD of ASK signals (i.e., second term of Eq.(6.4.7)) is out-side the bandwidth of IF filter of the desired channel, so that the crosstalk is only caused by the first term of Eq.(6.4.7), which is common to both schemes.

B. Crosstalk penalty in multichannel systems with FSK modulation format

The single-side NSD of FSK signals is dependent on the modulation index Δ, and is given as follows for integer $\Delta(=1, 2, 3,...)$:

$$G_{mF}(f) = \frac{1}{8R_b}\left[sinc\left(\frac{f}{R_b} - \frac{\Delta}{2}\right) - (-1)^{\Delta}\, sinc\left(\frac{f}{R_b} + \frac{\Delta}{2}\right)\right]^2 + \frac{1}{8}\left[\delta\left(\frac{f}{R_b} - \frac{\Delta}{2}\right) + \delta\left(\frac{f}{R_b} + \frac{\Delta}{2}\right)\right] \qquad (6.4.10)$$

For Δ=0.5, 1,5 2.5,...:

$$G_{mF}(f) = \frac{1}{2R_b}\left[sinc^2\left(\frac{f}{R_b}-\frac{\Delta}{2}\right)\cdot\cos^2\pi\left(\frac{f}{R_b}-\frac{\Delta}{2}\right)\right.$$
$$+ sinc\left(\frac{f}{R_b}-\frac{\Delta}{2}\right) sinc\left(\frac{f}{R_b}+\frac{\Delta}{2}\right)\cos 2\pi\frac{f}{R_b}$$
$$\left.+ sinc^2\left(\frac{f}{R_b}+\frac{\Delta}{2}\right)\cos^2\pi\left(\frac{f}{R_b}+\frac{\Delta}{2}\right)\right] \qquad (6.4.11)$$

Since BER of a multichannel FSK single-filter system is the same as that of ASK system, the crosstalk induced penalty can be calculated with Eqs.(6.4.5), (6.4.7), (6.4.10) and (6.4.11). However, in a multichannel FSK dual-filter system, noise power caused by the crosstalk is different for mark and space signals, giving different expressions of the BER (see Appendix A). In this case the noise power due to crosstalk is given as

$$\sigma_c^2 = A^2 \sum_{\substack{i=1\\ i\neq k}}^{N} \int_{f_{IF}-f_d-R_b}^{f_{IF}-f_d+R_b} G_m\left(f-f_{IF}+(i-k)D_{opt}\right) df$$
$$+ A^2 \sum_{\substack{i=1\\ i\neq k}}^{N} \int_{f_{IF}+f_d-R_b}^{f_{IF}+f_d+R_b} G_m\left(f-f_{IF}+(i-k)D_{opt}\right) df \qquad (6.4.12)$$

so that the crosstalk induced penalty can be calculated with Eq.(6.4.5), and (6.4.10)-(6.4.12).

Figure 6.6 shows the calculated crosstalk induced penalties at BER=10^{-9} for CPFSK (Δ = 0.5) and for FSK (Δ = 2) dual-filter scheme under different channel numbers, as functions of D_{opt}/R_b. It is found that the penalties in FSK schemes are almost independent of channel number, and that the channel spacings needed to keep the penalty less than desired levels in FSK schemes are smaller than that in ASK and PSK schemes. These are because that the NSDs of both ASK and PSK schemes are of second roll-off, while that of FSK scheme has a fourth roll-off, so that in FSK scheme noise power caused by adjacent channels (except for the nearest channel) becomes negligi-

bly small.

6.4.3 Crosstalk penalty considering the influence of laser phase noise

In a practical system using semiconductor lasers as both transmitter and LO, the carrier in each channel can not be considered to be a complete sine function because of the existence of laser phase noise. The laser phase noise $\phi_i(t)$ is a nonstationary Wiener process:

$$\phi_i(t) = \int_{-\infty}^{t} \dot{\phi}(t_1) dt_1 \tag{6.4.13}$$

where $\dot{\phi}(t_1)$ is the instantaneous angular frequency noise, which can be modeled as a white zero-mean Gaussian random process with the power spectral density (PSD) given as

$$S_{\dot{\phi}} = 2\pi\Delta\nu \qquad \text{for } -\infty<f<\infty \tag{6.4.14}$$

where $\Delta\nu$ is the full width half maximum (FWHM) linewidth at the IF stage, i.e.,

$$\Delta\nu = \Delta\nu_s + \Delta\nu_L \tag{6.4.15}$$

where $\Delta\nu_s$ and $\Delta\nu_L$ are the linewidths of transmitter and LO respectively. The PSD given by Eq.(6.4.14) corresponds to the Lorentzian laser line shape[64], the NSD of which is given as

$$G_{bi}(f) = \frac{2\pi\Delta\nu}{(2\pi f)^2 + (\pi\Delta\nu)^2} \tag{6.4.16}$$

so that the crosstalk induced penalty including the influence of laser phase noise can be calculated with Eqs.(6.4.4), (6.4.5), (6.4.8)-(6.4.11) and (6.4.16).

The calculated crosstalk induced penalties are shown in Fig.6.7 as functions of the ratio of channel spacing to bit-rate (here the channel spacing

in IF stage D_{ele}/R_b is considered, as will be described latter, $D_{ele} = D_{opt} - 2f_{IF}$), under different ratios of laser linewidth to bit-rate ($\Delta\nu/R_b$). Here a two-channel system is considered for simplicity. Figure 6.7(a), (b), (c) and (d) are the calculated results for ASK, PSK, CPFSK and FSK dual-filter schemes. Figure 6.8 shows the needed electrical channel spacings for various modulation schemes for a penalty of 0.1dB at BER=10^{-9}, as functions of $\Delta\nu/R_b$. It is found that the needed channel spacings are not equal to each other for ASK and PSK schemes when $\Delta\nu$ is large. This is because that when the carrier of light source is phase fluctuated, compared with the NSD of PSK scheme, the NSD of ASK scheme contains an additional Lorentzian-like component which is not band-limited, causing an appearance of noise power. It is also found that the penalty increases rapidly when $\Delta\nu/R_b$ exceeds 1/10 in ASK and PSK schemes, and in FSK schemes the influence of laser phase noise on crosstalk induced penalty is more critical than those in ASK and PSK schemes.

6.5 Discussion

6.5.1 Selections of IF and f_L

As has been described in Section 6.2, there are two approaches to arrange the frequency, f_L, of LO; one is to locate f_L closer to the desired channel than the nearest adjacent channel, and the other is to locate it closer to the nearest adjacent channel than the desired channel. In the former arrangement, $f_{IF} < D_{opt}/2$, and $D_{opt} = D_{ele} + 2f_{IF}$. In this case, the crosstalk generated by the (k-1)th channel is much stronger than that generated by (k-2)th or (k+1)th channels, because the (k-1)th channel is the closest to the desired channel. In the later arrangement, f_{IF} should be larger than $D_{opt}/2$ to separate the channels completely, and both the (k-1)th channel and the (k-2)th channel

may be the nearest adjacent channel depending on the selection of IF. When $f_{IF} = 3D_{opt}/4$, the $(k\text{-}1)$th and the $(k\text{-}2)$th channels are located symmetrically about the desired channel at the IF stage, generating the smallest crosstalk. In this case, $D_{opt} = 2D_{ele}$. For a certain D_{ele}, the second arrangement will have twice the crosstalk power as that of the first arrangement, because the same amount of crosstalk is generated by both the $(k\text{-}1)$th and the $(k\text{-}2)$th channels. Therefore, the first arrangement is more advantageous than the second one except for the special case that a large IF is needed.

6.5.2 Influences of IF and power level of adjacent channels

In the analyses of Section 6.4, a fixed IF ($=R_b$), and the same light power for all channels are assumed. In a practical system, these may not be all the case, so that different crosstalk penalties can be resulted. The influences of these factors are discussed here. In following calculation a two-channel system is assumed for simplicity.

Since the channels in multichannel coherent systems are separated at IF stage, the crosstalk induced penalty at IF stage depends on the electrical channel spacing, D_{ele}, rather than on the optical channel spacing, D_{opt}. Therefore, it is important to arrange IF because when the optical channel spacing is fixed, an increase of IF will cause a decrease of D_{ele} at IF stage, and consequently an increase of penalty.

Figure 6.9 shows the needed optical channel spacings for a crosstalk penalty of 0.1dB at BER=10^{-9} versus the ratio of IF to bit-rate (f_{IF}/R_b) for various modulation formats. It is found that the normalized permissible channel spacing, D_{opt}/R_b, increases by 2Hz for every 1Hz increase of f_{IF}. Figures 6.10 and 6.11 show the needed optical channel spacings for a crosstalk penalty of 0.1dB at BER=10^{-9} for various modulation formats, as functions of the

ratio of channel powers ρ, where ρ is defined as P_{si}/P_s. It is found that the permissible channel spacing increases with the increase of signal power of adjacent channels in ASK or PSK scheme, while in FSK scheme it is almost maintained to be constant. This is again resulted from the fact that the NSD of ASK or PSK scheme is of second roll-off, while that of FSK scheme has a fourth roll-off.

6.5.3 Influence of type of IF filter

It is understood from Eq.(6.4.2) that the crosstalk induced noise is dependent on the transfer function of IF BPF used in the receiver for desired channel. All of the above analyses are performed under an assumption of use of an ideal filter. However, in a practical system, so-called Butterworth- or Tchebyshev-type filter rather than the ideal filter is commonly utilized. Here the influence of type of IF filter on crosstalk is discussed.

The transfer functions of Butterworth- and Tchebyshev-type filter are given respectively, as[63]

$$|H_B(f)|^2 = \frac{1}{1 + \left(\frac{f - f_{IF}}{B}\right)^{2n}} \tag{6.5.1}$$

and,

$$|H_T(f)|^2 = \frac{1}{1 + \epsilon^2 T_n^2(f)} \tag{6.5.2}$$

where B is the bandwidth of IF filter, ϵ a constant expressing the ripple of the filter, and $T_n^2(f)$ the Tchebyshev polynomial expression given as

$$T_n(f) = \frac{1}{2}\left(\frac{f - f_{IF}}{B} + j\sqrt{1 - \left(\frac{f - f_{IF}}{B}\right)^2}\right)^n + \frac{1}{2}\left(\frac{f - f_{IF}}{B} - j\sqrt{1 - \left(\frac{f - f_{IF}}{B}\right)^2}\right)^n \tag{6.5.3}$$

Thus the crosstalk induced penalty can be calculated similarly as done in Section 6.4.

The crosstalk penalty differences between the Butterworth-type filter and ideal filter for ASK and PSK schemes under different orders of filter are shown in Fig.6.12, as functions of D_{opt}/R_b, where P_I denotes the crosstalk induced penalty using the ideal filter, and P_B that using the Butterworth-type filter. Fig.6.13 shows the calculated results for the Tchebyshev-type filter, where P_T is the crosstalk induced penalty using the Tchebyshev-type filter. In the calculation, $B = 2R_b$ and a two-channel system are assumed for simplicity. Figure 6.14 shows comparisons among a 5th order Butterworth-type, a 5th Tchebyshev-type filter and the ideal filter. It is found that there are no difference among them when channel spacing is larger than 6 times bit-rate, suggesting that the error caused by the approximation of the filter transfer function can be ignored in the analysis.

6.5.4 Influence of pulse shape

It can be seen from Eq.(6.4.2) that the crosstalk induced noise is also determined by the NSD of signals. On the other hand, the NSD of signals is dependent on pulse shapes of received signals. In general systems the NRZ rectangular pulses with spectral of non-bandlimited are used as transmitting signals. However, the received signals are no longer a NRZ rectangular pulses because of the limited bandwidth of modulators and the bandpass filtering of the receiver. The crosstalk induced penalties for two-channel ASK and PSK schemes are calculated here using three types of signal pulse: Gaussian pulse, cosine pulse, and raised cosine pulse.

The power spectra of Gaussian pulse, cosine pulse and raised cosine pulse are given respectively as[65]

$$P(f) = \frac{\sqrt{\pi}}{2}\tau \exp\left[-\left(\frac{\pi f \tau}{2}\right)^2\right] \tag{6.5.4}$$

$$P(f) = \frac{2}{\pi}\tau \frac{\cos(\pi f \tau)}{1-(2f\tau)^2} \tag{6.5.5}$$

and

$$P(f) = \frac{\tau\, sinc(2f\tau)}{1-(2f\tau)^2} \tag{6.5.6}$$

where $\tau = \frac{1}{R_b}$.

The pulse shapes and corresponding spectral densities used in the calculation are shown in Fig.6.15, where curve "a" is the model for NRZ rectangular pulse, curve "b" that for cosine pulse, curve "c" that for Gaussian pulse, and curve "d" that for raised cosine pulse. The calculated crosstalk induced penalties for ASK and PSK schemes at BER=10^{-9} are shown in Fig.6.16. It is found that the penalty can be significantly reduced by choosing shapes of signal pulse. For example, the needed channel spacing of systems with the raised cosine pulse for a power penalty of 0.5dB is 1/3 times that of systems with the NRZ rectangular pulse.

6.5.5 Influence of bandwidth of IF filter

As described in Section 6.2, crosstalk due to image-band interference is caused by the powers of adjacent channels fell within bandwidth of IF filter of the receiver for desired channel, so that a wider bandwidth of IF filter will cause a larger crosstalk induced penalty. Figure 6.17 shows the calculated permissible channel spacings normalized by bit-rate for a penalty of the desired level for two-channel ASK, PSK and CPFSK with Δ = 0.5 (referred to as MSK) schemes, as functions of the normalized bandwidth of IF filter, where curves "a" and "c" show the results for a penalty of 0.1dB, and curves "b" and "d" show that for a penalty of 0.5dB. It is found that the needed

channel spacing is proportional to the bandwidth of IF filter with a factor of 1/2 in an MSK scheme, and that the same results are obtained in ASK and PSK schemes when the bandwidth of IF filter becomes wider.

In FSK scheme of modulation index larger than 0.5, the bandwidth of IF filter can not be chosen arbitrarily, and is limited by the modulation index. Therefore, the permissible channel spacing is directly dependent on the modulation index rather than the bandwidth of IF filter. Figure 6.18 shows the permissible channel spacing versus modulation index for FSK scheme to confine the penalty within a desired level, where an IF of $f_d + R_b$, and the bandwidth of IF filter of R_b are assumed. It is found that in an FSK single-filter scheme the permissible channel spacing is proportional to the modulation index with a factor of 1, and that in an FSK dual-filter scheme it is proportional to the modulation index with a factor of 2.

6.5.6 Comparison of calculated and experimental results

To confirm the present theory, the calculated results are compared with experimental results here. The crosstalk induced penalty considering the influence of laser phase noise in a two-channel ASK system has been calculated with the same parameters used in the experiment by Park et al.[35], where $\Delta\nu/R_b = 0.5$ and the bandwidth of IF filter of 6.7 times bit-rate are used. Figure 6.19 shows both the calculated and the experimental results, where open circles are the measured crosstalk penalties, and the solid curve the theoretical results obtained from the present analysis. It is found that a good agreement is obtained.

6.6 Conclusions

In this chapter, the crosstalk induced penalties due to excess shot noise and image-band interference are analyzed theoretically. It is found that

(1) The crosstalk penalty caused by excess shot noise is dependent on LO power, and at the same time it determines the bit-rate and channel number. When a typical LO power of 1mW is used, the permissible bit-rate and channel number for a penalty of 0.1dB is 2Gbit/s and 500.

(2) The crosstalk penalty due to image-band interference is dependent on modulation scheme, laser linewidth, type of IF filter, pulse shape and bandwidth of IF filter. In an idealized system, ASK and PSK schemes have similar crosstalk induced penalties and require larger channel spacing than FSK schemes.

(3) The existence of laser phase noise causes an increase of the crosstalk induced penalty, and FSK systems are more sensitive to laser phase noise than ASK and PSK systems.

(4) The noise power due to crosstalk is determined by the electrical channel spacing rather than the optical channel spacing. Therefore, an increase of IF causes a decrease of electrical channel spacing and consequently an increase of crosstalk when the optical channel spacing is fixed, and it is better to locate the LO frequency closer to the desired channel than the nearest adjacent channel.

(5) The crosstalk penalty depends also on the type of IF filter. However, in a system using the Butterworth- or Tchebyshev-type filter it can be approximately dealt with as ideal filter without causing any extra penalty.

(6) The crosstalk penalty can be significantly reduced by choosing proper shape of pulses as signal pulses. For example, the needed channel spacing

of systems with raised cosine pulse for a power penalty of 0.5dB is 1/3 times that of systems with NRZ rectangular pulse.

(7) The needed channel spacing is proportional to the bandwidth of IF filter with a factor of 1/2 in an MSK scheme, and similar results are obtained in ASK and PSK schemes when the bandwidth of IF filter becomes wider. In FSK scheme with modulation index larger than 0.5, the bandwidth of IF filter can not be chosen arbitrarily, but is limited by the modulation index. In an FSK single-filter scheme the permissible channel spacing is proportional to the modulation index with a factor of 1, and that in an FSK dual-filter scheme it is proportional to the modulation index with a factor of 2.

(8) The results obtained from the present theory show good agreements with the experimental results reported by others, suggesting the validity of the theory.

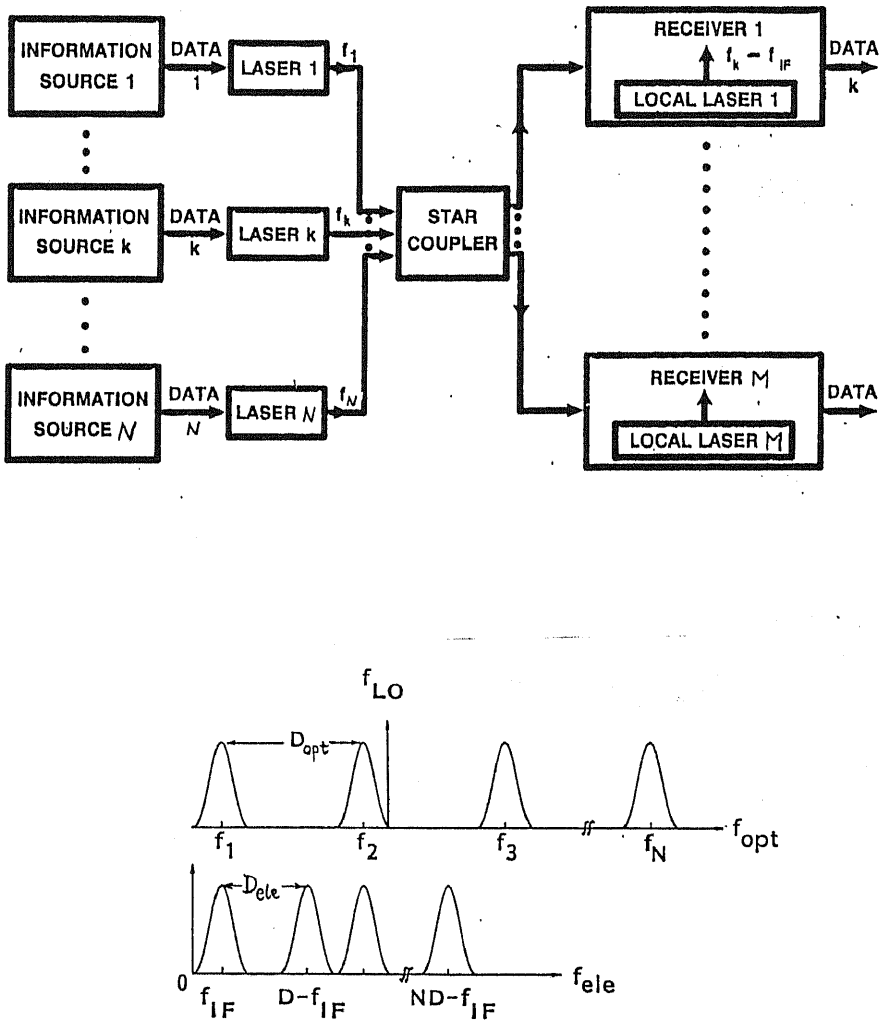

Fig. 6.1 Block diagram and channel arrangement of the N-channel coherent optical fiber communication system under investigation.

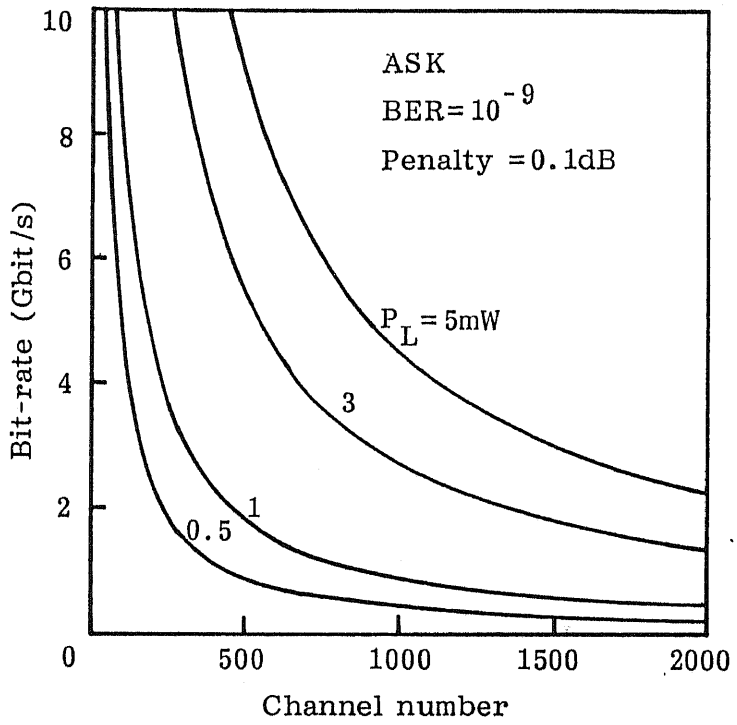

Fig. 6.2 Calculated maximal permissible bit-rate for ASK scheme under different LO powers for a power penalty of 0.1dB at BER=10^{-9}, as a function of channel number.

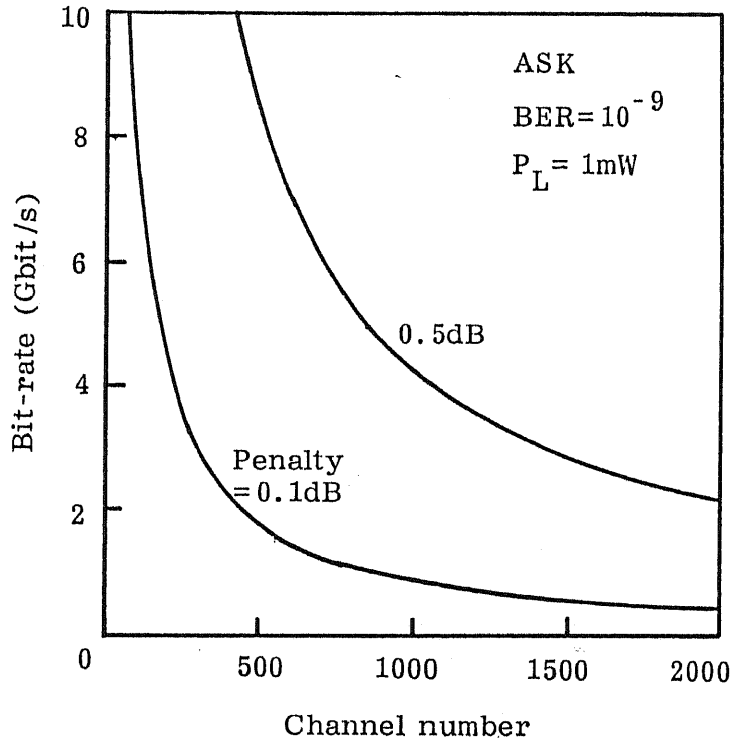

Fig. 6.3 Calculated maximal permissible bit-rate for ASK scheme to confine power penalty within a desired level at BER=10^{-9}, as a function of channel number, where an LO power of 1mW is assumed.

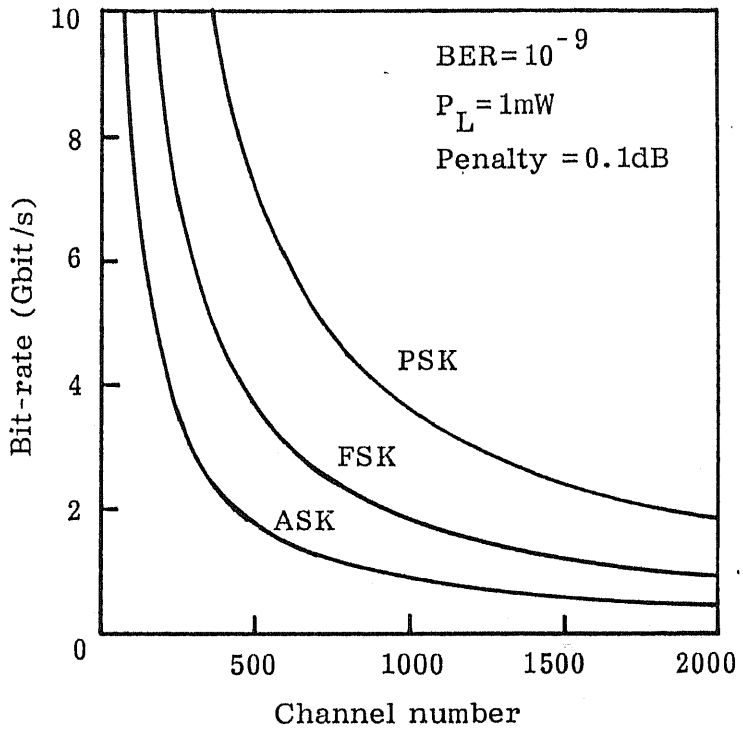

Fig. 6.4 Comparisons of maximal permissible bit-rate for ASK scheme with that for FSK single-filter, FSK dual-filter and PSK schemes, where an LO power of 1mW and a power penalty of 0.1dB are assumed.

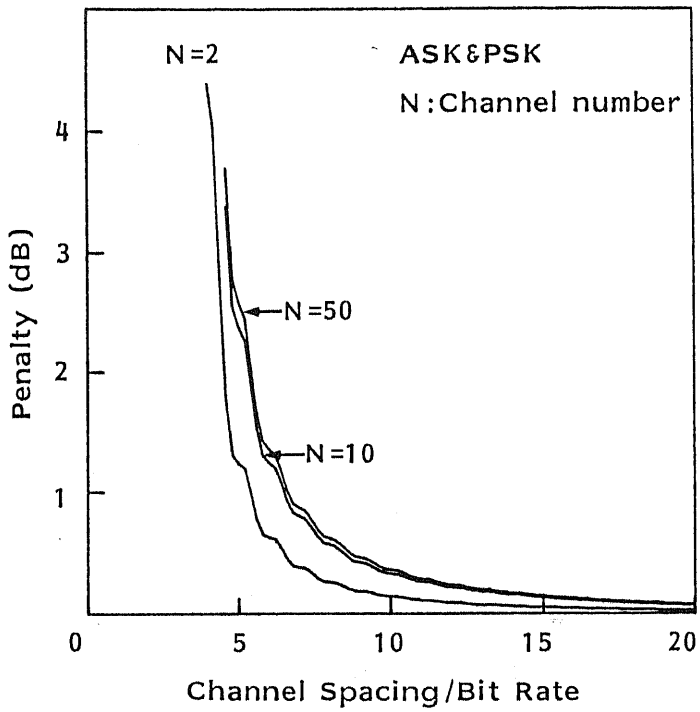

Fig. 6.5 Calculated crosstalk induced penalties at BER=10^{-9} for ASK and PSK schemes under different channel numbers, as functions of D_{opt}/R_b.

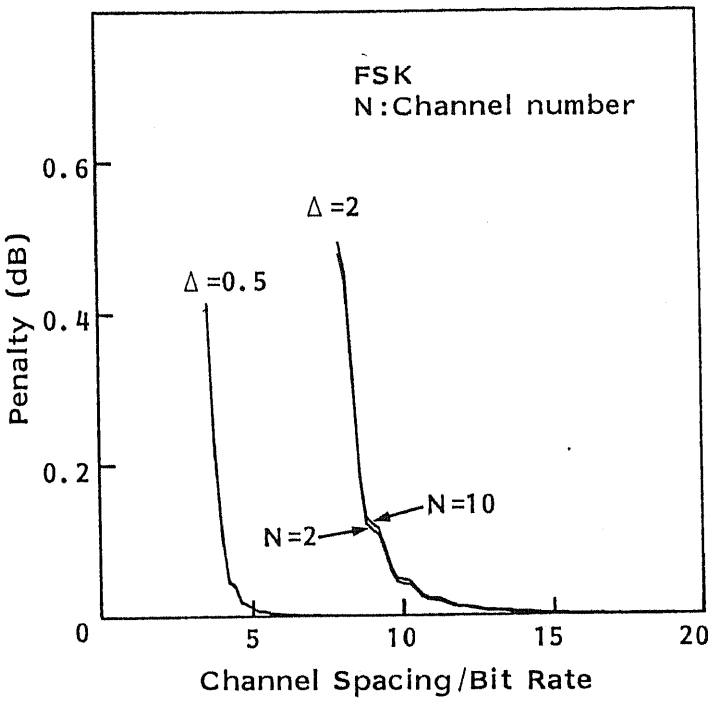

Fig. 6.6 Calculated crosstalk induced penalties at BER=10^{-9} for CPFSK (Δ = 0.5) and FSK dual-filter schemes (Δ = 2) under different channel numbers, as functions of D_{opt}/R_b.

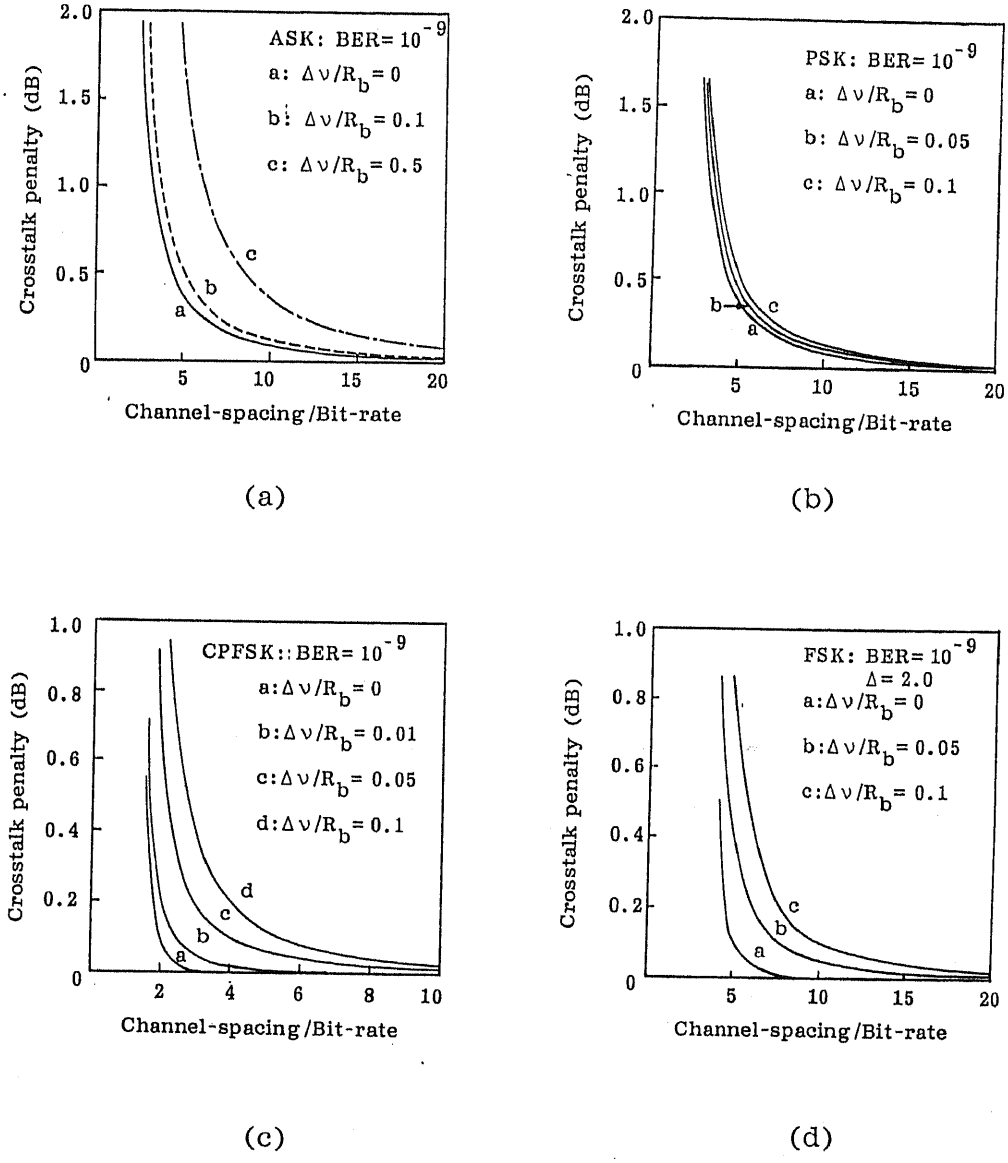

Fig. 6.7 Calculated crosstalk induced penalties for two-channel systems as functions of the ratio of channel spacing to bit-rate under different ratios of laser linewidth to bit-rate ($\Delta\nu/R_b$).

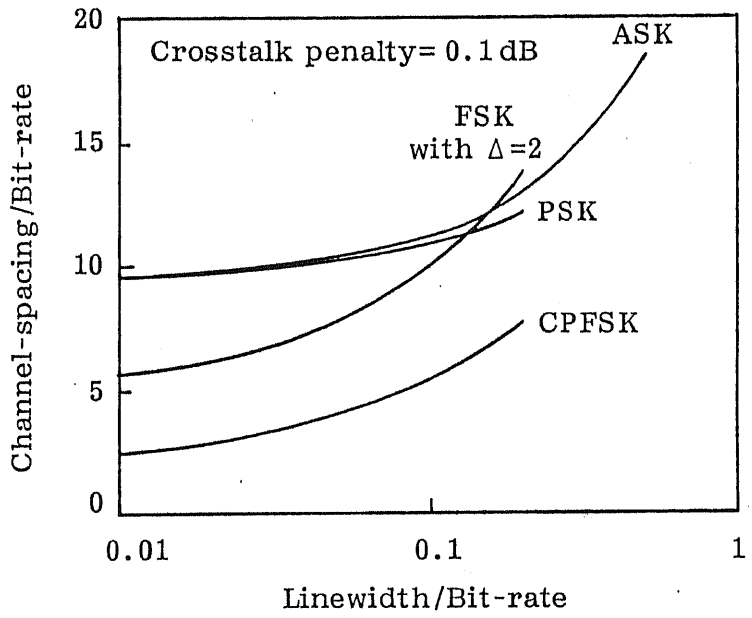

Fig. 6.8 Needed electrical channel spacings for various modulation formats for a crosstalk penalty of 0.1dB at BER=10^{-9}, as functions of $\Delta\nu/R_b$.

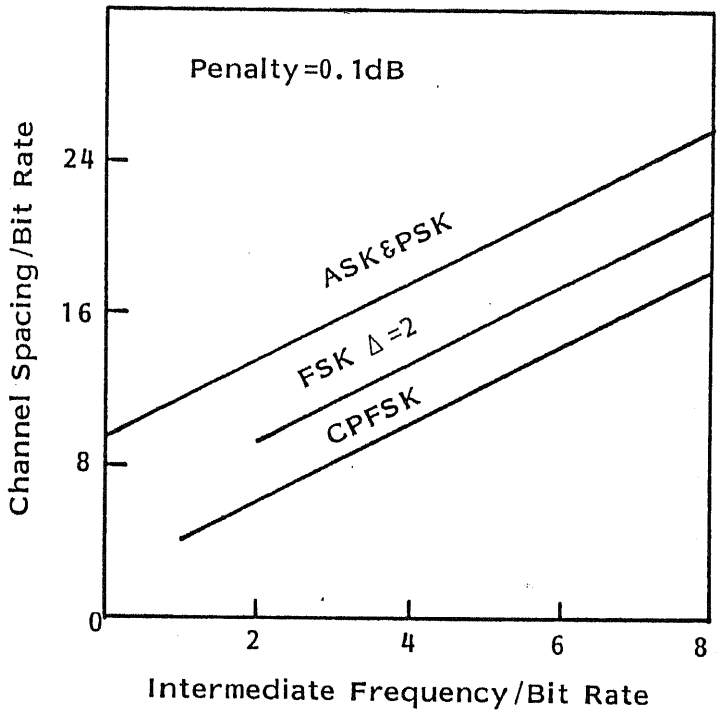

Fig. 6.9 Needed optical channel spacings for various modulation formats for a penalty of 0.1dB at BER=10^{-9}, as functions of the ratio of IF to bit-rate (f_{IF}/R_b).

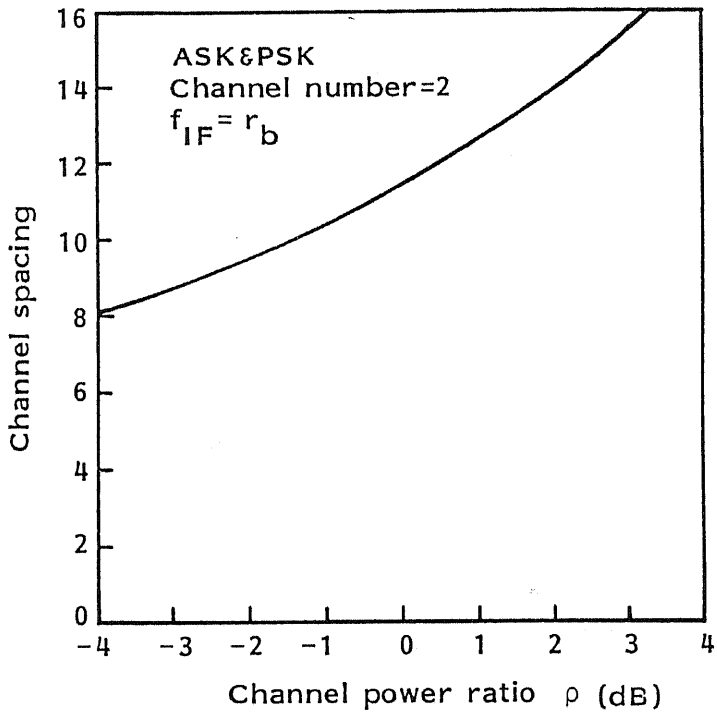

Fig. 6.10 Needed optical channel spacings for ASK and PSK schemes for a penalty of 0.1dB at BER=10^{-9}, as functions of the ratio of channel powers ρ, where ρ is defined as P_{si}/P_s.

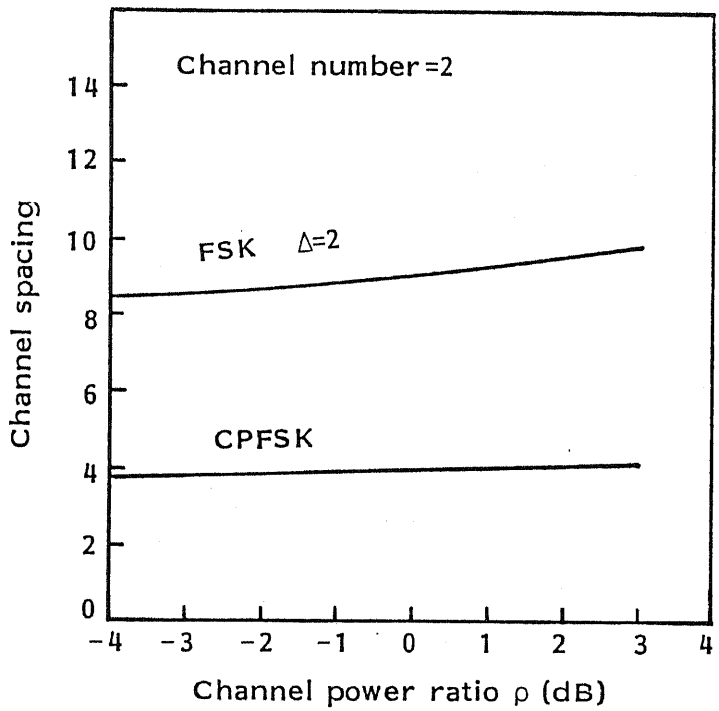

Fig. 6.11 Needed optical channel spacings for CPFSK and FSK dual-filter schemes for a penalty of 0.1dB at BER=10^{-9}, as functions of ρ.

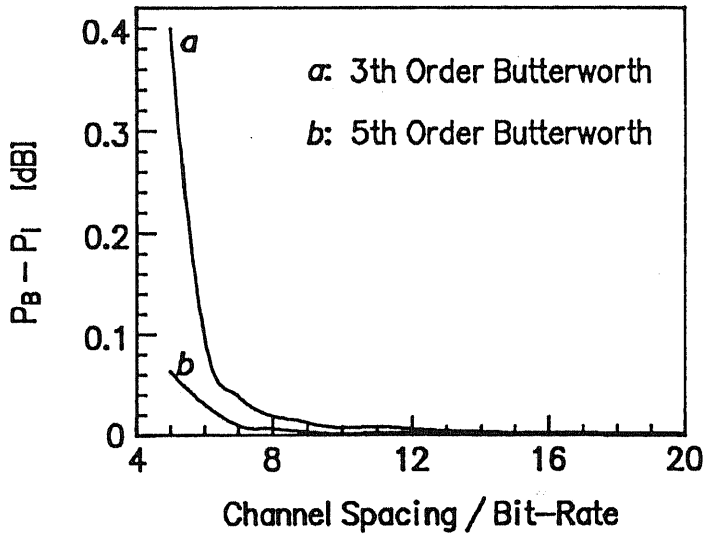

Fig. 6.12 Crosstalk penalty differences between a Butterworth-type filter and an ideal filter versus normalized channel spacing for ASK and PSK schemes under different orders of filter, where P_I denotes the crosstalk induced penalty using the ideal filter, and P_B that using the Butterworth-type filter.

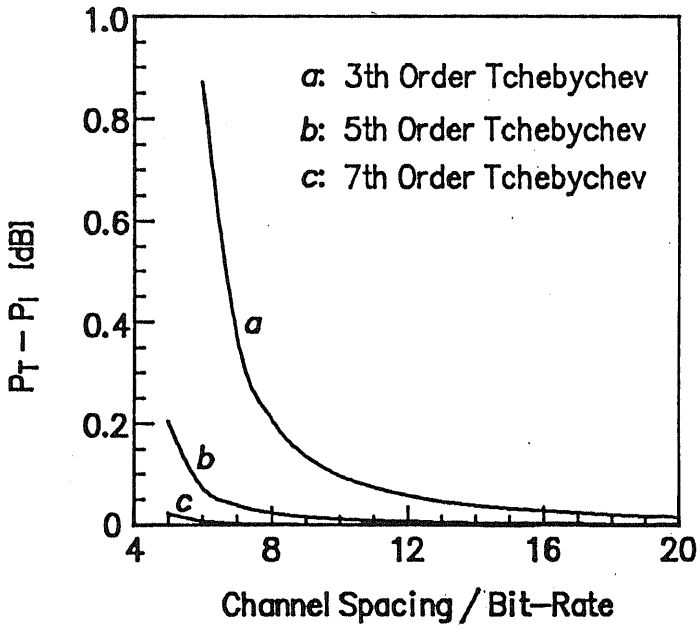

Fig. 6.13 Crosstalk penalty differences between a Tchebyshev-type filter and an ideal filter versus normalized channel spacing for ASK and PSK schemes under different orders of filter, where P_T is the crosstalk induced penalty using the Tchebyshev-type filter.

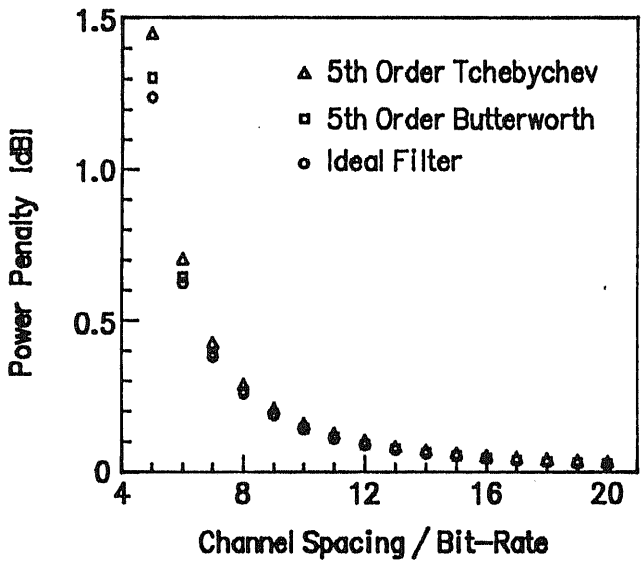

Fig. 6.14 Crosstalk comparisons of a 5th order Butterworth-type and a 5th Tchebyshev-type filter with an ideal filter, when they are used as IF BPF.

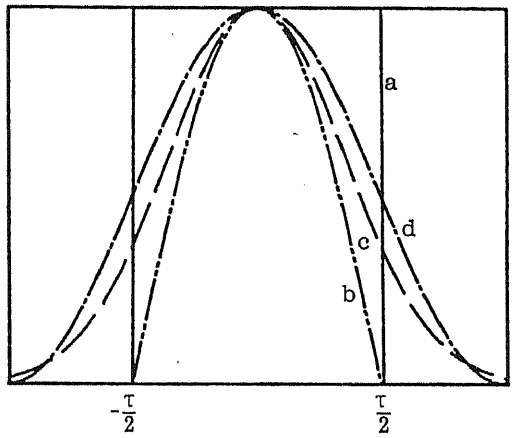

Various Pulse Shapes

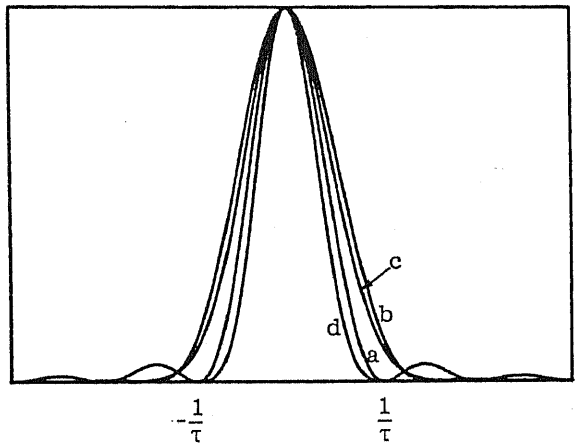

Power Spectrum

Fig. 6.15 Pulse shapes and corresponding spectral densities used in the calculation, a: NRZ rectangular pulse, b: cosine pulse, c: Gaussian pulse, and d: raised cosine pulse.

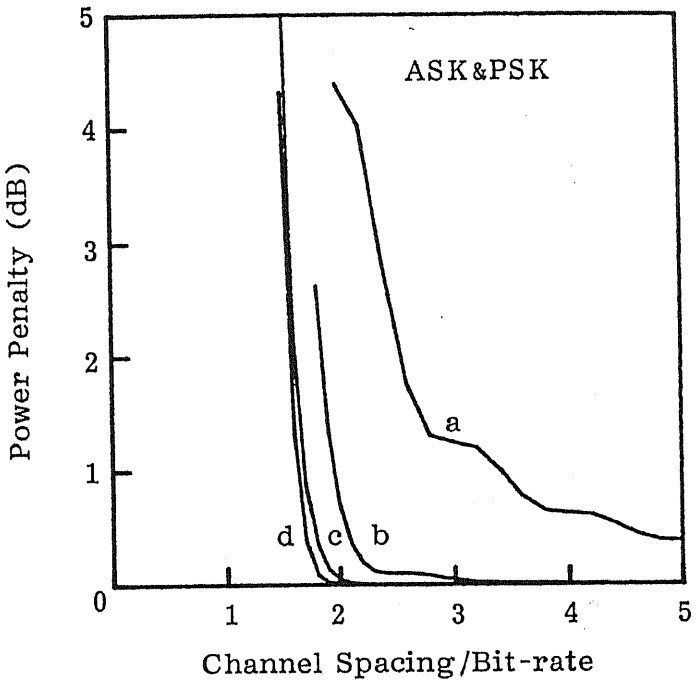

Fig. 6.16 Crosstalk induced penalties at BER=10^{-9} versus channel spacing for ASK and PSK schemes under various pulse shapes.

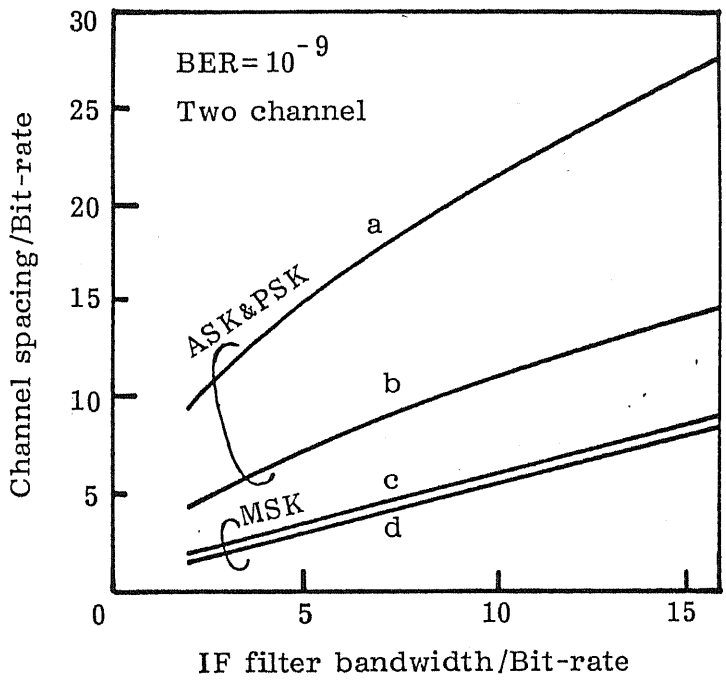

Fig. 6.17 Calculated permissible channel spacings for a penalty of the desired level versus the normalized bandwidth of IF filter, for two-channel ASK, PSK and MSK schemes, where curves "a" and "c" show the results for a penalty of 0.1dB, and curves "b" and "d" that for a penalty of 0.5dB.

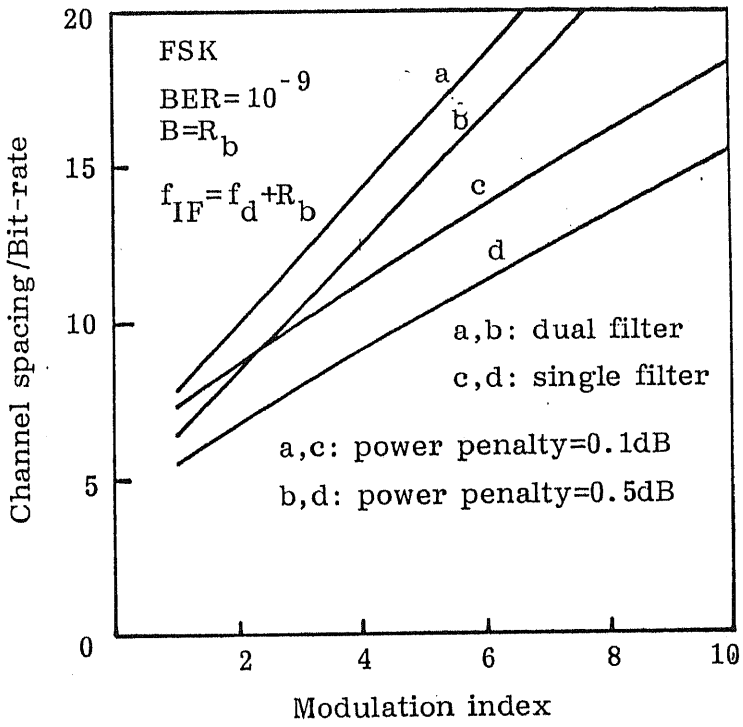

Fig. 6.18 The permissible channel spacing versus modulation index for FSK schemes to keep the penalty below desired levels.

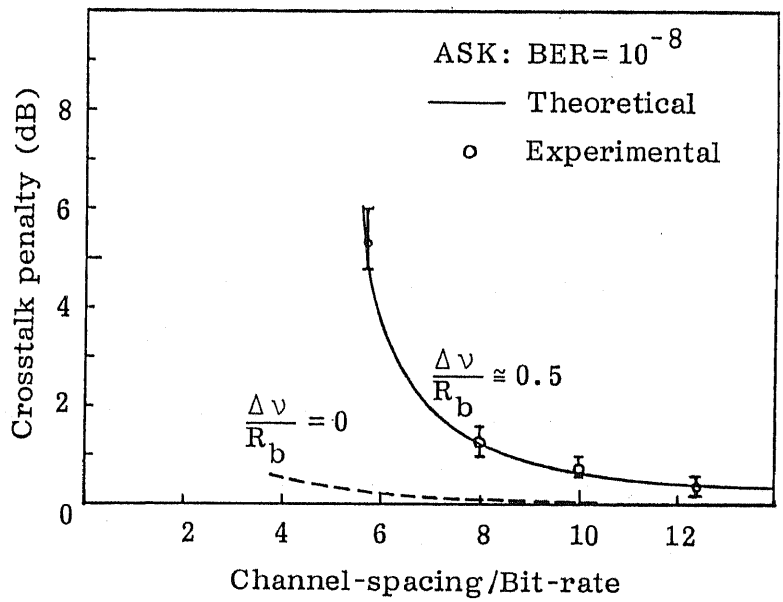

Fig. 6.19 Comparisons of the calculated and the experimental results, where the open circles show the measured crosstalk penalty, and the solid curve the theoretical results obtained from the present analysis.

CHAPTER 7

Conclusions

Phase-noise-canceling heterodyne schemes (PNCHSs) and multichannel coherent optical fiber communication systems are studied theoretically and experimentally in this thesis.

The theoretical analysis shows that a dual-polarization PNCHS is advantageous for low bit-rate systems in which lasers used as transmitter and LO have relatively large linewidth (>0.007 times bit-rate), and that the performance of dual-polarization PNCHS is sensitive to loss in orthogonality of polarization. For example, the permissible loss in orthogonality of polarization is about 9 degrees for a power penalty of 1dB. Theoretical and experimental studies indicate that the loss in orthogonality of polarization is small in typical fibers and fiber couplers, suggesting the feasibility of the scheme.

It is shown that the performance of dual-frequency PNCHS is the same as that of the dual-polarization PNCHS. A receiver sensitivity of -48.9dBm is obtained at BER=10^{-9} in the experiment of BER measurement of a 20Mbit/s PSK dual-frequency PNCHS. The measured BER curve shows that no BER floor appeared even for $\Delta\nu/R_b = 1$, which suggests the successful cancellation of laser phase noise. A polarization diversity dual-frequency PNCHS is also proposed and analyzed. It is found that the proposed scheme is available for low bit-rate systems having small frequency separation and using a fiber with small polarization dispersion.

A dual-waveguide PNCHS having the same performance as that of the dual-polarization and the dual-frequency PNCHSs is proposed and analyzed theoretically. It is shown that the receiver sensitivity of the scheme depends on the difference in propagating characteristics of fibers used as transmission paths, and that it should be less than 0.08π to keep power penalty below 1dB. An improved dual-waveguide PNCHS insensitive to fiber characteristics is also proposed and discussed.

Theoretical and experimental studies on a time-division PNCHS show that the proposed scheme has a better sensitivity than the conventional DPSK scheme when the ratio of laser linewidth to bit-rate is larger than 0.009, and that the permissible time delay difference for a penalty of 1dB is 0.04 times carrier frequency. The proposed scheme can be combined with polarization diversity receiver without causing any penalty. Experimental results of electronic simulation model of the time-division PNCHS confirmed the principle of the scheme.

Crosstalk induced sensitivity penalty of multichannel coherent systems are analyzed considering crosstalks due to excess shot noise and due to image-band interference. The crosstalk induced penalty due to excess shot noise is dependent on LO power, and determines bit-rate and channel number. When a typical LO power of 1mW is used, the bit-rate and channel number should be less than 2Gbit/s and 500 respectively, to confine the crosstalk induced penalty within 0.1dB.

Crosstalk induced penalties due to image-band interference for various modulation schemes are analyzed considering the influences of laser linewidth, type of IF filter, pulse shape and bandwidth of IF filter. In a phase noise free case, ASK and PSK systems have the same penalty and require larger channel spacing than FSK systems. The existence of laser phase noise

causes increase of penalty, and FSK systems are more sensitive to laser phase noise than ASK and PSK systems. Since noise power due to crosstalk is determined by electrical channel spacing rather than optical channel spacing, an increase of IF causes a decrease of electrical channel spacing and consequently an increase of crosstalk when the optical channel spacing is fixed. The crosstalk induced penalty can be significantly reduced by choosing signal pulses with narrow spectrum.

The needed channel spacing is proportional to the bandwidth of IF filter with a factor of 1/2 in MSK scheme, and similar results are obtained for ASK and PSK schemes when the bandwidth of IF filter becomes wider. In FSK schemes with modulation index larger than 0.5, the bandwidth of IF filter can not be chosen arbitrarily, but is limited by the modulation index. In an FSK single-filter scheme the permissible channel spacing is proportional to the modulation index with a factor of 1, and in an FSK dual-filter scheme, that is proportional to modulation index with a factor of 2. The calculated results from the present theory show good agreements with experimental results reported by others, suggesting the validity of the theory.

REFERENCES

[1] F.D.Kapron, D.B.Keck, and R.D.Maurer, "Radiation loss in glass optical waveguides," *Appl. Phys. Lett.*, Vol.17, pp.423-425, 1970.

[2] I.Hayashi, M.B.Panish, P.W.Foy, and S.Sumski, "Junction lasers which operate continuously at room temperature," *Appl. Phys. Lett.*, Vol.7, No.3, pp.109-111, 1970.

[3] T.Okoshi and K.Kikuchi, *Coherent Optical Fiber Communications*. KTK/Kluwer, 1988.

[4] O.E.DeLange, "Wideband optical communication systems: Part II-frequency division multiplexing," *Proc. IEEE*, Vol.58, No.10, pp.1683-1690, 1970.

[5] T.Okoshi, "Feasibility study of frequency-division multiplexing optical fiber communication systems using optical heterodyne or homodyne schemes (in Japanese)," *Pap. Tech. Group*, IECE Japan, No.OQE78-139, 1979.

[6] Y.Yamamoto, "Study on optical digital modulation-demodulation systems (in Japanese)," *Pap. Tech. Group*, IECE Japan, No.CS79-144, 1979.

[7] T.Okoshi and K.Kikuchi, "Frequency stabilization of semiconductor lasers for heterodyne-type optical communication schemes," *Electron.Lett.*, Vol.16, pp.179-181, 1980.

[8] F.Favre and D.LeGuen, "High frequency stability of laser diode for heterodyne communication systems," *Electron. Lett.*, Vol.16, No.18, pp.709-710, 1980.

[9] Y.Yamamoto, "Receiver performance evaluation of various digital optical modulation-demodulation systems in the 0.5-10μm-wavelength region," *IEEE J. Quantum Electron.*, Vol.QE-16, No.11, pp.1251-1259, 1980.

[10] T.Okoshi, "Single-polarization and single-mode optical fibers," *IEEE J. Quantum Electron.*, Vol.QE-17, No.6, pp.879-884, 1981.

[11] T.Okoshi, "Polarization-state control schemes for heterodyne or homodyne optical fiber communications," *J. Lightwave Technol.*, Vol.LT-3, No.6, pp.1232-1237, 1985.

[12] T.Okoshi, S.Ryu, and K.Kikuchi, "Polarization-diversity receiver for heterodyne /coherent optical fiber communications," in *IOOC'83*, (Tokyo Japan), Pap.30C3-2, 1983.

[13] S.Saito, Y.Yamamoto, and T.Kimura, "Optical FSK signal detection in a heterodyne system using semiconductor lasers," *Electron. Lett.*, Vol.18, No.11, pp.470-471, 1982.

[14] D.J.Malyon, T.G.Hodgkinson, D.W.Smith, R.C.Booth, and B.E.Daymond-John, "PSK homodyne receiver sensitivity measurements at 1.5μm," *Electron. Lett.*, Vol.19, No.4, pp.144-145, 1983.

[15] K.Emura, M.Shikada, S.Fujita, I.Mito, H.Honmou, and K.Minemura, "Novel optical FSK heterodyne single filter detection system using a directly modulated DFB-laser diode," *Electron. Lett.*, Vol.20, No.24, pp.1022-1023, 1984.

[16] R.A.Linke, B.L.Kasper, N.A.Olsson, and R.C.Alferness, "Coherent lightwave transmission over 150km fiber lengths at 400Mbit/s and 1Gbit/s data rates using phase modulation," *Electron. Lett.*, Vol.22, No.1, pp.30-31, 1986.

[17] K.Iwashita and N.Takachio, "2Gbit/s optical CPFSK heterodyne transmission through 200km single-mode fiber," *Electron. Lett.*, Vol.23, No.7, pp.341-342, 1987.

[18] B.Glance, L.D.Tzeng, T.L.Koch, O.Scaramucci, K.C.Reichmann, and U.Koren, "High-performance coherent optical communication system," *Electron. Lett.*, Vol.25, No.14, pp.932-933, 1989.

[19] K.Emura, S.Yamazaki, S.Fujita, M.Shikada, I.Mito, and K.Minemura, "Over 300km transmission experiment on an optical FSK heterodyne dual filter detection system," *Electron. Lett.*, Vol.22, No.21, pp.1096-1097, 1986.

[20] K.Emura, R.S.Vodhanel, R.Welter, and W.B.Sessa, "5Gbit/s optical phase diversity homodyne detection experiment," *Electron. Lett.*, Vol.25, No.6, pp.400-401, 1989.

[21] M.J.Creaner, R.C.Steele, I.Marshall, G.R.Walker, N.G.Walker, J.Mellis, S.Al Chalabi, I.Sturgess, M.Rutherford, J.Davidson, and M.Brain, "Field demonstration of 565Mbit/s DPSK coherent transmission system over 176km of installed fibre," *Electron. Lett.*, Vol.24, No.22, pp.1354-1356, 1988.

[22] R.H.Stolen and J.E.Bjorkholm, "Parametric amplification and frequency conversion in optical fibers," *IEEE J. Quantum Electron.*, Vol.QE-18, p.1062, 1982.

[23] D.Cotter, "Stimulated Brillouin scattering in monomode optical fiber," *J. Opt. Commun.*, Vol.4, No.1, pp.10-19, 1983.

[24] A.R.Chraplyvy, D.Marcuse, and P.S.Henry, "Carrier-induced phase noise in angle-modulated optical fiber systems," *J. Lightwave Technol.*, Vol.LT-2, No.1, pp.6-10, 1984.

[25] A.R.Chraplyvy and J.Stone, "Measurement of crossphase modulation in coherent wavelength-division multiplexing using injection lasers," *Electron. Lett.*, Vol.20, No.24, pp.996-997, 1984.

[26] G.P.Agrawal, "Four-wave mixing and phase conjugation in semiconductor laser media," *Opt. Lett.*, Vol.12, No.4, pp.260-262, 1987.

[27] G.P.Agrawal, "Amplifier-induced crosstalk in multichannel coherent lightwave systems," *Electron. Lett.*, Vol.23, No.22, pp.1175-1177, 1987.

[28] T.E.Darcie, R.M.Jopson, and R.W.Tkach, "Intermodulation distortion in optical amplifiers from carrier-density modulation," *Electron. Lett.*, Vol.23, No.25, pp.1392-1394, 1987.

[29] T.E.Darcie and R.M.Jopson, "Nonlinear interactions in optical amplifiers for multifrequency lightwave systems," *Electron. Lett.*, Vol.24, No.10, pp.638-640, 1988.

[30] P.Healey, "Effect of intermodulation in multichannel optical heterodyne systems," *Electron. Lett.*, Vol.21, No.3, pp.101-103, 1985.

[31] L.Kazovsky, "Multichannel coherent optical communications systems," *J. Lightwave Technol.*, Vol.LT-5, No.8, pp.1095-1102, 1987.

[32] E.-J.Bachus, F.Böhnke, R.-P.Braun, W.Eutin, H.Foisel, K.Heimes, and B.Strebel, "Two-channel heterodyne-type transmission experiment," *Electron. Lett.*, Vol.21, No.1, pp.35-36, 1985.

[33] Y.K.Park, S.W.Granlund, C.Y.Kuo, M.Dixon, T.W.Cline, R.W.Smith, and N.K.Dutta, "Crosstalk penalty in a two-channel ASK heterodyne detection system," *CLEO'87*, (Baltimore, U.S.A.), Pap. WH1, 1987.

[34] B.Glance, K.Pollock, C.A.Burrus, B.L.Kasper, G.Eisenstein, and L.W.Stulz, "Densely spaced WDM coherent optical star network,"

Electron. Lett., Vol.23, No.17, pp.875-876, 1987.

[35] Y.K.Park, S.W.Granlund, C.Y.Kuo, M.Dixon, T.W.Cline, R.W.Smith, N.K.Dutta, and G.Vannucci, "Crosstalk penalty in a two-channel ASK heterodyne detection system with non-negligible laser linewidth," *Electron. Lett.*, Vol.23, No.24, pp.1291-1293, 1987.

[36] A.Tomita, "Crosstalk caused by stimulated Raman scattering in single-mode wavelength-division multiplexed systems," *Optics Lett.*, Vol.8, No.7, pp.412-414, 1983.

[37] R.G.Waarts and R.P.Braun, "Crosstalk due to stimulated Brillouin scattering in monomode fibre," *Electron. Lett.*, Vol.21, No.23, pp.1114-1115, 1985.

[38] N.Shibata, R.P.Braun, and R.G.Waarts, "Crosstalk due to three-wave mixing process in a coherent single-mode transmission line," *Electron. Lett.*, Vol.22. No.12, pp.675-677, 1986.

[39] Y.K.Park, S.W.Granlund, L.D.Tzeng, N.A.Olsson, and N.K.Dutta, "Crosstalk in a two-channel coherent fibre-optic ASK system using an optical amplifier and non-negligible linewidth lasers," *Electron. Lett.*, Vol.24, No.8, pp.475-477, 1988.

[40] G.Grosskopf and R.Ludwig, "Effect of channel spacing in an optical two-channel DPSK transmission system with optical amplifier," *Electron. Lett.*, Vol.24, No.16, pp.1052-1054, 1988.

[41] B.Glance, G.Eisenstein, P.J.Fitzgerald, K.J.Pollock, and G.Raybon, "Optical amplification in a multichannel FSK coherent system," *Electron. Lett.*, Vol.24, No.18, pp.1157-1159, 1988.

[42] K.Kikuchi, T.Okoshi, M.Nagamatsu, and N.Henmi, "Degradation of bit-error rate in coherent optical communications due to spectral spread

of the transmitter and the local oscillator," *J. Lightwave Technol.*, Vol.LT-2, No.6, pp.1024-1033, 1984.

[43] L.G.Kazovsky, "Impact of laser phase noise on optical heterodyne communication systems," *J. Opt. Commun.*, Vol.7, No.2, pp.66-78, 1986.

[44] I.Garrett and G.Jacobsen, "Theoretical analysis of heterodyne optical receivers for transmission systems using (semiconductor) lasers with nonnegligible linewidth," *J. Lightwave Technol.*, Vol.LT-4, No.3, pp.323-334, 1986.

[45] S.Kakimoto, Y.Nakajima, Y.Sakakibara, H.Watanabe, A.Takemoto, and N.Yoshida, "Narrow spectrum linewidth and low chirp of 1.5μm InGaAs MQW-DFB-PPIBH laser diodes," *ECOC'89*, (Gothenburg, Sweden), Pap.TuB10-4, 1989.

[46] K.Emura, M.Shikada, S.Yamazaki, K.Komatsu, I.Mito, and K.Minemura, "Optical DPSK heterodyne detection experiment using DBR laser diodes with external optical feedback," *Electron. Lett.*, Vol.21, No.24, pp.1121-1122, 1985.

[47] E.Meissner, "116photons/bit in a 565Mbit/s optical DPSK heterodyne transmission experiment," *Electron. Lett.*, Vol.25, No.4, pp.281-282, 1989.

[48] K.Tamura, S.B.Alexander, and V.W.S.Chan, "Phase-noise-canceled differential-phase-shift-keying PNC-DPSK modulation for coherent optical communication systems," *OFC'88*, (Louisiana, U.S.A.), Pap.WG2, 1988.

[49] M.Schwartz, W.R.Bebbett, and S.Stein, *Communication Systems and Techniques*. McGraw-Hill, New York, 1965.

[50] K.S.Miller, *Multidimentional Gaussian Distributions*. Wiley, New York, 1964.

[51] T.Okoshi, K.Emura, K.Kikuchi, and R.Th.Kersten, "Computation of bit-error rate of various heterodyne and coherent-type optical communication schemes," *J. Opt. Commun.*, Vol.2, No.3, pp.89-96, 1981.

[52] R.E.Wagner, C.D.Poole, H.J.Schulte, N.S.Bergano, V.P.Nathu, J.M.Amon, R.L.Rosenberg, and R.C.Alferness, "Polarization measurements on a 147-km undersea cable," *OFC'86*, (Atlanta, U.S.A.), Pap.PDP7, 1986.

[53] J.P.Dakin, C.A.Wade, and G.H.Ellis, "A novel 3-wave mixing heterodyne approach to coherent optical communications," *ECOC'86*, (Barcelona), pp.33-36, 1986.

[54] S.Ryu, S.Yamamoto, and K.Mochizuki, "Polarization-insensitive operation of coherent FSK transmission system using polarization diversity," *Electron. Lett.*, Vol.23, No.25, pp.1382-1384, 1987.

[55] T.G.Hodgkinson, R.A.Harmon, and D.W.Smith, "Performance comparison of ASK polarization diversity and standard coherent optical heterodyne receivers," *Electron. Lett.*, Vol.24, No.1, pp.58-59, 1988.

[56] L.D.Tzeng, T.W.Cline, and A.A.M.Saleh, "Measurement of excess sensitivity penalty of a four-diode polarization diversity coherent receiver," *Electron. Lett.*, Vol.24, No.6, pp.330-332, 1988.

[57] S.Watanabe, T.Naito, T.Chikama, T.Kiyonaga, Y.Onoda, and H.Kuwahara, "Power penalty analysis due to polarization diversity on 1.2Gbit/s optical DPSK heterodyne transmission," *Electron. Lett.*, Vol.25, No.6, pp.383-384, 1989.

[58] C.D.Poole, N.S.Bergano, R.E.Wagner, and H.J.Schulte, "Polarization

dispersion and principal states in a 147-km undersea lightwave cable," *J. Lightwave Technol.*, Vol.LT-6, No.7, pp.1185-1190, 1988.

[59] A.Hirose, E.A.J.Marcatili, and T.Okoshi, "Proposal of tandem differential detection scheme for time-division phase-noise-canceled (PNC) DPSK coherent optical communi-cations," unpublished work.

[60] L.G.Kazovsky, "Impact of laser phase noise on optical heterodyne communication systems," *J. Opt. Commun.*, Vol.7, No.2, pp.66-78, 1986.

[61] G.Jacobsen and I.Garrett, "Theory for optical heterodyne DPSK receivers with post-detection filtering," *J. Lightwave Technol.*, Vol.LT-5, No.4, pp.478-484, 1987.

[62] L.G.Kazovsky and J.L.Gimlett, "Sensitivity penalty in multichannel coherent optical communications," *J. Lightwave Technol.*, Vol.6, No.9, pp.1353-1365, 1988.

[63] A.B.Carlson, *Communication Systems*. McGraw-Hill, 1986.

[64] A.Yariv, *Quantum Electronics*. John Wiley & Sons, 1975.

[65] M.Schwartz, *Information Transmission, Modulation, and Noise*. McGraw-Hill, 1970.

PUBLICATIONS

Periodicals:

[1] Y.H.Cheng and T.Okoshi, "Effect of laser linewidth on crosstalk penalty in two-channel ASK heterodyne detection system," *Electron. Lett.*, Vol.24, No.14, pp.830-831, 1988.

[2] Y.H.Cheng, T.Okoshi, and O.Ishida, "Performance analysis and experiment of a homodyne receiver insensitive to both polarization and phase fluctuations," *J. Lightwave Technol.*, Vol.7, No.2, pp.368-374, 1989.

[3] Y.H.Cheng and T.Okoshi, "Phase-noise-cancelling dual-frequency heterodyne optical fibre communication system," *Electron. Lett.*, Vol.25, No.13, pp.835-836, 1989.

[4] Y.H.Cheng, E.A.J.Marcatilli, and T.Okoshi, "Analysis of phase-noise-canceling heterodyne schemes for coherent optical communications," to be submitted to *J. Opt. Commun.*.

International Conferences:

[5] Y.H.Cheng and T.Okoshi, "Crosstalk penalty in two-channel ASK, FSK and PSK heterodyne detection systems considering effect of laser linewidth," *OEC'88*, (Tokyo, Japan), Pap.3A3-3, 1988.

[6] Y.H.Cheng, E.A.J.Marcatili, and T.Okoshi, "Phase-noise-canceling heterodyne receivers for coherent optical communication systems,"

OFC'89, (Houston, U.S.A.), Pap.TU17, 1989.

[7] Y.H.Cheng and T.Okoshi, "Bit-error rate and feasibility analyses of dual polarization phase-noise-canceling heterodyne receiver," *IOOC'89*, (Kobe, Japan), Pap.19B3-18, 1989.

Institutional Meetings:

[8] Y.H.Cheng and T.Okoshi, "Impact of the crosstalk on frequency division multiplexing (FDM) coherent optical fiber communications," *IEICE Technical Report*, No.OQE87-124, pp.1-8, 1987 (in Japanese).

[9] Y.H.Cheng and T.Okoshi, "Effect of laser linewidth on crosstalk penalty in frequency division multiplexing coherent communication systems," *IEICE Technical Report*, No.OCS88-13, pp.25-30, 1988 (in Japanese).

Domestic Conferences:

[10] Y.H.Cheng and T.Okoshi, "Impact of the excess shot noise on frequency division multiplexing coherent optical communications," *1987 National Convention Record*, The Institute of Electronics, Information and Communication Engnieers, Pap.332, 1987 (in Japanese).

[11] Y.H.Cheng and T.Okoshi, "Crosstalk penalty in frequency-division multiplexing coherent optical communication systems," *1989 Spring National Convention Record*, The Institute of Electronics, Information and Communication Engnieers, Pap.B-770, 1989 (in Japanese).

APPENDIX

BER formula of a multichannel FSK dual-filter envelope detection system considering crosstalk induced noise

BER formula of a single-channel FSK dual-filter scheme can be found in common text books. However, because crosstalk induced noise in a multichannel FSK dual-filter scheme is different for mark and space time-slots, BER formula of multichannel FSK dual-filter scheme is not equal to that of single-channel scheme. Here BER formula of a multichannel FSK dual-filter envelope detection scheme is derived.

Assuming that the received signal power is A^2, and noises for mark and space signals are N_m and N_s respectively, we have

$$N_m = \sigma_0^2 + \sigma_{cm}^2 \tag{A1}$$

and

$$N_s = \sigma_0^2 + \sigma_{cs}^2 \tag{A2}$$

where σ_0^2 is the shot noise, and σ_{cm}^2 and σ_{cs}^2 the crosstalk induced noises for mark and space signals respectively. In general, σ_{cm}^2 is different from σ_{cs}^2.

When a mark signal is transmitted the probability density function of the receiver for mark signal is given by a Rice distribution as

$$p(r_m) = \frac{r_m}{N_m} I_0\left(\frac{Ar_m}{N_m}\right) \exp\left(-\frac{r_m^2 + A^2}{2N_m}\right) \tag{A3}$$

whereas that of the receiver for space signal is given as

$$p(r_s) = \frac{r_s}{N_s} \exp\left(-\frac{r_s^2}{2N_s}\right) \tag{A4}$$

An error occurs so long as $r_s > r_m$, then BER is given as

$$BER^m = prob.(r_s > r_m) = \int_0^\infty p(r_m) \int_{r_m}^\infty p(r_s)\, dr_s\, dr_m \tag{A5}$$

By substituting Eqs.(A3) and (A4) into Eq.(A5), Eq.(A5) is simplified as

$$BER_m = \frac{N_s}{N_m + N_s} \exp\left(-\frac{A^2}{2(N_m + N_s)}\right) \tag{A6}$$

Similarly, when a space signal is transmitted the probability density function of the receiver for space signal is given as

$$p(r_s) = \frac{r_s}{N_s} I_0\left(\frac{Ar_s}{N_s}\right) \exp\left(-\frac{r_s^2 + A^2}{2N_s}\right) \tag{A7}$$

whereas that of the receiver for mark signal is given as

$$p(r_m) = \frac{r_m}{N_m} \exp\left(-\frac{r_m^2}{2N_m}\right) \tag{A8}$$

An error occurs so long as $r_m > r_s$, thus BER is given as

$$BER^s = prob.(r_m > r_s) = \int_0^\infty p(r_s) \int_{r_s}^\infty p(r_m)\, dr_m\, dr_s \tag{A9}$$

By substituting Eqs.(A7) and (A8) into Eq.(A9), Eq.(A9) is simplified as

$$BER_s = \frac{N_m}{N_m + N_s} \exp\left(-\frac{A^2}{2(N_m + N_s)}\right) \tag{A10}$$

Thus the total BER is

$$BER = \frac{1}{2}(BER_m + BER_s) = \frac{1}{2} \exp\left(-\frac{A^2}{2(N_s + N_m)}\right) \tag{A11}$$